UNIVERSITY OF CALIFORNIA SAN DIEGO

Biofuel Cells for Self-Powered Biosensors and Bioelectronics Toward Biomedical Applications

A dissertation submitted in partial satisfaction of the requirements for the degree
Doctor of Philosophy

in

NanoEngineering

by

Itthipon Jeerapan

Committee in charge:

Professor Joseph Wang, Chair
Professor Zheng Chen
Professor Patrick P. Mercier
Professor Tse Nga Ng
Professor Sheng Xu

2019

The Dissertation of Itthipon Jeerapan is approved, and it is acceptable in quality and form for publication on microfilm and electronically:

_____

_____

_____

_____

_____

Chair

University of California San Diego

2019

DEDICATION

This dissertation is dedicated to my parents and all members in my home. This is also to my Great Teacher, teachers, and friends. To all beings and all things that have the spirit of good teachers and good friends.

EPIGRAPH

Uppādā vā tathāgatānaṃ anuppādā vā tathāgatānaṃ, ṭhitāva sā dhātu
dhammaṭṭhitatā dhammaniyāmatā idappaccayatā.

อุปฺปาทา วา ตถาคตานํ อนุปฺปาทา วา ตถาคตานํ ฐิตา ว สา ธาตุ ธมฺมฏฺฐิตตา ธมฺมนิยามตา อิทปฺปจฺจยตา

เพราะเหตุที่ตถาคตทั้งหลาย จะบังเกิดขึ้นก็ตาม จะไม่บังเกิดขึ้นก็ตาม ธรรมธาตุนั้น ย่อมตั้งอยู่แล้ว นั่นเทียว
คือ ธัมมัฏฐิตตา *(ความตั้งอยู่ แห่งธรรมดา)*
คือ ธัมฺมัฏฐิตตา *(ความเป็นกฎตายตัว แห่งธรรมดา)*
คือ อิทัปปัจจยตา *(ความที่เมื่อมีสิ่งนี้ สิ่งนี้เป็นปัจจัย สิ่งนี้ สิ่งนี้จึงเกิดขึ้น)*

Whether a Buddha emerges in the world or whether he has not emerged in the world,
the Dharmadhātu *(elements and properties of nature)* stands.
Dhammaṭṭhitatā *(steadfastness of nature)*,
Dhammaniyāmatā *(inevitability about nature, orderliness of nature, natural law)*,
and Idappaccayatā *(specific conditionality and the principal of causality – that all things arise and exist due to certain causes (or conditions) and cease once the causes (or conditions) are removed.)* remain.

The Buddha

TABLE OF CONTENTS

LIST OF FIGURES

LIST OF TABLES

ACKNOWLEDGEMENTS

First, I would like to thank my advisor, professor Joseph Wang. He allowed me to learn about the broad scope of interdisciplinary research. In addition, joining his team graciously broadened my horizons in many aspects. Professor J. Wang is also the most primary and significant resource for getting me to learn about the world of publications. These experiences are invaluable and unforgettable. I would also like to spread my appreciation to my other valuable committee members. These include Professor Sheng Xu and Professor Zheng Chen from the Department of NanoEngineering. These also include Professor Tse Nga Ng and Professor Patrick P. Mercier from the Department of Electrical and Computer Engineering. They have greatly enriched my work and provided treasured experiences throughout this dissertation. I would like to specially acknowledge professor P. P. Mercier and his wonderful research group for our collaborations and the integrated knowledge and grateful contributions of electronics that he and his group provided. I would also like to extend my acknowledgement to Dr. Krishnan Chakravarthy, who has been very supportive of our fantastic interdisciplinary research. I very much appreciated his time, allowing me to learn new and very exciting experiences. We conjugated our exciting disciplines together to transform new frontier technologies for future translational biomedicine.

I have been fortunate to meet many friends and co-workers, all contributing to my research in Prof. Wang's laboratory and in a large part during my Ph. D. study. These include, but not limited to, A. Abellán-Llobregat, Abbas Barfidokht, Adriana Pavinatto, Aida Martin, Alan S. Campbell, Aleksandar Karajić, Amay Bandodkar, Amir Nourhani,

Berta Esteban-Fernandez de Avila, Bianca Ciui, Caleb Christianson, Cristian Abraham Silva-Lopez, Deniz Aktaş Uygun, Emil Karshalev, Ernesto De La Paz, Farshad Tehrani, Fernando Soto, Gabriela Valdés-Ramírez, Hazhir Teymourian, Hongsen Yang, Jayoung Kim, Ji-Hyun Jang, Jian Lv, Jonas F. Kurniawan, Juliane R. Sempionatto, Jung-Min You, Lee J. Hubble, Lu Yin, Miguel Angel Lopez-Ramirez, Murat Uygun, Nikhil Harsha Maganti, Paulo A. R. Pereira, Rajan Kumar, Rupesh K. Mishra, Rushabh Shah, Sadagopan Krishnan, Somayeh Imani, Ta-Yu Huang, Tamas Szabo, Tatsuo Nakagawa, Thomas N. Cho, Vinu Mohan, Wanxin Tang, and Xiaoyang Wang. Amay Bandodkar was a graduate student and a very first support for my initial projects in the UCSD. Dr. Jung-Min You is the first person to let me see the fantastic opportunity of research in biofuel cells. Juliane R. Sempionatto helped and supported a big part for my research described in this dissertation. My wonderful friends, such as Ta-Yu Huang, Jian Lv, Cristian Abraham Silva-Lopez, Ernesto De La Paz, etc., sat near me and joined many interesting research projects.

I would especially like to acknowledge my research assistants, including Aidan Kennedy, Gustavo Andres. Hassler Bueno, Ian Martin, Isac Lazarovits, Julian Ramirez, Martin C. Hartel, Nicholas Tostado, Nicolás Ma, Paul Warren, Philippe Eisenberg, Ranawat Trisiripisal, Rogelio Nuñez-Flores, Ruining Piao, Shuyang Liu, Tiffany Chen, and Won Jung. It is their efforts that supported me in an immeasurable way. Many of them have also trained me to gain real and valuable experiences of being a research mentor.

In addition, I very much appreciated A. M. Vinu Mohan, Amay Bandodkar, Jung-Min You, Fernando Soto, and Rajan Kumar. They kindly helped and supported me when I was going through a hard time due to the appendicitis and health issues.

I would also like to thank a few special friends. The help and grateful support of my friends and colleagues made my Ph.D. possible. I would like to express my special appreciation and thanks to my Thai friends and roommates that I have spent a great time with in the USA, including Anusorn Mudla, Chochanon Moonla, Korrawee Pruegsanusak, Nantawat Udomchatpitak, Narupat Hongdilokkul, Nitit Sunthorn, Pichaya Lertvilai, Praopim Limsakul, Richard Samakapiruk, Siraphob Boonvanich, Sumaetee Tangwancharoen, Tossapol Pholcharee, Wasut Pornpatcharapong, Watcharapong Hongjamrasilp, Wisarut Kiratitanaporn, Woraphong Janetanakit, Cheng-Yi Fang, Dulce Rodriguez-Ponciano, Erlend U. Ambjørndalen, and Keith Cheung. I also thank to my landlord, Charles Lu, for a nice place. My time in the USA was made entertaining in a great part because of many friends and groups that supported an important part of my life. In addition, I would also like to extend my great appreciations to my friends, including Panyapon Sudkaow, Sasikarn Seetasang, and Sununta Panyasang. I value their friendship and admirable support. Although they are not in the USA, they are a significant part of my success. Being with our good friends (kalyāṇa-mitta) is all the therapy and power we need.

My acknowledgement is also directed to the scholarship from the Development and Promotion of Science and Technology Talents Project (DPST), Thailand. Without this financial support, I definitely could not have studied abroad outside my home country. I

also give thanks to Dr. Proespichaya Kanatharana, Dr. Chongdee Thammakhet, Dr. Panote Thavarungkul, and so many other supports from the Department of Chemistry, Faculty of Science, Prince of Songkla University, Thailand. This acknowledgement is extended to Dr. Sirilak Sattayasamitsathit and Dr. Soracha Dechaumphai, who helped me take the beginning step to start life in UCSD. These contributions made my study in the USA possible.

My heartfelt appreciations are extended to my parents and sister: Nopporn Jeerapan, Ampon Jeerapan, and Pornpimon Jeerapan. I would also like to extend my appreciation to my relatives and my beloved dogs. There are not enough words to describe the gratitude. I would like to express my thanks for being such a good support and always cheering me up.

I would also like to spread my thanks to anyone, anything, and to many experiences involved. I very much appreciate everyone and everything in my heart. All contributions made my Ph. D. possible and successful. If I had to write all the names on my dissertation acknowledgement, this section would be seen in the Guinness World Records as the longest dissertation in the history.

Chapter 1 is based, in part, on the material as it appears in Advanced Functional Materials, 2019, by Itthipon Jeerapan, Juliane R. Sempionatto, and Joseph Wang. The dissertation author was the primary investigator and author of this paper.

Chapter 2 is based, in part, on the material as it appears in Journal of Materials Chemistry A, 2016, by Itthipon Jeerapan, Juliane R. Sempionatto, Adriana Pavinatto, Jung-Min You, and Joseph Wang. The dissertation author was the primary investigator and author of this paper.

Chapter 3 is based, in part, on the material as it appears in Journal of Materials Chemistry B, 2018, by Itthipon Jeerapan, Bianca Ciui, Ian Martin, Cecilia Cristea, Robert Sandulescu, and Joseph Wang. The dissertation author was the primary investigator and author of this paper.

Chapter 4 is based, in part, on the material as it appears in Biosensors and Bioelectronics, 2018, by Itthipon Jeerapan, Juliane R. Sempionatto, Jung-Min You, and Joseph Wang. The dissertation author was the primary investigator and author of this paper.

Chapter 5 is based, in part, on the materials as they appear in Journal of Materials Chemistry A, 2016, by Itthipon Jeerapan, Juliane R. Sempionatto, Adriana Pavinatto, Jung-Min You, and Joseph Wang; Journal of Materials Chemistry B, 2018, by Itthipon Jeerapan, Bianca Ciui, Ian Martin, Cecilia Cristea, Robert Sandulescu, and Joseph Wang; in Biosensors and Bioelectronics, 2018, by Itthipon Jeerapan, Juliane R. Sempionatto, Jung-Min You, and Joseph Wang. The dissertation author was the primary investigator and author of these papers.

VITA

2013 Bachelor of Science in Chemistry (First Class Honor), Prince of Songkla University, Songkhla, Thailand

2016 Master of Science in Nanoengineering, University of California San Diego, California, The United States of America

2019 Doctor of Philosophy in Nanoengineering, University of California San Diego California, The United States of America

SELECTED PUBLICATIONS

1. **Jeerapan, I.**; Sempionatto, J. R.; Wang, J., On-Body Bioelectronics: Wearable Biofuel Cells for Bioenergy Harvesting and Self-Powered Biosensing. *Advanced Functional Materials* **2019**. DOI: 10.1002/adfm.201906243.
2. **Jeerapan, I.**; Sempionatto, J. R.; Pavinatto, A.; You, J.-M.; Wang, J., Stretchable biofuel cells as wearable textile-based self-powered sensors. *Journal of Materials Chemistry A* **2016,** *4* (47), 18342-18353. DOI:10.1039/C6TA08358G.
3. **Jeerapan, I.**; Ciui, B.; Martin, I.; Cristea, C.; Sandulescu, R.; Wang, J., Fully edible biofuel cells. *Journal of Materials Chemistry B* **2018,** *6* (21), 3571-3578. DOI: 10.1039/C8TB00497H.

4. **Jeerapan, I.**; Sempionatto, J. R.; You, J.-M.; Wang, J., Enzymatic glucose/oxygen biofuel cells: Use of oxygen-rich cathodes for operation under severe oxygen-deficit conditions. *Biosensors and Bioelectronics* **2018,** *122,* 284-289. DOI: 10.1016/j.bios.2018.09.063.

FIELDS OF STUDY

Major Fields: Biomedical Nanotechnology, Energy

Studies in Nanoengineering

Professor Joseph Wang

ABSTRACT OF THE DISSERTATION

Biofuel Cells for Self-Powered Biosensors and Bioelectronics

Toward Biomedical Applications

By

Itthipon Jeerapan

Doctor of Philosophy in NanoEngineering

University of California San Diego, 2019

Professor Joseph Wang, Chair

Considerable efforts in research have been dedicated to the advancement of enzyme-based biofuel cells (BFCs) for various applications. BFCs can be used as energy-conversion devices, converting biofuels into electricity. Self-powered biosensors can also be engineered from BFCs. Such self-sustainable BFC-based biosensors and bioelectronics open opportunities for various biomedical applications, ranging from wearable, ingestible,

to implantable applications. However, irrespective of purposes, bioelectronics mandates sustainable energy sources. The goal in the research is to expand the spectrum of new BFCs for biomedical technologies. Valuably, BFCs working as self-powered biosensors and energy harvesters simplify overall systems by minimalizing energy-consuming compartments, allowing the miniaturization of biodevices that traditional devices cannot enable. This dissertation describes an example of the first textile-based BFCs as stretchable self-powered sensors that can autonomously extract the electricity from perspiration and use this electricity as an analytical signal to indicate metabolite levels. This successful demonstration of wearable self-powered sensors with real-time wireless communication is expected to step further the progress of energy-harvesting systems and self-sustainable bioelectronics. Moreover, this dissertation will describe the fully edible ethanol BFC, based merely on biocompatible mushroom/plant extracts and food-based materials without any additional external mediators. These edible BFC energy harvesters represent attractive opportunities for modernizing biosensors and bioelectronics for the use in the digestive system. Furthermore, the grand challenges of BFCs including oxygen dependency will be discussed. For example, this dissertation includes an approach to address the oxygen limitations by developing a nanocomposite of oxygen-rich cathode material to provide the internal oxygen for the BFC cathodic reaction. Therefore, the effect of fluctuating oxygen levels during the operation of BFCs can be mitigated. Understanding challenges and opportunities are significant to transform BFCs to new devices for diverse domains, such as wearable, ingestible, and biomedical technologies.

Chapter 1 Introduction

1.1 On-Body Bioelectronics: Wearable Biofuel Cells for Bioenergy Harvesting and Self-Powered Biosensing

The growing power demands of wearable electronic devices have stimulated the development of on-body energy-harvesting strategies. This chapter reviews the recent progress on rapidly emerging wearable biofuel cells (BFCs), along with related challenges and prospects. Advanced on-body BFCs in various wearable platforms, e.g., textiles, patches, temporary tattoo, or contact lenses, enable attractive advantages for bioenergy harnessing and self-powered biosensing. These noninvasive BFCs open up unique opportunities for utilizing bioenergy or monitoring biomarkers present in biofluids, e.g., sweat, saliva, interstitial fluid, and tears, toward new biomedical, fitness, or defense applications. However, the realization of effective wearable BFC requires high-quality enzyme-electronic interface with efficient enzymatic and electrochemical processes and mechanical flexibility. Understanding the kinetics and mechanisms involved in the electron transfer process, as well as enzyme immobilization techniques, is essential for efficient and stable bioenergy harvesting under diverse mechanical strains and changing operational conditions expected in different biofluids and in a variety of outdoor activities. These key challenges of wearable BFCs are discussed along with potential solutions and future

prospects. Understanding these obstacles and opportunities is crucial for transforming traditional bench-top BFCs to effective and successful wearable BFCs.

Bioelectronics involves the interface of biomaterials and electronic devices toward a variety of biomedical applications.[1-2] The growing recent interest in bioelectronics has been driven by the rapid rise of wearable devices.[3-4] While early efforts in wearable sensing devices have been devoted to on-body physical sensors for monitoring body motion and electrophysiological signs (e.g., blood pressure, heart rate), recent efforts have shifted toward the development of wearable bioelectronic devices for noninvasive detection of target chemical markers (e.g., electrolytes and metabolites).[4-7] These wearable biosensing devices are "energy hungry" due to the growing demands for multiparameter detection, complex data processing, and real-time wireless data transmission. Such sensing devices rely also on advanced body-compliant soft electrochemical platforms in connection to diverse flexible and stretchable materials.[8-9] However, progress of wearable energy devices has not been fast enough to cope with these rapidly growing energy demands of wearable sensing devices (and of wearable electronics, in general) and has been hindered by the lack of similar anatomically-compliant viable power sources.[8, 10-11] Existing power sources, are rigid, large and heavy, and hence limit the wearer's activity. Among the emerging wearable energy-harvesting devices, miniaturized body-compliant flexible noninvasive biofuel cells (BFCs), that rely on various biofluids for generating electricity, offer an attractive approach for addressing the challenge of wearable power sources.[12-15]

This chapter reviews the current state-of-arts of wearable BFCs and discusses key challenges and obstacles for achieving and maintaining efficient electron transport between the enzyme and the conducting electrode during diverse on-body operations, along with future opportunities and prospects. Wearable BFCs are promising for the powering of noninvasive wearable platforms, particularly noninvasive sensors, as they harvest energy from the same biofluids of interest, operating as self-powered biosensors. BFCs belong to a class of fuel cells that uses biocatalysts (e.g., enzymes and microorganisms) instead of metallic inorganic catalysts. There are basically two types of BFCs. The first type, known as secondary or indirect BFC, involves a biocatalyst that generates the fuel which is subsequently oxidized by an inorganic catalyst at the electrode surface to produce the electrical power. In the second type, known as primary or direct BFC, the biocatalyst is directly involved in the redox reaction that generates the power.[16] The latter case is preferred for on-body wearable systems, where the redox reaction can be carried out in mild physiological conditions of temperature and pH.[17]

Figure 1.1 shows a schematic of a typical primary enzymatic BFC based on glucose and oxygen, where the glucose oxidase (GOx) enzyme is immobilized at the anode electrode to promote the electron-generating fuel (glucose) oxidation reaction generating protons and electrons. At the cathode, the bilirubin oxidase (BOx) enzyme is immobilized to promote the oxygen reduction to water. These bioelectrochemical reactions at the electrode surfaces are utilized to generate current and power. The intensity of the electrical current involved in these redox reactions and the corresponding electrical energy are thus

proportional to the fuel concentration and can be used to power biosensors, or to charge batteries and supercapacitors (Figure 1.1A, left). In addition, the BFC can act as a self-powered biosensor via several mechanisms, including measuring the concentration of the fuel (target analyte) or of reaction inhibitors or activators. All these mechanisms represent an attractive type self-sustainable bioelectronic device[18-19] (Figure 1.1A, right). The power density (PD) of wearable BFCs thus depends strongly on the availability of the chemical fuel in biofluids. Wearable BFCs rely on biofluids, such as sweat or tears, which contain several metabolites that can be used as fuels, to generate usable electrical energy. Such BFCs are thus promising for the powering of noninvasive bioelectronic sensing platforms since they harvest bioenergy from the same biofluids that the corresponding sensors analyze. It should be noted that the terminology of BFCs can include a nonfully enzymatic BFC, with an enzymatic electrode in one side and a regular (nonenzymatic) electrode on the other half side. This includes, for example, a BFC that uses an enzymatic bioanode coupled with an abiotic catalytic cathode (such as Pt-based cathode). Owing to their continuous operations in biofluids, wearable BFCs often suffer from similar issues facing wearable biosensing platforms. Among them, the device stability is one of the most crucial challenges that researchers have to address.

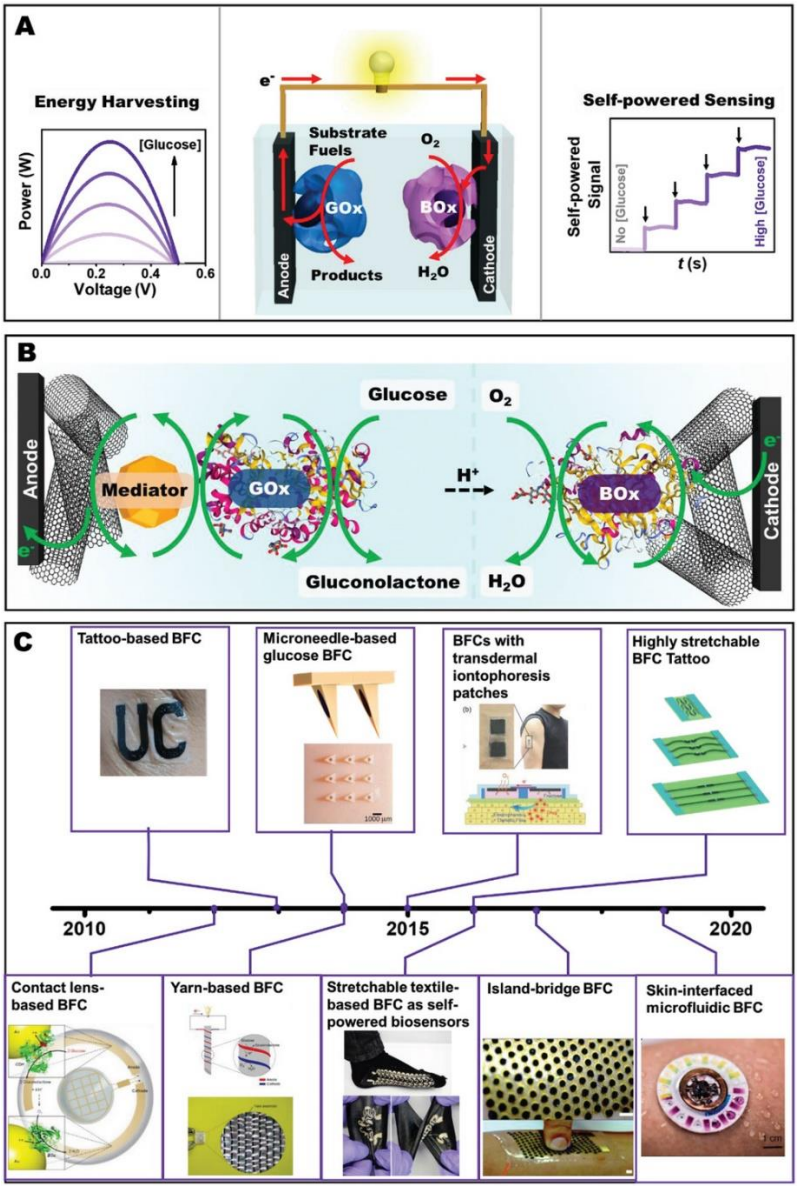

Figure 1.1 A) Conceptual illustration of an enzymatic biofuel cell (BFC), showing the key working principle and applications for energy harvesting and self-powered sensing. Adapted with permission.[20] Copyright 2019, Wiley-VCH. B) A scheme of the composition and operation of a typical glucose/oxygen BFC consisting of a glucose oxidase (GOx)-mediated bioanode and bilirubin oxidase (BOx) biocathode. Adapted with permission.[20] Copyright 2019, Wiley-VCH. C) Historical timeline showing the key progress of wearable BFCs in connection to different platforms and body fluids. The key initial conceptual demonstration of different main platforms is included. (Top row, left to right): Adapted with permission.[21] Copyright 2013, Wiley-VCH. Adapted with permission.[22] Copyright 2014, Elsevier. Adapted with permission.[23] Copyright 2015, Wiley-VCH. Adapted with permission.[24] Copyright 2016, American Chemical Society. (Bottom row, left to right): Adapted with permission.[25] Copyright 2012, Elsevier. Adapted with permission.[26] Copyright 2014, Nature Publishing Group. Adapted with permission.[27] Copyright 2016, Royal Society of Chemistry. Adapted with permission.[28] Copyright 2017, Royal Society of Chemistry. Adapted under the terms and conditions of the CC-BY license.[29] Copyright 2019, The Authors, published by AAAS.

The successful implementation of wearable BFCs depends on addressing major challenges to realize effective electrochemical communication between the enzyme and the electrode surface, to the uncontrollable parameters of wearable devices, including unexpected dynamic variations of the corresponding biofluids and surrounding environment (e.g., changes in the temperature, pH, humidity, or oxygen levels), as well as to material challenges for ensuring the necessary flexibility, stretchability and overall mechanical resiliency of the system under severe strains.

The electrochemical communication challenge is related to the efficiency of transferring electrons between the biocatalyst and the electrode. In order to effectively harvest the electrons involved in bioelectrocatalytic reactions, the active site of the enzyme needs to be in close proximity to the electrode surface. The enzyme thus needs to be oriented and immobilized on the electrode surface so that it can effectively communicate with the electrode while promoting the diffusion of fuel and products. The efficiency of the electron transfer in the enzyme-electrode interface, and hence the resulting power output, are greatly influenced by the enzyme immobilization strategy. Different physical and chemical, approaches have been used for immobilizing enzymes on electrode surfaces. A comprehensive discussion of this topic has been presented in early reports.[4, 14-15] In the case of wearable BFCs, the immobilization protocol must ensure that the reagent layer is also resilient against mechanical strains, that the enzyme resists rapid temperature or pH changes and that all the species involved in the bioelectrocatalytic process are confined onto the corresponding bioanode and cathode. These include the redox-active mediators,

often introduced into the electrode-enzyme interface to improve the electrochemical communication between the enzyme active site and the electrode surface.[30] The redox reaction between the mediator and the enzyme must be efficient with fast kinetics and reversibility at low overpotentials.[30] Small mediator molecules can easily diffuse away from the surface and such leaching can lead to poor BFC stability and toxicity. Strategies to bypass the use of mediators in BFC will be discussed in the following sections of this chapter.

The efficiency of the BFC system strongly depends on the temperature, pH, and oxygen levels. Unlike traditional BFCs, wearable BFCs commonly operate under conditions that differ from the physiological ones (pH 7.4, 0.15 M NaCl, 37 °C). Variations in the body temperature, humidity, and outdoor conditions, including exposure to unknown substances, are some of the examples which can affect the performance of BFCs. Fluctuations in the biofluid pH can vary depending on the specific fluid. For instance, the pH of human sweat can fluctuate from 4.5 to 6.0[31] while the tears pH varies from 6.5 to 7.6.[32] The fluctuated pH of acidic sweat can degrade the performance of the skin-worn BFC, and may eventually lead to their complete inactivation. Other variations in the specific biofluid, e.g., ionic strength and viscosity, should also be carefully considered. To successfully operate a wearable BFC in complex dynamic biofluids, the enzyme needs to be immobilized efficiently on the electrode surface to maintain its biocatalytic activity under extreme conditions (e.g., of temperature or pH). The biocathode commonly rely on the enzyme BOx or laccase for the oxygen reduction. The former can be inhibited by urate

anions present in sweat while the latter is inhibited by chloride ions and requires a low pH.[33] Another inherent challenge to BFC operating in complex biofluids is the biofouling of the active surface. The biofouling of wearable BFCs is less severe than that of implantable BFCs, as they do not come into direct contact with whole blood and do not involve skin piercing. Yet, the prolonged exposure of a wearable BFC to biofluids with high concentrations of proteins (such as present in saliva[34]) leads to nonspecific adsorption of large biomolecules onto the surface of the bioanode and cathode. Such surface fouling hinders the fuel diffusion to the BFC, and gradually decreases the power output. Biofouling effects can be minimized by using additional antifouling protective layers on the electrode surface,[35-36] although such layers can also reduce the fuel transport. Other parameters and strategies to increase the stability of BFCs operating in dynamic biofluids will be discussed in the following sections.

Conventional BFCs are rigid with low conformability and mechanical compliance against the body multiaxial deformations, resulting in discomfort of worn traditional BFC. Thus, wearable BFCs require additional mechanical properties compatible with the soft and curvilinear human tissues so that they can intimately mate with the tissue. Hence, the material aspects of wearable BFCs are important, not only to meet the criteria of the body-compliance parameters, such as comfort, simplicity of operation, flexibility, and stretchability, but also affect directly the power output generated by the BFC. The power generated by the BFC strongly depends on the active surface area. The use of 3D porous electrodes enables high loading of the active species, which in turn promotes a substantial increase in the generated power. The active electrode area and electrocatalytic activity can

also be enhanced by the incorporation of nanomaterials into BFC systems. In addition, smart functional fabrics hold considerable promise as supporting platforms for textile-based BFCs, as desired for facilitating fully integrated wearables in daily life. These and other material challenges, solutions, and innovations toward high-performance wearable BFC will be further discussed in the following sections.

Overall, this review in this chapter discusses recent advances in wearable BFC, with particular emphasis on noninvasive BFCs harnessing bioenergy from sweat and tears, and discusses key materials, fabrication and operational challenges associated with continuously changing on-body conditions. Finally, we will discuss the future outlook, toward a wide spectrum of wearable BFC applications, ranging from fitness to personalized healthcare.

1.2 Fundamentals and History of Wearable Biofuel Cells

Here, we cover several key historical contributions to the development of wearable BFCs. This is not intended to be a comprehensive coverage of wearable and implantable BFC devices. Other past efforts and activities, not covered in the short section of this review, can be found in recently published reviews.[3, 11, 13, 37-39]

The use of BFCs for producing electric power out of body fluids of animals was envisioned first in the 1970's in connection to the use of blood glucose as the biofuel.[40] During this half century, enzymatic fuel cells have evolved from large and rigid

compartment cells to membraneless systems,[41-42] miniaturized implantable devices,[43-44] and now, into flexible wearable energy harvesters.[13]

As we briefly discussed, the design and operation of an enzymatic BFC are similar to that of a conventional fuel cell, consisting of the anode and the cathode, as shown in Figure 1.1B. Initially, the fuel (such as glucose) undergoes an enzyme-catalyzed oxidation at the bioanode, generating electrons that flow through an external circuit and reach the cathode. Next, when electrons reach the cathode, an oxidant (usually oxygen, present in natural fluids) receives those electrons, leading to a net electrical current.[14] Figure 1.1B shows a detailed schematic of a BFC composed of a GOx-based anode and a BOx-based cathode. Equation 1.1 and Equation 1.2 illustrate the corresponding electron generation and reduction reactions with the assistance of biocatalysts on the anode and cathode, respectively. For simplicity of the illustration, note that the proton generation and transfer in Figure 1.1A are not included

$$2\ glucose \rightarrow 2\ gluconolactone + 4H^+ + 4e^- \qquad \textbf{Equation (1.1)}$$

$$O_2 + 4H^+ + 4e^- \rightarrow 2H_2O \qquad \textbf{Equation (1.2)}$$

In order to generate power, the electron transfer rate between enzyme and electrode needs to be as efficient as the biocatalytic reaction rate. The electron transfer in a BFC can be divided into direct or mediated electron transfer (DET or MET, respectively). DET is achieved when the enzyme redox-active site is close enough to the electrode surface to enable effective electrons transfer directly from the active center of the enzyme to the current collector. In the case of GOx, this is extremely difficult to achieve, or even

impossible, as the active center is buried deeply in the protein structure for realizing short-distance electron tunneling. A recent article has discussed that the DET in native GOx is not possible due to the physical insulation of the flavin active sites by the enzyme structure, and that even conductive nanomaterials, such as carbon nanotubes (CNTs), graphene or nanoparticles, are not able to communicate with these sites.[45] However, as the majority of the literature cited in this chapter considers the DET of GOx, we report their discussion. In order to address the challenges of the GOx DET, several attempts have been made to "wire" the enzyme by incorporating nanomaterials such as CNTs[46-47] and gold nanoparticles (AuNPs).[48] Several reports have discussed the important topic of enzyme "wiring."[49-50] Alternately, small redox molecules, called mediators, are attractive candidates for improving the electron transfer between electrode surface and the enzyme, regardless of its orientation. Such MET represents a common strategy used when the electron transfer between the enzymes to the electrodes is not efficient. The role of a mediator molecule is to shuttle electrons between the enzyme redox center and the electrode, as illustrated in the bioanode of Figure 1.1B. The use of mediators has shown to improve the power density of several BFCs; however, it may add an extra level of complexity as well as safety and stability concerns (due to potential leaching) into the wearable system. Mediator immobilization is thus an important step in the preparation of wearable BFC. These issues and challenges will be discussed further in Section 1.3.3 "Achieving Efficient Electrical Communications in Wearable Bioelectrodes: While Eliminating Redox Mediators".

The simple design of BFCs and their ability to operate under mild physiological conditions have made these bioelectronic devices extremely attractive for harvesting power

from living species. BFCs represent very versatile systems that can harvest energy from the inside or outside of the body.[44, 51] The ability of enzymes to produce electricity, combined in a fuel cell system, was demonstrated over 50 years ago.[40] Glucose BFCs were thus used in the early 70's to harvest energy from dogs[52] and sheep;[53] however, the power generated from these early devices was unstable, presenting a fast decay until complete nonoperative state. In 2010, Cosnier and coworkers demonstrated the first example of a stable enzymatic glucose BFC implanted in the retroperitoneum of a rat;[33] following this pioneering work, BFCs have been implanted and used successfully by Katz and Scherson in living insects,[54-55] snail,[56] clams and lobsters,[57] rabbits,[58-59] and rats.[33] These implantable BFCs were reviewed recently by Katz.[44, 60]

Unlike implantable BFCs, the development of wearable noninvasive BFCs is relatively new and reflects the tremendous recent attention given to wearable electronics and mobile devices. Using wearable BFCs, instead of implantable ones, also minimizes concerns about biocompatibility, stability, oxygen fluctuations, and issues associated with exposure to the immune system.[61-63] In 2012, Falk et al. demonstrated the first wearable contact-lens glucose BFC operating in human tears.[25] Subsequently, several research groups developed innovative wearable BFCs based on different platforms and biofluids. In 2013, Prof. Joseph Wang' team presented the initial concept of epidermal tattoo BFCs[21] followed by microneedle BFCs in 2014.[22] Also, in 2014, engineered yarns were developed as effective components of textile-based BFCs.[26] These innovations represent a key motivation that moves the traditional BFCs closer to potential practical wearable

applications. After the initial demonstration of different body-worn BFCs, further efforts have been devoted to address challenges, such as electrode robustness and conformability of the device. Moving forward toward practical wearable applications, new materials and novel applications were presented during 2015 and 2016 in connection to more body conformal and versatile systems,[23-24] and eventually toward the first demonstration of an on-body self-powered biosensing in 2016.[27] In 2017, the first high-power (mW range) island-bridge stretchable sweat BFC was demonstrated,[28] and more recently, integrated microfluidic systems have been evaluated toward high-performance sweat BFCs.[29] These flow-through fluidic BFC configurations offer great promise for maintaining a fresh fuel "supply" and hence preventing decrease in the power density. Such progress in wearable BFCs is summarized in the timeline shown in Figure 1.1C.

1.3 Meeting the Material Challenges of Wearable Biofuel Cells

1.3.1 Mechanically Durable and Stretchable Materials for Biofuel Cells

Traditional BFCs are rigid, planar, and nonstretchable devices. However, the multiplexed movements of our body and direct contact of the wearable BFC with different nonplanar soft areas of the skin create major material demands for mechanical resilient,

lightweight, soft, and stretchable wearable energy-harvesting devices. Stretchable devices have recently received a tremendous attention in personalized bioelectronics.[11, 64] The realization of flexible and stretchable BFCs requires functional stress-enduring material and rational device structures (e.g., serpentines). The substrates for many stretchable electrodes are mainly textiles and elastomeric polymers with intrinsic stretchability. A variety of stretchable polymers, such as polydimethylsiloxane (PDMS),[65] polyurethane,[24] Ecoflex (silicone rubber),[24] and styrene–(ethylene–butylene)–styrene (SEBS),[66] can serve as the underlying platforms for stretchable bioelectronics. For example, an elastomeric thin film, based on Ecoflex and PU, was introduced as a stretchable underlying base material for fabricating temporary-tattoo BFCs (Figure 1.2A).[24] It is important to note the importance of maintaining a small gap between the tattoo and skin for improving the biofluid flow over the enzyme reagent layer and avoiding detachment of the BFC due to the built up pressure.[21] This skin-worn all screen printed BFC relied on a stress-enduring CNT-based material ink formulated to offer the desirable stretchability. Key for realizing this stretchable BFC is the combination of the attractive electrochemical and mechanical properties of CNTs with the intrinsic stretchability of a polyurethane binder, along with a free-standing serpentine electrode structure. Such coupling of stress-enduring materials and serpentine structures offers two degrees of stretchablity and device stretchability up to 500%.

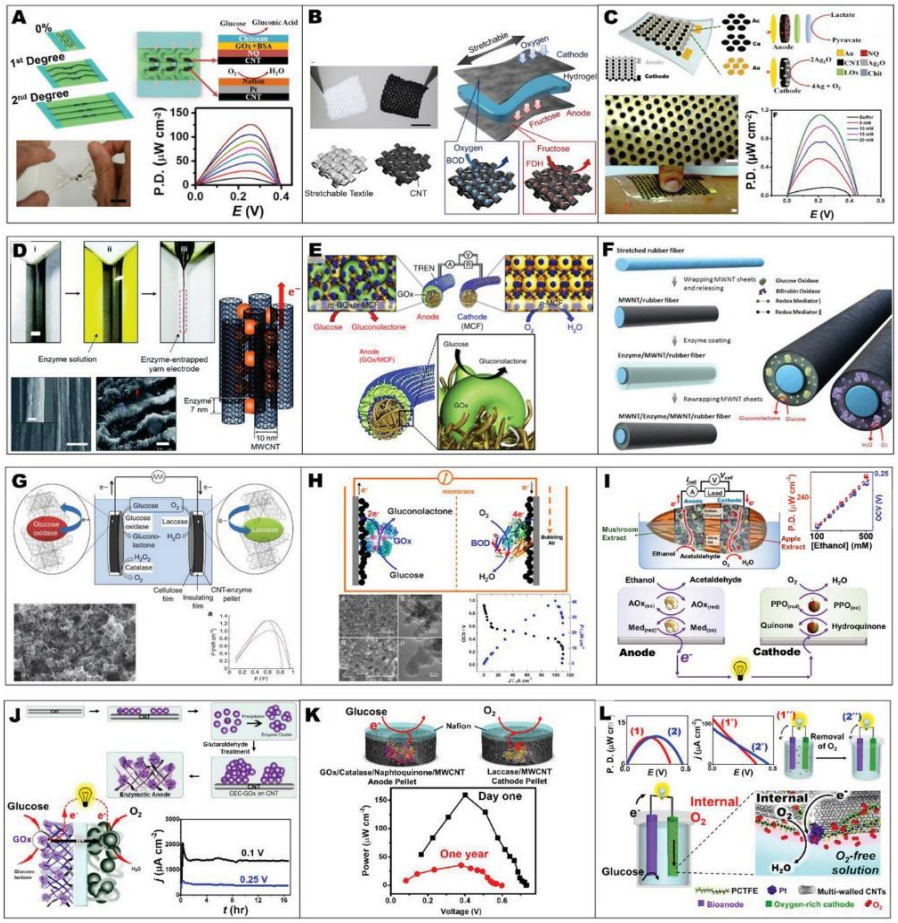

Figure 1.2 Material aspects to address challenges in BFCs. Stretchable materials: A) Highly stretchable CNT-based glucose/oxygen BFCs, combining intrinsic and design-induced stretchability. Adapted with permission.[24] Copyright 2016, American Chemical Society. B) Fructose/oxygen BFCs with enzyme-modified conductive CNT-based textiles. Adapted with permission.[67] Copyright 2015, Elsevier. C) Island-bridge high power density electronic skin-based lactate/Ag_2O BFCs. Adapted with permission.[28] Copyright 2017, The Royal Society of Chemistry. Materials for fiber-based BFCs: D) Mediator-free CNT yarn glucose/oxygen BFCs. Adapted with permission.[68] Copyright 2016, The Royal Society of Chemistry. E) Glucose/oxygen BFCs based on metallic cotton fibers. Adapted with permission.[69] Copyright 2018, Nature Publishing Group. F) Stretchable fiber glucose/oxygen BFCs, fabricated by rewrapping CNT sheets. Adapted with permission.[70] Copyright 2018, American Chemical Society. Alternative approaches for eliminating chemical mediators: G) Mediatorless high-power glucose/oxygen BFCs based on compressed CNT-enzyme electrodes. Adapted with permission.[46] Copyright 2011, Nature Publishing Group. H) Mediatorless and direct electron transfer type glucose/oxygen BFCs based on carbon nanodots. Adapted with permission.[71] Copyright 2015, American Chemical Society. I) Ethanol/oxygen BFCs based on highly biocompatible and fully edible materials without external mediators. Adapted with permission.[72] Copyright 2018, The Royal Society of Chemistry. Strategies to mitigate the effects of changing environmental conditions: J) Miniaturized glucose/oxygen BFCs with improved stability under continuous operation. Adapted with permission.[73] Copyright 2006, Wiley-VCH. K) One-year stability study for a glucose/oxygen BFCs combined with pH reactivation of the laccase/CNT biocathode. Adapted with permission.[74] Copyright 2015, Elsevier. L) Enzymatic glucose/oxygen BFCs, employing oxygen-rich cathodes for operation under oxygen-deficit conditions. Adapted with permission.[75] Copyright 2018, Elsevier.

A stretchable nylon/polyurethane-based textile has been used as a support for a textile-based fructose-dehydrogenase bioanode and a gas-diffusion BOx biocathode (Figure 1.2B).[67] The stretchable fabric was coated by CNTs (dispersed in sodium deoxycholate or Triton X-100), toward a highly conductive CNT-modified textile with conductivity up to 200 mS cm^{-1}. This textile-based anode employed the fructose fuel, stored in a double-network hydrogel sheet, placed in between the anode and the cathode, with the fructose oxidation carried out on the anode, along with oxygen reduction reaction (ORR) process at the cathode. The stretchable BFC offered a power of ≈0.2 mW cm^{-2} and was stable for 30 cycles of 50% stretching.

Further efforts have been made to increase the power density of stretchable BFC by enhancing the loading of the immobilized enzyme, mediator, and the conductive base via packing as bioanode pellets. In this approach, the enzyme and mediator are part of the electrode composition, being distributed in a 3D structure, as opposed to the superficial coverage obtained by drop casting. In addition, the performance is optimized by maximizing the loading of active species within the 3D pellets (Figure 1.2C).[28] The mechanical resiliency has been realized through stretchable island-bridge structures, integrating these highly-packed rigid pellet islands with stretchable serpentine bridges. The resulting lactate oxidase (LOx)-based island-bridge BFC displayed a high power density up to 1.2 mW cm^{-2} using sweat lactate fuel to power electronics, with the assistance of DC/DC converter, including light-emitting diode and a Bluetooth Low Energy radio.

1.3.2 Yarn-Based and Textile-Based Materials for Wearable Biofuel Cells

Electronic yarns and textiles represent very promising platforms for wearable devices but require attention to several material challenges. Textile and yarn-based electronic-textiles (E-textiles), capable of performing electronic functions, present large geometric area for integrating body-compliant bioelectronic devices.[76] Such garment-based E-textiles have already demonstrated considerable promise for diverse wearable bioelectronic applications. Early efforts have relied on integrating conformal electrodes onto textiles by applying screen-printing technology[27, 66] or by depositing conducting materials on nonconductive textiles.[67, 77] Yet, E-textiles based on electrically conductive yarns or fibers, in which electrical signals are transmitted through a garment, have attracted a considerable recent attention toward the preparation of on-body bioelectronic devices, owing to their direct integration with normal clothing.[78]

One of the main challenges for textile-based wearable electronics is the washability. High performance E-textiles should endure repeated washing cycles while maintaining their attractive properties. Due to the increasing interest in textile-based wearable, several recent studies described washing resistant E-textiles.[79] Some approaches rely on the use of modified conductive yarns, which are intrinsically robust, or printing protocols with modified inks, such as CNT-based inks, containing ionic liquid and gel-based nanoparticles.[80] However, developing washable BFCs remains a major challenge.

Additional challenge for such yarn-based bioelectronic systems is the fabrication of continuous, robust, and weavable conductive yarn. Carbon nanomaterial sheets are attractive to serve as host materials for entrapping enzymes owing to their high electrical conductivity and electrochemical properties. In addition to the preparation of underlying conductive yarns, the immobilization of enzyme and active moieties onto small materials in a linear shape is another major issue. For example, multiwalled CNT (MWCNT) sheets with vertically aligned structure, were coated with poly(3,4-ethylenedioxythiophene) (PEDOT), and served for supporting the enzyme immobilization (Figure 1.2D).[68] The fabrication of enzyme-loaded PEDOT/MWCNT self-assembled yarn electrodes relied on the contraction between the enzyme and MWCNTs caused by surface tension in the drying enzyme solution. Advantageously, hydrophobic interactions between MWCNTs offered stable yarn electrode with a small diameter of 28 μm. Importantly, this enzyme-entrapped material displayed direct electron transfer between GOx and aligned multiwalled CNTs. The resulting GOx/BOx yarn BFC thus exhibited a maximum of 236 μW cm^{-2} and an open circuit voltage (OCV) of 0.61 V in 30×10^{-3} M glucose solution, without any mediators or cross-linkers.

Nobel metals represent another group of conducting materials that support the fabrication of conductive yarns. AuNPs could be assembled layer-by-layer with small organic linkers onto cotton fibers to form metallic cotton fibers with high conductivity (2.1×10^4 S cm^{-1}) (Figure 1.2E).[69] These metallic cotton fibers can act as underlying base material for efficient electrical communication with an oxidase enzyme on the anode. In addition, such fibers with AuNPs could also act as an enzyme-free electrocatalytic cathode

for ORR. This approach enables layer-by-layer assembled GOx-coated anode to fabricate the glucose/oxygen BFC with boosted DET between the oxidase enzyme and the conductive fibers. This yarn BFC resulted a power density of 3.7 mW cm^{-2}.

Additional efforts have been made to impart stretchability to yarn-based BFC by employing rewrapping MWCNT sheets on the rubber fiber (Figure 1.2F).[70] The MWCNT sheet-wrapped rubber fiber was an underlying electrode for immobilizing an enzyme, Os-based redox polymeric mediators, and a cross-linker. Then, the active biocatalytic layer-coated electrode was wrapped again with MWCNT sheets. Trapping the enzyme between CNT sheets, forming a fiber of ≈380 μm, could stabilize the BFC and retain the power density when applying external stretching. The anode relied on GOx mediated oxidation, while the cathode used a BOx mediated ORR process. The fiber-based BFC could endure up to 100% stretching strain while generating maintainable electrical power. After 1000 stretch–release cycles, the power density of BFC fiber declined by only 5% from the initial ≈40 μW cm^{-2} power density.

1.3.3 Achieving Efficient Electrical Communications in Wearable Bioelectrodes: While Eliminating Redox Mediators

As we discussed earlier, enzymatic BFCs commonly require a redox mediator to facilitate operative electro-communication between the enzyme redox center and the

electrode surface. However, the MET approach may be limited, particularly for continuous wearable applications, due to potential toxicity of some redox mediators, and related leaking and stability issues. In addition to MET-based BFCs, in which redox species are employed to shuttle electrons to/from the electrode surface, DET-based BFCs offer another attractive yet challenging alternative. Several papers and reviews have described various strategies to realize DET-type bioelectrocatalysis between enzymes and nonwearable electrodes without the use of mediators.[50, 71, 81-83] Unfortunately, only few enzymes are capable of nonmediated direct electron transfer with the supporting electrode. This mediatorless strategy thus often requires nanomaterials that can induce the enzyme to communicate directly with the electrode surface. Conductive carbon nanomaterials are outstanding candidates for supporting enzymatic wiring for both MET and DET. For example, GOx and laccase could be compressed in CNT disks by hydraulic compression, allowing DET-based anode and cathode, respectively, as illustrated in Figure 1.2G.[46] Remarkably, this DET displayed an OCV in agreement with the redox potentials of the respective enzymes, and enhanced current outputs for glucose oxidation and oxygen reduction. This concept of the mediatorless packed BFC has resulted with a power density up to 1.3 mW cm^{-2} and an optimum OCV of 0.95 V.

Carbon nanodots (CNDs) have been demonstrated to promote DET reactions of GOx and BOx (Figure 1.2H).[71] The GOx-immobilized CND anode showed a high rate constant (ks) of 6.28 s^{-1}. In addition, the BOx-immobilized CND cathode displayed an efficient ORR catalytic property at the onset potential of +0.51 V (vs Ag/AgCl). The assembled mediator-free glucose/air BFC, based on the modification of spherical carbon

nanostructures (50–60 nm), generated an OCV as high as 0.93 V and a maximum power density of 40.8 μW cm^{-2} at 0.41 V.

Mainstream BFCs utilize mediated biocatalytic reactions of the pure enzyme in connection to common solid (metal or carbon) electrode materials. Alternately, the biocatalytic reactions of enzyme-rich plant tissues can be used for creating "green" BFC biocatalytic reactions, analogous to tissue-based electrochemical sensors.[72, 84] Highly biocompatible "green" BFCs, utilizing natural and edible processed food materials, were demonstrated recently (Figure 1.2I).[72] Such edible BFCs device relied on paste bioelectrodes containing various sources of natural plant/mushroom extract, along with a vegetable oil binder and a conductive dietary charcoal paste. The resulting anode and the cathode paste materials utilized natural biocatalysts found in mushroom, apple, plum, and banana plant tissues, for fabricating ethanol/air BFCs without using toxic mediators or a membrane. This strategy utilized the natural availability of biocatalytically-rich systems, allowing the oxidation of ethanol on the anode and the ORR on the cathode (e.g., via mushroom-based and apple-based biocatalytic electrodes, respectively). Such BFCs, based on fully edible materials, displayed a power density up to ≈280 μW cm^{-2} with an OCV of 0.24 V. Moreover, the power and OCV signals were proportional to ethanol levels, indicating great promise for self-powered alcohol sensing.

1.3.4 Uncontrolled Conditions Affecting Wearable Biofuel Cells

The susceptibility of enzymatic BFCs toward a variety of environmental conditions expected in real-life scenarios represents another challenge for energy-harvesting wearable devices, and has stimulated efforts to develop new strategies aimed for stabilizing the biocatalytic activity and hence the BFC performance. Long-term and operational stabilities become particular concerns in wearable applications. Several strategies to stabilize enzymes[85-91] suggest potential solutions toward prolonged operation of wearable enzymatic BFCs. These include engineering of amino acid sequence, introducing additional covalent and noncovalent attachments of enzymes to an external matrix, or protecting the electrode with antibiofouling coatings. These all aim at maintaining the catalytic activity of enzymes, particularly under operational conditions.

An example of maintaining GOx activity in operating conditions was demonstrated by Fischback et al. who attached cross-linked enzyme clusters onto the surface of CNT materials (Figure 1.2J).[73] The crosslinked enzyme clusters were formed by ammonium sulfate-induced precipitation in the mixture of covalently-attached GOx and excess GOx enzymes, near the CNTs. Additionally, glutaraldehyde was used to crosslink these enzyme cluster precipitates, therefore forming stable cross-linked biocatalyst clusters on the CNT surface. This enabled stable enzyme/CNT composites for the BFC bioanode. Such immobilization strategy could extend the BFC lifetime as the performance was stabilized in unbuffered fuel solution.

Another approach to improve and extend the BFC performance relies on the compression fabrication of carbon nanomaterial-based pellets. For example, a pellet-based glucose/oxygen BFC was demonstrated, with the anode and the cathode prepared by soft grinding of the active and conducting MWCNTs and subsequent compression (Figure 1.2K).[74] The anode composed of 1,4-naphthoquinone (NQ), GOx, catalase, and MWCNTs, while the cathode employed ORR biocatalytic laccase. Nafion was also drop-coated on the pellet surface. The resulting BFC maintained 22% of its initial maximum power after one year. Note that, at neutral pH, the laccase activity can be inhibited by the presence of hydroxide ion. Therefore, the cathode displayed maximum current densities of 0.24 and 0.06 mA cm^{-2} at pH 5 and 7, respectively (at 0.2 V vs SCE). However, the pellet biocathode could be reversibly reactivated via immersion in phosphate buffer (pH 5). The pH reactivation could maintain the OCV of the biocathode after each discharge. The operation of this BFC in air-saturated phosphate buffer (pH 7) containing 5×10^{-3} M glucose at 37 °C exhibited a maximum power of 160 μW cm^{-2} with an OCV of 0.75 V. This enzyme-entrapping strategy offers also a compressed CNT network for the wiring and provides high enzyme loading, leading to a prolonged BFC energy harvesting.

Oxygen deficiency and fluctuations can also compromise the performance of wearable BFCs, particularly in anaerobic or oxygen fluctuating situations.[75, 92-94] The power performance of metabolite/oxygen BFC (e.g., glucose/oxygen BFC) strongly relies on the oxygen level acting as the cathode fuel. Oxygen can also cause a secondary competing reaction at the anode. As a result, fluctuating oxygen level can negatively affect the BFC output. A recent approach to address this challenge involved the use of oxygen-

rich bioanode and cathode, i.e., a built-in internal oxygen supply (Figure 1.2L).[75] Such oxygen-rich electrodes have been realized using the fluorocarbon polychlorotrifluoroethylene as the binding material of the carbon-paste anode and cathode.[75] While the bioanode utilized the GOx-mediated reaction, the oxygen-rich cathode provided internal oxygen supply toward its platinized carbon materials. This approach holds promise for the development of efficient energy-harvesting and self-powered devices operating in oxygen-deficit and oxygen-fluctuating conditions. The use of oxygen-insensitive dehydrogenase enzymes, which is common in traditional BFCs, requires a challenging coimmobilization of the NAD^+ cofactor, which is usually complex for wearable BFCs and can lead to unstable devices.

1.3.5 Operation of Biofuel Cells in Different Biofluids

The tremendous progress related to advanced materials used for wearable BFCs has led to successful and diverse applications of these systems for harvesting energy from different biofluids such as sweat, saliva, tears, and interstitial fluid (ISF).

Human sweat is an attractive biofluid for harvesting energy owing to its high concentrations (millimolar) of metabolites, such as lactate and urea, and broad distribution of sweat glands around our body. In addition, sweat can also provide a constant flow for replenishing the substance at the BFC site.[95] However, a major drawback of sweat BFCs is the need of exercising for sweat generation. This issue may be addressed by local sweat stimulation using iontophoresis, at the cost of additional complexity. Saliva, on the other

hand, is an easily-accessible biofluid rich in metabolites but characterized with high viscosity that may impair the electron transfer. In addition, in mouth oral devices may be subject to safety issues. Tears sampling is a common challenge for ocular wearable devices; usually, the amount of produced tear is very small and if increased, it may dilute the fuel concentrations and decrease the BFC power efficiency. Sterilization after use (using disinfecting solutions) may limit the utility of tear BFCs. The cleaning process represents a barrier for repeated use of the same lenses, forcing their application as single-use disposable devices. Recent efforts have focused on ISF-based wearable devices, owing in part to the correlation of the level of ISF molecules with their blood concentration. The main disadvantage of ISF BFCs is the limited accessibility and volume of this biofluid. ISF devices require the use of microneedles or reversed iontophoretic patches. Despite the various challenges, the above biofluids contain a wide variety of metabolites, which can be utilized as potential fuels for on-body bioenergy harvesting.

Sweat produced during intense physical activity contains high lactate concentration (as high as 50×10^{-3} M);[95] hence, wearable sweat BFCs usually use lactate as fuel. Our group has demonstrated the first example of an epidermal tattoo lactate BFC for harvesting energy from sweat during exercise activity.[21] The tattoo was designed with a cathode and an anode using the letters "UC," acronym for "University of California" (Figure 1.3Aa). Screen-printing technology was used to print carbon ink onto a temporary tattoo paper. The letter "U" (anode) was modified with LOx, CNT, and tetrathiafulvalene (TTF), as a mediator, to promote electron shuttling between the enzyme and the LOx active site. The letter "C," serving as cathode, employed platinum black, catalyst for oxygen reduction, on

the printed carbon surface (Figure 1.3Aa). The exposed area was 6 mm^2 for the bioanode and 12 mm^2 for the cathode. The tattoo BFC was tested on-body during exercise activity, resulting in a power density varying from ≈5–70 μW cm^{-2}, depending on the persons fitness level (Figure 1.3Aa). Unlike implantable devices, such low-cost printed tattoo BFCs can be discarded following short operations. Prof. Joseph Wang's team also reported, recently, on a high-power density LOx/Ag_2O wearable BFC with an OCV of 0.5 V and a power density of nearly 1.2 mW cm^{-2} at 0.2 V.[28] (Figure 1.3Ab) The perspiration-based BFC system, briefly discussed in the previous sections, consisted of an array of pellet island electrodes, coupled with a gold bridge serpentine structures to impart stretchability. The anode comprised the islands and was composed of highly packed 3D CNT-NQ bounded by chitosan biopolymer. After packing, the enzyme LOx was drop casted on the pellet anode islands. The cathode consisted in compact 3D CNT-Ag_2O structures, firmly held by the water-insoluble Nafion polymer. The system was able to generate 1.2 mW during exercise on the human skin. The use of Ag_2O cathodes can mitigate the natural oxygen fluctuations, improving the BFC performance; on the other hand, Ag_2O is consumed during the BFC operation, affecting the operational stability of the system. Previously reported Ag_2O cathodes had an operational time of ≈6 h with high power output;[93] an on-body operation of 50 min was reported.[27]

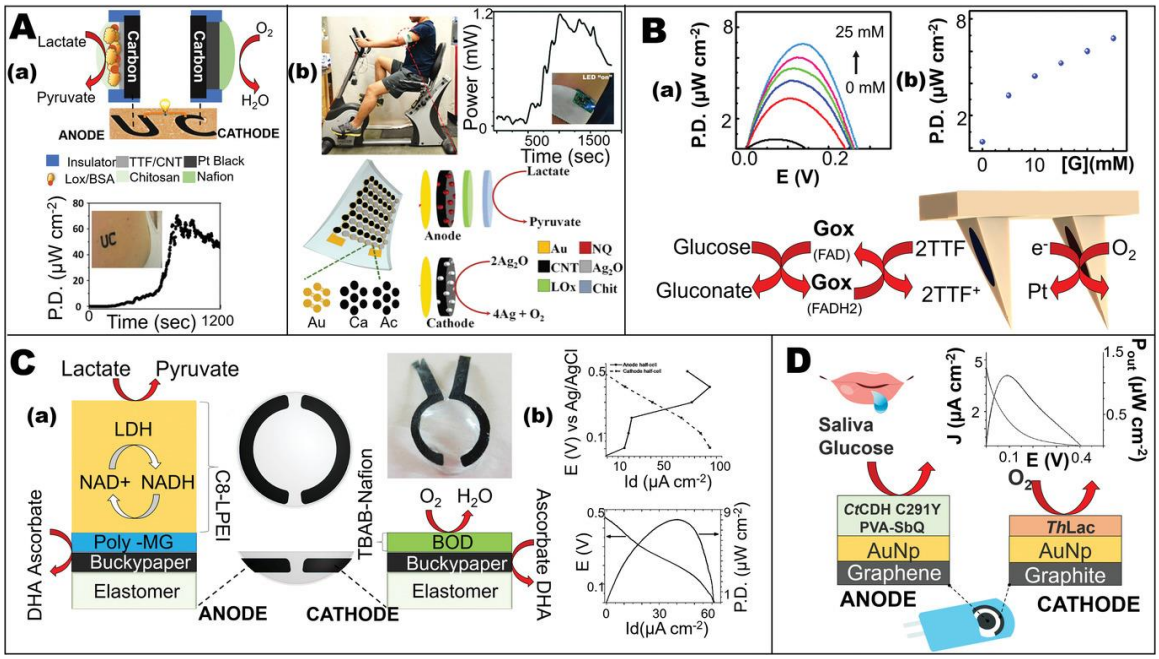

Figure 1.3 BFCs operating in different biofluids. Images and schematics illustrating: A) Epidermal sweat lactate BFC a); tattoo-based LOx/Pt BFC schematic using sweat lactate as fuel and with respective sweat power density (PD) obtained during exercising. Adapted with permission.[21] Copyright 2013, American Chemical Society. b) Soft and stretchable island-bridge LOx/Ag_2O BFC placed on a volunteer's arm, followed by the power density obtained during exercising and respective BFC schematic. Adapted with permission.[28] Copyright 2013, Wiley-VCH. B) Microneedle-based ISF BFC using glucose ISF as fuel and respective power curves obtained in artificial ISF for several glucose concentration. Schematic showing the anode enzymatic reaction and the platinum reduction process in the cathode. Adapted with permission.[22] Copyright 2014, Elsevier. C) Contact-lens based BFC using tears lactate as fuel. Contact lens with integrated cathode and anode; cathode and anode characterization with respective power curve in artificial tears. Adapted with permission.[96] Copyright 2015, Elsevier. D) Screen-printed electrode for saliva-based BFC using salivary glucose as fuel with power curves obtained in saliva. Adapted with permission.[97] Copyright 2018, Elsevier.

Following the work on epidermal BFC,[21, 28, 98] several research groups have demonstrated BFCs for harnessing bioenergy from sweat using different fuels. Sweat glucose was often explored as energy harvesting source. In 2014, Falk et al.[99] demonstrated a miniature mediator-less enzymatic BFC using gold microwires modified with AuNPs and immobilized cellobiose dehydrogenase as anode, in combination with a BOx cathode, operating in human sweat with a power density of 0.26 μW cm^{-2}; such low power density reflected the very low sweat glucose concentration. In contrast, the

glucose levels in ISF are considerable higher, displaying close correlation to blood glucose concentrations[100] and hence ISF BFCs commonly use glucose as fuel. Our group demonstrated the first example of a minimally-invasive glucose/O_2 microneedle BFC based on a carbon-paste bioanode and cathode, packed into a hollow microneedle array (Figure 1.3B).[22] The bioanode consisted of a carbon paste mixed with the enzyme GOx and the TTF mediator, while the microneedle cathode consisted of a carbon paste mixed with Pt black nanoparticles. The BFC system was tested in the normal, hyperglycemia, and hypoglycemia levels using artificial ISF, and indicated considerable promise for self-powered biosensing, with a maximum response of 7 μWcm^{-2} observed at 25 × 10^{-3} M glucose (Figure 1.3B). An iontophoresis-based BFC, extracting power from iontophoresis extracts, was demonstrated by Toit et al.[101] The system generated power from glucose-spiked iontophoresis extracts, obtained from pig skin, using a system of three glucose/oxygen BFCs embedded into a fluidic device. The bioanode consisted of highly-porous gold electrodes, modified electrostatically with GOx; laccase was similarly immobilized onto the porous gold cathode. Peak values of 0.7 mW were obtained in a flow-through mode, while a power of 0.4 mW was generated in a batch mode using 27 × 10^{-3} M glucose.

BFC operating successfully in lacrimal fluid and saliva have also been demonstrated. Reid et al. demonstrated a BFC system mounted on contact lens that relied on a tears lactate fuel (Figure 1.3C).[96] The tears BFC was realized by integrating buckypaper electrodes and silicon-based contact lens. Lactate dehydrogenase (LDH) and NAD^+ were used to functionalize the anode, while the cathode was functionalized with 1-

pyrenemethyl anthracene-2-carboxylate and BOx (Figure 1.3Ca). Using artificial tears, the BFC contact lens generated an OCV of 0.413 V and maximum current and power density of 61.3 μA cm^{-2} and 8.01 μW cm^{-2}, respectively (Figure 1.3Cb). Other tears metabolites, such as glucose, have also been explored for energy harvesting using the BFC. For example, Falk et al. demonstrated an enzymatic glucose/oxygen BFC, operating in basal human lachrymal liquid and generating a power density of ≈1 μW cm^{-2} along with more than 20 h operational half-life.[25] These efforts represent useful steps toward realizing ocular devices with a built-in power supply.

The operating ability of a glucose/oxygen BFC was also demonstrated in real saliva samples. A screen-printed electrode was used by Bollella et al. to assemble a graphene bioanode and a graphite biocathode (Figure 1.3D).[97] AuNPs were immobilized on the anode and cathode surface. The anode was realized by immobilizing the enzyme cellobiose dehydrogenase from *Corynascus thermophilus* (CtCDH) C291Y on the AuNPs graphene surface via photopolymerization of poly(vinyl alcohol) N-methyl-4(4′-formylstyryl)pyridinium methosulfate acetal (PVA-SbQ), while the cathode was prepared by immobilizing *Trametes hirsuta* laccase on the graphite/AuNPs surface in order to reduce the overpotential of the enzymatic O_2/H_2O redox reaction (Figure 1.3D). The BFC strip generated a maximal power output of 1.57 and 1.10 μW cm^{-2}, with an OCV of 0.58 and 0.41 V in a 100 × 10^{-3} M glucose solution and in human saliva, respectively (Figure 1.3D). Salivary BFCs have also been demonstrated by Conghaile et al.[102] A graphite electrode was modified with a mixture of pyranose dehydrogenase, an osmium redox polymer as mediator, along with CNT, with glutaraldehyde crosslinking with the drop

casted mixture. The bioanode was prepared by modifying gold electrodes with a dispersion of BOx and AuNPs. When tested in unstimulated human saliva, a maximum power density of 6 μW cm^{-2} was obtained.

1.4 Self-Powered Biosensors

BFCs can act as self-powered electrochemical biosensors because they can simultaneously provide a viable power source and biosensing signals, and since their power output is commonly proportional to the concentration of metabolites that operate these devices.[4, 18] The simple system that allows a BFC to act as a self-powered biosensor requires the anode and/or a cathode to convert the chemical fuels (such as glucose target analyte) into electricity with a well-defined power-concentration relationship (often a good linear dependence). For instance, as was shown earlier in Figure 1.1A, the self-powered quantification of glucose can be achieved by the generated current (via glucose oxidation), while the ORR on the cathode is not a limiting factor, i.e., relying on the substrate (analyte) level. The higher the glucose level, the higher the electrical output. Additional approaches could also be applied.[18-19] Some examples include the inhibition-based sensing route commonly applied for detecting toxic substances that inhibit the enzyme activity on the BFC electrodes[103] and the hindering-based approach that contains the biorecognition layer to bind the target analyte.[104-105] Advantageous, this unique capability of self-powered biosensors based on BFCs significantly simplifies the integrated biosensor system, particular for wearable devices which prefer simplicity and self-sustainability. Such self-

powered sensing devices thus allows a simplified two-electrode cell without externally applied potentials to operate and are powered by biological fluids and hence they are ideal as wearable sensors. In 2001, Katz et al. demonstrated the concept of self-powered enzyme-based biosensors by using glucose or lactate analyte as biofuels on the anodes.[106] The BFC consisted of pyrroloquinolino quinone (PQQ)-flavin adenine dinucleotide (FAD)/GOx-functionalized anode and an ORR-based cytochrome c/cytochrome oxidase (Cyt c/COx)-functionalized cathode. In addition to glucose/oxygen BFC, the other BFC, consisting of PQQ- NAD+/ LDH-functionalized anode and the same configuration of the cathode, was used for lactate sensing. These systems could thus sense glucose or lactate by reading the OCV, which corresponds to their metabolite levels.

Smart textiles can be seamlessly integrated with human skin toward diverse applications.[76, 78, 107] By leveraging BFCs, Jeerapan et al. reported on the first textile-based self-powered textile biosensors (Figure 1.4A).[27] Glucose and lactate BFCs, with single-enzyme and membraneless formations, were thus fabricated on stretchable printed electrodes. The success behind stretchability relied on intrinsic properties of custom-made stress-enduring materials and serpentine patterns, screen printed onto the textile substrates. These glucose and lactate BFCs generated the maximum power density of 160 and 250 $\mu W\ cm^{-2}$ with the OCVs of 0.44 and 0.46 V, respectively. These self-generated signals (obtained without any applied potential) were proportional to sweat glucose or lactate fuel concentrations, and were highly selective to the target fuel analyte in the presence of relevant electroactive sweat constituents. In addition to high specificity of enzymatic characteristic, the attractive advantage to minimize analytical interference effects is also

since no additional external potential is applied to the sensor, decreasing the interfering signal from coexisting electroactive species. The device integrated with a sock was coupled with a compact wireless device for recording in real-time the lactate signal on a smartphone. The on-body demonstration confirmed the feasibility of using the textile BFC biosensors during common activities, such as biking. This first concept in wearable self-powered biosensors opens up new opportunities for self-sustainable devices when mechanical resiliency is mandatory.

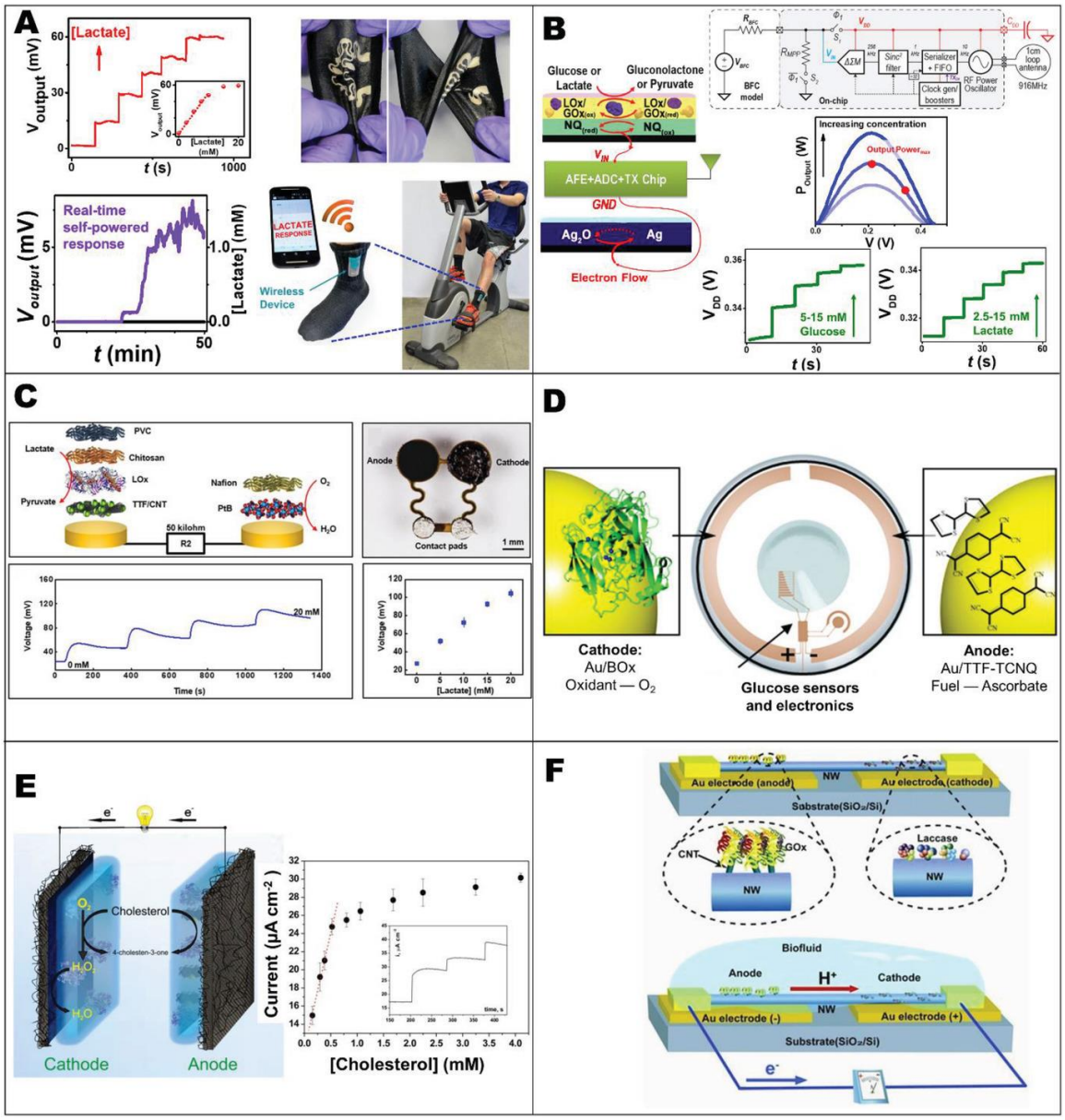

Figure 1.4 Self-powered sensors. A) Stretchable textile-based self-powered sensors. Adapted with permission.[27] Copyright 2016, The Royal Society of Chemistry. B) A 0.3 V complementary metal-oxide-semiconductor (CMOS) biofuel-cell-powered wireless glucose/lactate biosensing system. Adapted with permission.[108] Copyright 2018, IEEE. C) Skin-interfaced microfluidic/electronic systems. Adapted under the terms and conditions of the CC-BY license.[29] Copyright 2019, The Authors, published by AAAS. D) Contact lenses-based BFCs for glucose sensing. Adapted with permission.[109] Copyright 2013, American Chemical Society. E) Cholesterol self-powered biosensor. Adapted with permission. [110] Copyright 2014, American Chemical Society. F) Nanowire-based BFC for self-powered nanodevices. Adapted with permission.[111] Copyright 2010, Wiley-VCH.

The energy generated by BFCs is sufficient to power a fully integrated circuit. For example, the electronic complementary metal-oxide-semiconductor (CMOS) BFC-powered chip has been designed to utilize the BFC output voltage of 0.3 V (Figure 1.4B).[108] This technology relies on an analog-to-digital converter and a wireless 920 MHz radio frequency (RF) transmitter without any DC-DC converter. In general, previously, it should be noted that a DC-to-DC converter electronic circuit, that boosts a source of direct current (DC) from one voltage level to another (higher) one, was required. The demonstrated chip consumed a small power of 1.15 μW. The self-powered sensing model eliminated the need for complex collections of a battery, DC-DC converter, or a potentiostat.

The concept of a battery-free wireless electronic sensing has received a considerable recent attention. Continuous efforts have thus been devoted to the development of self-sustainable biosensing devices. Recently, thin, soft, skin-interfaced microfluidic platform for noninvasive sweat monitoring, based on self-powered glucose and lactate biosensors, was demonstrated by Bandodkar et al. (Figure 1.4C).[29] The lithographically-patterned microfluidic device relied on soft materials and offered an efficient interface with eccrine glands, independent of the sensor location, to minimize contamination and cross-talk in the electrochemical sensing chamber. The self-powered signals, generated by the glucose- or lactate-based BFCs, led to detection limits of 43×10^{-6} M glucose and 2.1×10^{-3} M lactate. Coupled with near-field communication (NFC), wirelessly connected to the smartphone, this soft fluidic system allowed battery-free sensors for monitoring sweat.

Noninvasive tear monitoring has also received tremendous attention in connection to self-powered sensors. For example, a miniaturized lens-based membraneless ascorbate/O_2 BFC was demonstrated by Falk et al. to serve as alternative power supply for glucose-sensing contact lenses (Figure 1.4D).[109] The BFC anode and cathode relied on a thin Au-microwire-based electrode, decorated with AuNPs. The anode employed the gold electrode functionalized with the tetrathiafulvalene 7,7,8,8-tetracyanoquinodimethane (TTF-TCNQ) complex to electrooxidize ascorbate, while the cathode relied on a BOx-based Au electrode to reduce oxygen. The BFC operated in human tears produced an OCV of 0.54 V with a maximal power of 3.1 μW cm^{-2} at 0.25 V. This harvested electricity has been proposed to power a contact lens-based glucose sensor.[112]

A self-powered cholesterol biosensor was designed by Sekretaryova et al. utilizing a single-enzyme (namely, cholesterol oxidase, ChOx) membrane-free, self-powered biosensor (Figure 1.4E).[110] The BFC was constructed on high surface-area carbon cloth electrodes, that offered enhanced sensitivity. The cholesterol oxidation anode relied on electron transfer between the ChOx active site and a phenothiazine mediator, while the cathode relied on the electrocatalytic reduction of hydrogen peroxide, generated via the ChOx biocatalytic cholesterol oxidation. Note that both the anode and cathode relied on cholesterol reactions to offer enhanced sensitivity compared to the separate counterparts. The system thus provided an analytical range from 0.15×10^{-3} to 4.1×10^{-3} M cholesterol, with a detection limit of 2.3×10^{-6} M, and offered a good correlation with the results obtained from the standard kit, confirming negligible interference effects. Koushanpour et al. described also membraneless BFC based on biocatalytic reactions of lactate on both the

anode and cathode toward sweat lactate analysis.[113] This bioelectronic system coupled the lactate oxidation via NAD-dependent LDH anode reaction and a hydrogen-peroxide reduction via hemin reaction on the LOx/hemin cathode. The OCV values obtained from this LDH/LOx BFC system minimally changed upon varying the lactate concentration over the range of 8–20 × 10^{-3} M, while the short-circuit current increased from 1.36 to 1.66 mA. Such minor effect of the lactate concentration upon the outputs suggested a limiting NADH oxidation reaction, related to the overall lactate oxidation. The BFC operating in real human sweat exhibited an OCV of 0.79 V and short-circuit current of 1 mA, and generated a maximum power of 450 μW with an external load resistance of 0.28 kΩ.

The use of only small dead-volume drop of a few microliters of bodily biofluids is one of the most interesting topics in miniaturized biosensors. An extremely small single nanowire offers the fabrication of nanowire-based BFCs. For instance, a single proton conductive Nafion/poly(vinyl pyrrolidone) polymeric nanowire (200–800 nm) was functionalized with GOx and laccase on the glucose-oxidation anodic side and the ORR cathodic side, respectively (Figure 1.4F).[111] The single-nanowire BFC can produce a net current because of the electrochemical potential difference between the anode and cathode caused by the reactions at those bioelectrodes, inducing the movement of protons in the nanowire and electrons via the external load, resulting in a power of 0.5–3 μW. This capability illustrates the feasibility of self-powered nanodevices for small volume analysis. For example, this nanowire BFC was integrated with a single nanowire-based pH sensor or glucose sensor. The nanowire-based BFC could thus drive self-powered nanodevice systems.

1.5 Designs and Potential Applications of Wearable Biofuel Cells

Innovative approaches have been directed to the design, materials, and applications of BFCs. Hybrid systems, offering diverse applications and capabilities, have been demonstrated. For example, the dissertation author and co-authors demonstrate a hybrid textile-based stretchable BFC/supercapacitor wearable system, capable of harvesting and storing energy from human sweat (Figure 1.5A).[66] Such a hybrid device was realized by screen-printing on both sides of the fabric, with the BFC on the side facing the skin for harvesting the sweat-lactate bioenergy, while the outer side was comprised of a MnO_2/carbon nanotube composite supercapacitor. The screen-printed carbon-based BFC anode was modified with LOx and NQ mediator. Silver oxide was employed as the cathode active material. The BFC demonstrated an OCV of 0.49 V and a maximum power density of 252 mW cm^{-2} at 0.28 V. The integration of energy-harvesting wearables with energy-storage devices is very attractive toward self-powered systems that store the scavenged energy simultaneously.[114] Different approaches were also demonstrated integrating such hybrid devices. Xiao et al, presented a similar approach for the integration of BFCs with MnO_2-based supercapacitors.[115] Such device was composed of a nanoporous gold electrode modified with glucose dehydrogenase (GDH) based anode and a solid-state nanoporous gold electrode/MnO_2 as cathode. The cathode was able to supply oxygen to the BFC system while operating as supercapacitor. The ability of recovering the discharged MnO_2 allowed fabrication of a hybrid device that withstands 50 cycles of self-recovery and

galvanostatic discharge at 0.1 mA cm^{-2} over a period of 25 h. The instantaneous power density generated by the supercapacitor was 294 times higher than the power density generated by the BFC system alone, 676 µW cm^{-2} versus 2.3 µW cm^{-2} (OCV of 0.21 V) of the BFC. Another approach was also explored by Chen et al. in 2019.[116] It involves a stretchable and flexible lactate/O_2 BFC, fabricated using flexible buckypaper, and mounted on a screen-printed island/bridge configuration. The buckypaper was developed by crosslinking of MWCNTs with polynorbornene linear polymers comprising of pyrene groups. Squared flexible buckypaper island electrodes (3 mm × 3 mm) were modified with NQ and LOx to function as the anode while rectangular electrodes (3 × 6 mm) were modified with protoporphyrin IX and BOx to function as cathode and supercapacitor. The supercapacitor performance was evaluated and a maximum power density of 6.5 mW cm^{-2} at 20 mA cm^{-2} was achieved. The power density delivered by the supercapacitor pulse mode was 13 times higher than the BFC mode (for BFC the power density was 520 µW cm^{-2} with an OCV 0.74 V).

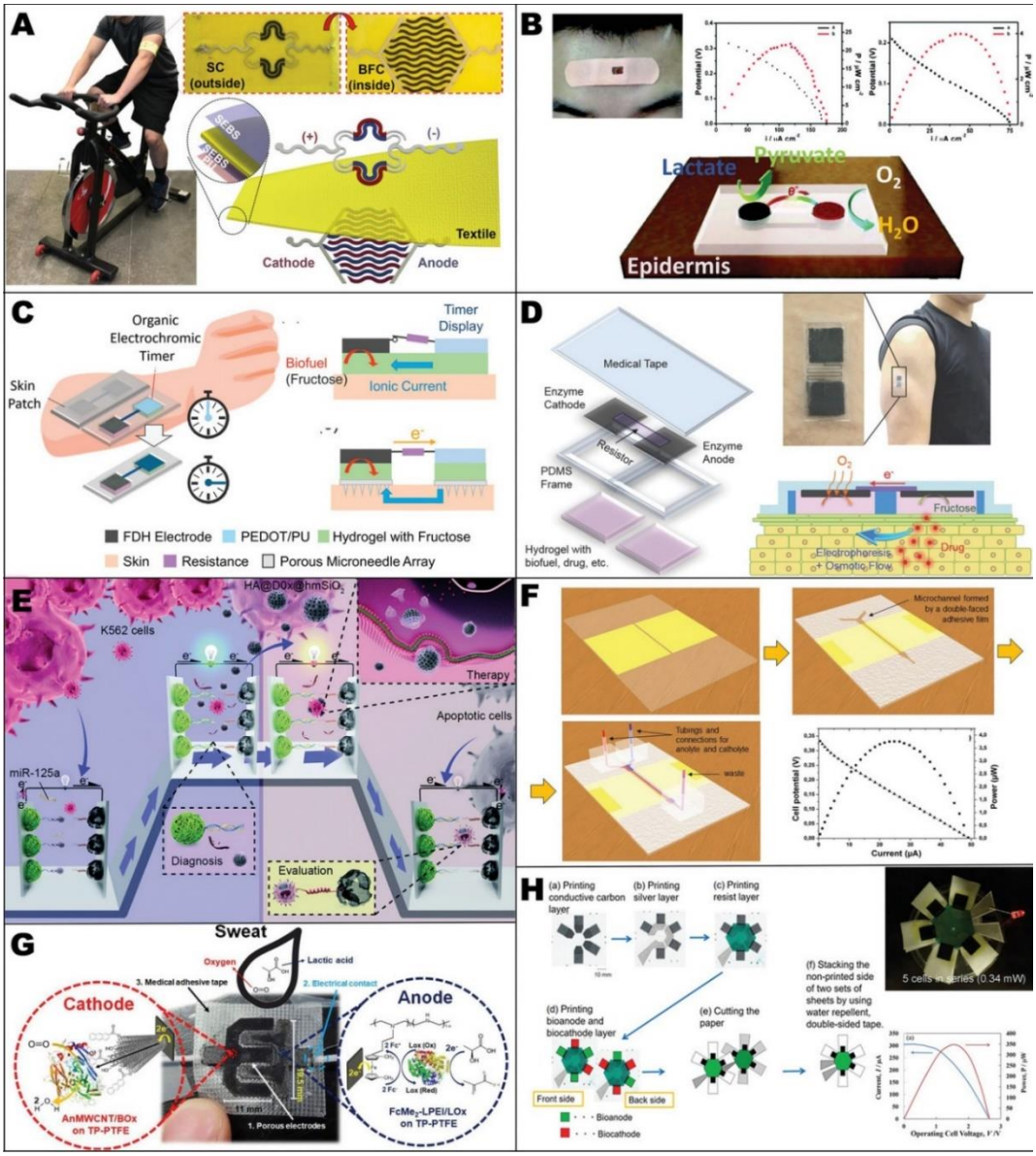

Figure 1.5 Examples of BFCs designs and potential wearable applications: A) Hydrid BFC and supercapacitor on a textile-based platform for harvesting bioenergy from sweat lactate and storing it in the supercapacitor. Adapted with permission.[66] Copyright 2018, The Royal Society of Chemistry. B) Hybrid photoelectric BFC for the simultaneous measurement of illumination and sweat lactate levels. Adapted with permission.[117] Copyright 2017, The Royal Society of Chemistry. C) Wearable flexible colorimetric timer based on hybrid electrochromic BFC. Adapted with permission. Copyright 2019, Elsevier. D) Transdermal iontophoresis patch with built-in BFC for independent drug delivery. Adapted with permission.[23] Copyright 2015, Wiley-VCH. E) Self-powered glucose sensor coupled with drug delivery and treatment evaluation system for cancer detection and treatment. Adapted with permission.[118] Copyright 2018, The Royal Society of Chemistry. F) Microfluidic BFC system for using catholytic and anolytic solution in a single channel. Adapted with permission.[119] Copyright 2015, Springer. G) Wearable flexible Toray carbon paper-based BFC using sweat lactate as fuel. Adapted with permission.[120] Copyright 2019, Elsevier. H) Cost-effective paper-based BFC for disposable BFCs. Adapted with permission.[121] Copyright 2017, Elsevier.

Other hybrid systems have also been demonstrated by Yu et al. They introduced the first example of the self-powered wearable photoelectric BFC for detecting simultaneously sweat lactate and ambient light.[117] The bioanode was prepared by immobilizing LOx into a Meldola's-blue-modified buckypaper, while the cathode was modified by electrodeposition of the organic semiconductor polyterthiophene film on an indium tin oxide (ITO)-polyethylene terephthalate (PET) electrode (Figure 1.5B). The electrons generated in the photocathode under illumination were used to drive the reduction reaction on the cathode. The simultaneous detection of illumination and lactate was carried out by monitoring the BFC open circuit potential, that increases with the light intensity, and the short-circuit current, which was directly proportional to the sweat lactate levels. The maximum power density of the BFC under xenon lamp (visible light) approached 22 $\mu W\ cm^{-2}$ and the maximum power density of the BFC under LED light was 3.99 $\mu W\ cm^{-2}$.

Kai et al. demonstrated recently, a versatile wearable timer hybrid electrochromic BFC, where the cathode consisted of PEDOT and polyurethane composite electrochromic film while the carbon electrode anode modified with fructose dehydrogenase (FDH) and hydrogel containing the fructose fuel (Figure 1.5C).[122] The electrochromic BFC display indicated the elapsed time since the application of the patch by monitoring gradual changes in the color intensity of the PEDOT/polyurethane cathode. Such color changes reflect the current generated by the BFC redox reaction. This electrochromic BFC timer can be used to indicate the right time to replace the integrated wearable sensor, a drug delivery system, or wound healing device.

The combination of BFCs with other systems allows synergetic applications. For example, Ogawa et al. demonstrated the first example of an iontophoretic patch with a built-in BFC, consisting of a fructose dehydrogenase (FHD)-modified carbon fabric anode and a BOx-modified carbon-fiber based cathode electrode (Figure 1.5D).[23] The fructose fuel was loaded in the iontophoretic gel along with the drug to be delivered. The hydrogels were placed in a PDMS frame while a conducting polymer served as an internal resistor. The current generated by the fructose BFC was thus used for delivering the drug. The BFC generated an open circuit of 0.75 V and a current density of ≈300 μA cm^{-2}, using a pig skin, with an operational stability of 6 h. Combining BFCs with innovative systems was used by Amir et al. for computational operations using logic gates.[123] Such application represents the first example of a BFC controlled by biochemical reactions toward on-demand power delivery.[19] The system consisted of an enzyme-based BFC with a pH-switchable cathode. The cathode was composed of a laccase enzyme immobilized on an ITO electrode modified with a pH-sensitive redox polymer, capable of switching between redox active and inactive states upon pH changes provoked by the enzymatic reaction; such changes in the polymer state were thus responsible for switching the BFC power ON (active polymer) and OFF (inactive polymer) by allowing or blocking the electron transfer, respectively.

The integration of a self-power sensor with a drug-delivery and a self-evaluation system was described recently by Wang et al. for the effective diagnostic, treatment, and treatment evaluation of cancer (Figure 1.5E).[118] The device consisted of a glucose/oxygen abiotic fuel cell with a porous gold anode and cathode composed of hollow mesoporous N-

doped carbon sphere modified with phosphatidylserine-binding peptide. The porous gold anode was modified with silica particles, loaded with anticancer drug doxorubicin which was released in the presence of circulating mRNA (a cancer biomarker). Upon releasing the drug-loaded particles from the anode surface, the power density increased, and this served as signal for positive diagnostic. After released in the medium, the drug acted on the cancer cell, producing apoptotic cells which were captured by the peptide-modified cathode and led to decreased power. Such decrease served as positive signal to confirm the effective action of the delivered drug.

Low-volume BFC systems are desired for expanding the scope of applications of wearable BFCs. The feasibility of a microfluidic BFC chip was demonstrated by Renaud et al.[119] A single fluidic channel with two inlets, in a "Y" shape, was assembled on a glass substrate with gold sputtered electrodes. Such assembly was prepared so that each gold current collector was in contact only with the side-walls of the fluidic channel (Figure 1.5F). An anolyte solution cocktail was pumped into the anode inlet while pumping the catholyte solution in the cathode inlet. Due to the low flow rate and laminar flow, there was no mixture of the fluids inside of the channel, eliminating the need for a membrane. The catholyte solution consisted of laccase and the 2,2′-azino-bis-3-ethylbenzothiazoline-6-sulfonic acid (ABTS) redox mediator, while the anolyte consisted of GOx and $Fe(CN)_6^{3-}$. The electrons involved in each redox reaction were collected by the gold electrodes on the channel's side walls. The system generated an OCP of 0.33 V with a power density of 3.75 μW. Integration of such system with wearable fluidic devices can be easily performed. A wearable fluidic system capable of sampling and measuring sweat analytes was

demonstrated by Bandodkar et al.[124] In their work, an inorganic fuel cell was used at the entrance of each collecting chamber and the OCP variations were monitored and correlated with the elapsed time on which sweat was first in contact with the system, thus allowing the time stamp for each sweat collection. Such battery-free operation allowed the unique feature of collecting sweat with a time stamp, while studying the sweat dynamics filling into the device.

Besides novel designs and integrations, the successful performance of BFCs demands the use of specific materials. Escalona-Villalpando et al. demonstrated a simple approach for fabricating wearable BFCs by using flexible Toray carbon paper (Figure 1.5G).[120] The patch-type BFC device relied on the immobilization of LOx and a redox polymer dimethylferrocene with linear polyethylenimine (FcM2-LPEI) at the anode. The cathode was modified with BOx by brushing a paste mixture of BOx with MWCNT-modified with anthracene. The resulting skin-worn BFC produced an OCV of 0.55 V and a short circuit current of 140 μA cm^{-2}.

The material choice employed in the BFC construction can affect directly the final cost of the system. Shitanda et al. demonstrated a cost-effective and disposable energy-harvesting BFC device based on five individual BFCs constructed on a paper substrate.[121] The cathode and anode were screen-printed using carbon ink onto a filter paper substrate (Figure 1.5H). The bioanode was composed of immobilized GOx and TTF while the cathode was based on the BOx enzyme. The BFC presented an OCV of 2.65 V and maximum power of 350 mW at 1.55 V, sufficient to illuminate an LED. In addition,

we also demonstrated the successful use of several low-cost disposable BFCs platforms based on textile detachable care textile labels,[98] temporary tattoos,[21, 24] and edible materials.[72]

1.6 Conclusions, Prospects, and Opportunities of On-Body Bioelectronics: Biofuel Cells for Bioenergy Harvesting and Self-Powered Biosensing

In this chapter, we highlighted the energy harvesting capabilities of wearable BFCs, along with key recent developments, future prospects, and challenges toward efficient on-body operation. Similar to traditional BFCs, the energy harvesting capability of wearable BFCs strongly depends on the electron-transfer efficiency between the enzyme active sites and the conducting electrodes and on the availability of the chemical fuel. However, unlike conventional BFCs, the development of wearable BFCs requires special attention because of the dynamic and uncontrolled body changes and conditions that can influence the behavior of enzymes, including dynamically changing biofluids and diverse outdoor activities. Meeting these challenges require further attention to the stability of wearable BFC devices through the rational design of the enzyme-electrode interface and by imparting mechanical flexibility to these systems. Wearable BFCs have been demonstrated on diverse on-body platforms and in connection to different biofluids and fuel metabolites. Despite many advances, the development of wearable BFC devices is still in its early stage

and existing devices have limited power density and stability. In the near future, we thus expect major efforts for addressing these limited power and stability issues using new approaches for faster electron transfer between enzymes and electrodes, high enzyme loadings and advanced biotechnological enzyme engineering strategies.

The research of wearable BFCs is still an incubating or emerging stage of technology. Currently, there are no mutual conventional protocols or setups for characterizing the performance of BFCs. Many factors can significantly affect the BFC behavior, including the temperature, pH, electrode size, fuel concentration, and electrochemical methods. In order to compare the performance clearly, the mutual standards and recommendations of BFC characterization should be established. We expect that such universal standards and definitions will further help to compare the actual performance of different laboratories and countries, hence pushing the field to move forward faster.

Many of the challenges hindering the development and application of wearable BFCs have been addressed using innovative approaches and advanced materials. Although the obstacles for such on-body energy harvesting are different, when designing a high-performance BFC, all parameters are intrinsically linked. For example, the chemical and biochemical challenges related to the enzyme-electrode interface can be mitigated by engineering new conductive flexible large-area materials able to increase the enzyme payload and improve the direct electron transfer while enduring mechanical strains encountered during body movements. Such developments will ensure an attractive

electrochemical performance and favorable biocatalytic activity under diverse on-body operations and settings.

Apart from the mechanical aspects toward conformal wearable platforms, researchers are aiming at eliminating mediators, commonly used in traditional BFCs, through new advanced functional materials. As we discussed, the use of mediators can compromise the performance, stability and biocompatibility of wearable BFCs, since these small molecules can easily leach out the system and increase the overall toxicity of the BFC. Addressing the challenges of mediator-free wearable BFCs requires proper attention to the charge transfer processes and enzyme orientation. The study of conductive enzyme-like biomolecules for direct electron transfer process seems promising to mitigate this issue.[125] Besides mutant enzymes, efforts toward the study of more efficient enzyme wiring and immobilization methodologies should be considered. An additional safety consideration is also the challenge to sterilize the BFC electrodes upon applying the device on highly sensitive biological tissues, such as eyes.

Stability is another significant aspect that impacts the operation and longevity of wearable BFC devices. Particular attention should be given to the susceptibility of the enzyme activity to variety of operating conditions, such as fluctuating pH, changing temperatures or low oxygen. The human body is a dynamic system and fluctuations in a specific biofluid can occur continuously, impacting directly the BFC performance. To address these issues, enzyme immobilization strategies that impart higher stability and pH tolerance should play a larger role when wearable applications are involved. Achieving

such favorable enzyme confinement will minimize changes in the enzyme structure and activity during these dynamically changing operating conditions. The integration of sensors (pH, temperature, etc.), adjacent to BFCs, could be used for tracking (and correcting for) fluctuations of wearer's surrounding conditions.

Overall, the human body is a very efficient machine that can minimize energy losses, as any other system; harvesting energy from body fluids is thus a demanding task. The amount of fuel available in body fluids is quite limited, resulting in limited net energy of the BFCs. In addition to the fuel availability, the incomplete oxidation of the biofuels at the anode also limits the obtained power.[126] While in living organisms, complex molecules are oxidized in an intricate system of enzymes, BFCs are usually composed by a single enzyme, and can hardly lead to complete oxidation of the fuel. Several research groups have studied enzymatic cascade and combinations of bio- and inorganic-catalysts to achieve complete fuel oxidation for maximizing the energy-conversion performance.[14, 127-128] Finally, the integration of BFCs with other wearable energy systems, both energy-harvesting devices (e.g., solar cells, triboelectric, and piezoelectric systems), and energy-storage devices (such as batteries and supercapacitors) is extremely attractive for developing comprehensive wearable “green”-energy system, capable of harvesting and storing energy under a variety of conditions.[66] The safety aspect of developing new wearable devices must always be considered carefully, with extra attention given to the use of nanomaterials and of toxic chemicals, and to the prevention of their direct contact with skin. To conclude, with such innovative solutions to major challenges, along with collaborative efforts of chemists, chemical engineers, and materials scientists, wearable

BFCs are expected to have an important impact on wearable electronics toward diverse biomedical, fitness, and defense applications.

1.7 Acknowledgements

Itthipon Jeerapan and J.R.S. contributed equally to this work. This work was supported by Defense Threat Reduction Agency Joint Science and Technology Office for Chemical and Biological Defense (HDTRA 1-16-1-0013). Itthipon Jeerapan and J.R.S. acknowledge support from the Thai Development and Promotion of Science and Technology Talents Project (DPST) and National Council for Scientific and Technological Development (CNPq-216981/2014-0), respectively.

Chapter 1 is based, in part, on the material as it appears in Advanced Functional Materials, 2019, by Itthipon Jeerapan, Juliane R. Sempionatto, and Joseph Wang. The dissertation author was the primary investigator.

Chapter 2 Stretchable Electrochemical Devices: Stretchable Biofuel Cells as Wearable Textile-Based Self-Powered Sensors

2.1 Introduction

Advanced soft materials for sensors and electronic devices are particularly interesting and used as wearable devices for diverse fitness[5, 21, 129] and biomedical[130-132] applications. Irrespective of applications, almost all wearable devices mandate viable energy sources, leading to a considerable research activity aimed at advancing wearable energy systems.[11] Among all the energy storage devices that typically require re-charging and operate under non-physiological conditions, energy bio-harvesting devices, *e.g.*, enzymatic biofuel cells (BFCs), have received considerable attention. Wearable BFCs can scavenge biochemical energy from the wearer, allowing the design of power-harvesting devices for *in vivo* applications and fully integrated miniaturized and self-powered sensors. Since most wearable devices are designed to be integrated with human epidermis, skin-worn BFCs thus have wide applications. Our group demonstrated minimally-invasive microneedles for harvesting energy from subcutaneous glucose[22] and a non-invasive

epidermal tattoo for generating energy from human sweat.[133] The net power extracted from them is limited due to small contact areas with the body. Textiles have become an important platform for wearable innovations and can cover a larger surface area. Textile-based BFCs thus have the potential to scavenge significant amounts of energy. Nevertheless, in real scenarios of daily life, multiplexed movements can cause adverse deformations to wearable devices, including both power sources and sensors, leading to one of the major challenges in wearable chemical sensors. Therefore, the dissertation author and co-authors herein attempted to overcome these challenges by creating a highly stretchable textile-based BFC as a fully integrated personalized self-powered sensor.

Despite the distinct advantages of textile-based devices, very few reports on textile-based BFCs have tried to address these major mechanical challenges. Nishizawa's group reported fabric-based BFCs that could convert 200–500 mM fructose to energy.[67, 134] In fact, these devices that are based on a biobattery idea showed that stretching 30 cycles at 50% strain provoked a power decrease of 20–30%, indicating key challenges to address both energy and stretchability issues. In addition, unlike the biobattery type, BFC harvesters can operate continuously, as fresh fuels are unceasingly provided by the human body, and more advantageously, they can act as self-powered sensors simultaneously. As will be demonstrated below, our new stretchable textile BFCs can serve as efficient self-powered biosensors. Self-powered biosensors have received considerable attention since the pioneering work of Katz *et al.*[106] Such bioelectronic devices obviate the need for a power source and provide power signals proportional to the level of the fuel analyte. Owing to their distinct advantages, including minimal interference effects in complex samples, self-powered sensors have

been developed by several groups.[11, 22, 105-106, 110, 135] However, to date, there are no reports on any wearable and stretchable self-powered biosensors.

This chapter describes the first example of highly stretchable textile-based BFCs as self-powered sensors that extract the electrical power from perspiration for probing the sensing events of sweat metabolites (Figure 2.1). The new bioelectronic devices have been fabricated by screen-printing technology that offers simple ink patterning over highly stretchable fabrics or other surfaces of wearable accessories, as well as enables engineering of any extra desirable functionalities to the inks.[136-138] However, printing electronics on wearable textiles is challenging. For example, it requires viable inks that adhere to substrates and endure high stretchability, while retaining high electrical conductivity and a favorable electrochemical performance.[24, 139] Here, we engineered the printable inks to meet these desired functionalities. Coupling the new ink formulations and serpentine electrode design, the resulting self-powered devices can display the highest stretchability for textile-based bioelectronics and endure a stable performance even upon repeated (>100 times) strains as large as 100%. Such a highly stretchable textile-based BFC has been integrated as a device that can "scavenge" biochemical energy from the wearer's perspiration, "sense" the biomarker level, and simultaneously "display" to the readout, minimizing the external energy sources. This "scavenge-sense-display" system is an example of a Stretchable Textile-based Autonomous Sensor ("STAS") for advancing wearable non-invasive sensors and bioelectronic devices, as demonstrated in the following sections toward the sock-based BFC and the self-powered wearable sensor. Such textile-based stretchable energy harvesters and self-powered sensors thus hold considerable

promise for enhancing the functionality of our clothing toward diverse wearable applications.

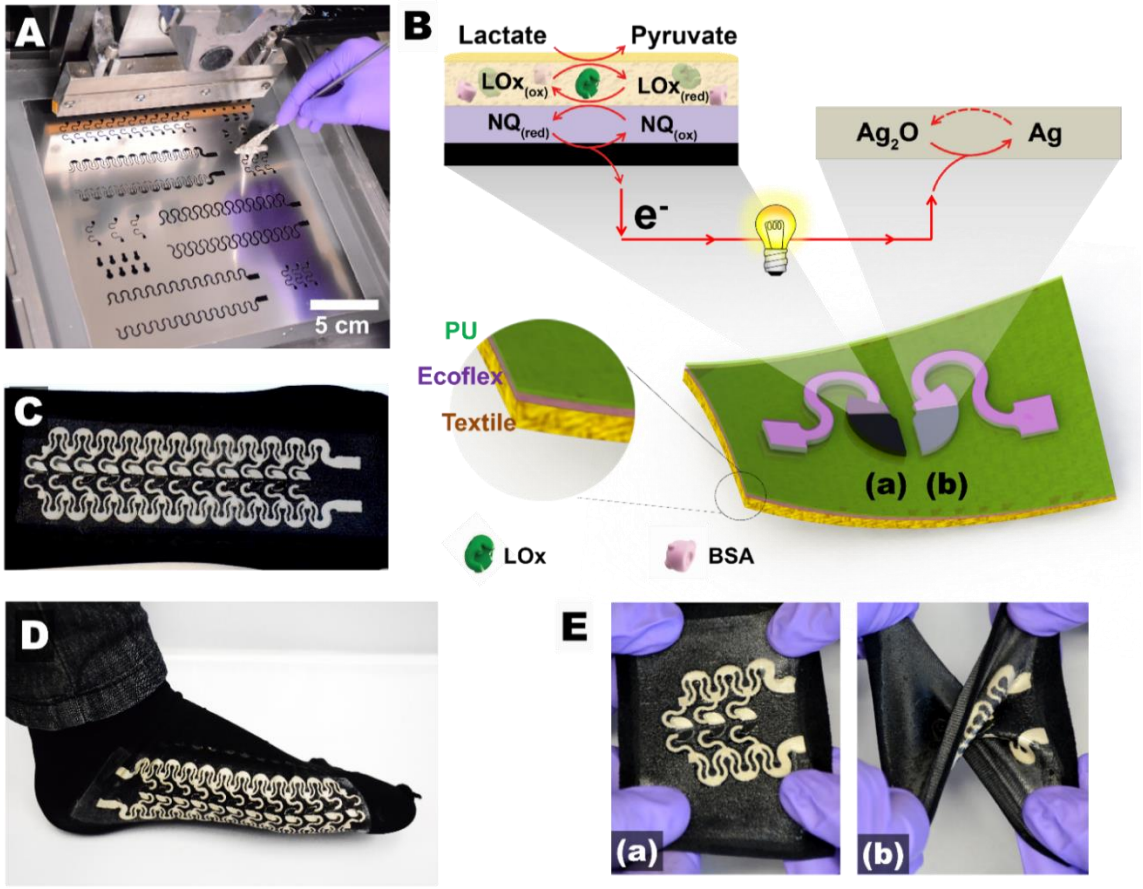

Figure 2.1 (A) Photograph of the designed stencil used for printing stretchable devices and the screen-printing process. (B) The components of the stretchable lactate BFC and the redox reactions that occur on the anode (a) and cathode (b). For glucose BFC, lactate, pyruvate and LOx in the reactions are replaced by glucose, gluconolactone and GOx, respectively. (C) Photograph of the stretchable BFC array printed on stretchable textile as wearable sock-based self-powered sensors. (D) A volunteer wearing the sock-based BFC array that can act as self-powered sensors. (E) Mechanical resilience tests on the stress-enduring BFC and self-power sensor printed array. Before (a) and during the multiplex deformations, such as twisting (b). Adapted with permission.[27] Copyright 2016, The Royal Society of Chemistry.

2.2 Experimental Section

2.2.1 Chemicals and Reagents

Carboxylic acid functionalized multi-walled carbon nanotubes (COOH-CNTs) and hydroxyl functionalized multi-walled carbon nanotubes (OH-CNTs) (purity > 95%, diameter = 10–20 nm, length = 10–30 μm) were purchased from Cheap Tubes Inc. Polyurethane (PU) (Tecoflex® SG-80A) was obtained from Lubrizol Life Sciences. Ecoflex® 00-30 was purchased from Smooth-On, Inc., PA. Lactate oxidase (LOx) was purchased from Toyobo. Potassium ferricyanide(III), mineral oil, *N*,*N*-dimethylformamide (DMF), tetrahydrofuran (THF), chitosan, glucose oxidase (GOx) from *Aspergillus niger*, type X-S (EC 1.1.3.4), 1,4-naphthoquinone (NQ), bovine serum albumin (BSA), glutaraldehyde, D(+)-glucose, L(+)-lactic acid, potassium phosphate dibasic (K_2HPO_4), potassium phosphate monobasic (KH_2PO_4), ethanol, and acetone were purchased from Sigma-Aldrich. All chemicals were of analytical grade and were used without further purification. Ultra-pure deionized water (18.2 MΩ cm) was used for all the aqueous electrolyte solutions. Ecoflex® 00-30 was prepared by mixing equal volumes of pre-polymers A and B, provided by the supplier. Ag/AgCl ink (E2414) was purchased from Ercon Inc., Wareham, MA. Glucose stock solution was allowed to mutarotate for at least 24 hours prior to use and stored at 4 °C. Stretchable textile (0.9 mm thickness, 87% nylon, 13% spandex) was purchased from Keyser-Roth Corp., USA.

2.2.2 Preparation of Stretchable CNT and Silver Inks

Stretchable inks were prepared by following our previous report with modifications.[24] The inks were optimized to suit the stretchable textile-based device. CNT stretchable ink was prepared by mixing 100 mg of COOH-CNTs with 70 mg of mineral oil. This composition was dispersed in THF for one hour in an ultrasonic bath and then homogenized in a shaker for five hours. After that, 91.5 mg of PU was added, and the resulting cocktail was shaken overnight. For printing, the solid content was controlled to be the solid-to-solvent ratio of 1 mg : 9 μL. For stretchable silver ink, 90 mg of Ag/AgCl ink were mixed with 10 mg of Ecoflex® to obtain a final weight percentage of 90 : 10, Ag/AgCl ink : Ecoflex®.

2.2.3 Fabrication of Stretchable BFC Array

The fabrication process was carried out by using an MPM-SPM semi-automatic screen printer (Speedline Technologies, Franklin, MA). Stretchable patterns were designed by the authors in AutoCAD (Autodesk, San Rafael, CA) and chemically etched on a stainless steel 12″ × 12″ framed stencil of 150 μm thickness (Metal Etch Services, San Marcos, CA). The printing process was carried out as per the following steps. The first step was screen printing a 75 μm thick layer of Ecoflex® on a stretchable textile. The layer was cured at 65 °C for 10 minutes. Then 15% (wt/vol) polyurethane in DMF was screen-printed over the Ecoflex layer and cured in an oven at 50 °C for 20 minutes to obtain a 75 μm thick layer of PU. Afterward, a sequence of stretchable Ag/AgCl and CNT inks were printed to obtain the designed BFC array. These printed patterns of the Ag/AgCl and CNT inks were

cured at 90 °C for 4 minutes and at 85 °C for 10 minutes in a conventional oven, respectively. Finally, Ecoflex® was used to define the electrode area and isolate the contact pads, and cured at 65 °C for 10 minutes.

2.2.4 Preparation of Enzymatic Anodes

The printed CNT anode was first activated by applying a potential of +1.2 V for 100 s in a saturated sodium carbonate solution. Next, the electrode was washed with water and dried in air. After activation, the modification was performed by drop casting the solution, step-by-step, as follows: 6 μL of 5 mg mL^{-1} OH-CNTs dispersed in 0.2 M NQ in ethanol/acetone (9 : 1 (vol/vol)), 4 μL of 40 mg mL^{-1} GOx or LOx solution dissolved in 10 mg mL^{-1} of BSA, 2 μL of 1% glutaraldehyde solution and 2 μL of 1% wt of chitosan in 0.1 M acetic acid. Each step was performed when the electrode from the previous step had completely dried. Chitosan solution was then added and left to dry overnight.

2.2.5 Preparation of Silver Oxide/Silver (Ag_2O/Ag) Cathode

The stretchable Ag_2O/Ag electrode was prepared by using the following procedure. 3% COOH-CNTs : 10% Ecoflex® : 87% pristine Ag/AgCl (by wt) ink was printed over the layer of the stretchable silver ink and then anodized at constant potential of +0.2 V for one hour at room temperature under alkaline conditions (1 M NaOH) in order to generate Ag_2O. Finally, it was rinsed with water and dried in air.

2.2.6 Resistance and Electrochemical Measurements

The resistance and short circuit current data were measured through an Agilent multimeter (6½ digit model 34411A) and Keysight BenchVue software (version 3.0). Electrochemical experiments were performed using a μAutolab Type II controlled by NOVA software version 1.11. The three-electrode system was carried out. The working electrode was the stretchable electrode. The counter and reference electrodes were platinum and Ag/AgCl (3 M KCl) electrodes, respectively. 10 mM ferricyanide in 0.1 M potassium phosphate buffer solution (PBS, pH 7.0) was used as a probe to evaluate the electrochemical performance. For the BFC characterization, open circuit potentials were obtained in 0.1 M PBS (pH 7.0) before and after the addition of the glucose or lactate solutions. Polarization curves were taken from open circuit potential to 0 V with a scan rate of 1 mV s^{-1} in 0.1 M PBS (pH 7.0). The autonomous current response was recorded after a 60 s incubation in the sample solution. The biosensor selectivity was evaluated in the presence of relevant constituents of human perspiration in physiological levels, *i.e.*, 84 μM creatinine, 10 μM ascorbic acid, 0.17 mM glucose, and 59 μM uric acid.[95] All experiments were carried out at room temperature, unless otherwise indicated. The "scavenge-sense-display" concept was demonstrated by using a dial analog ammeter (uxcell DMiotech Class 2.5 Accuracy DC Analog Panel Meter μA Ammeter). On body measurements were performed by using a compact wireless device with an integrated rechargeable battery (Vernier Go Wireless® Electrode Amplifier) to collect the data *via* Bluetooth in a smart phone.

2.2.7 Mechanical Resiliency Studies

Initially, the two-probe method for resistance measurements was employed to observe the mechanical resiliency. The printed designs (Figure 2.2C and Figure 2.3) were connected with the probes, multimeter, and computer. The external force was applied to stretch the device until reaching the input strains. Afterward, it was unconstrained to its original location. During the procedure, the resistance was measured. Cyclic voltammetry (CV) was also used to monitor the resilient ability of the stretchable device. CV was first recorded on the non-stretched device. Subsequently, various forms of mechanical deformations were applied to the device and then the device was allowed to relax to its original form. Afterward, CV was recorded again to monitor the changes in the electrochemical behavior of the textile-based electrodes. Power characterization and mechanical resiliency tests were carried out in a similar way.

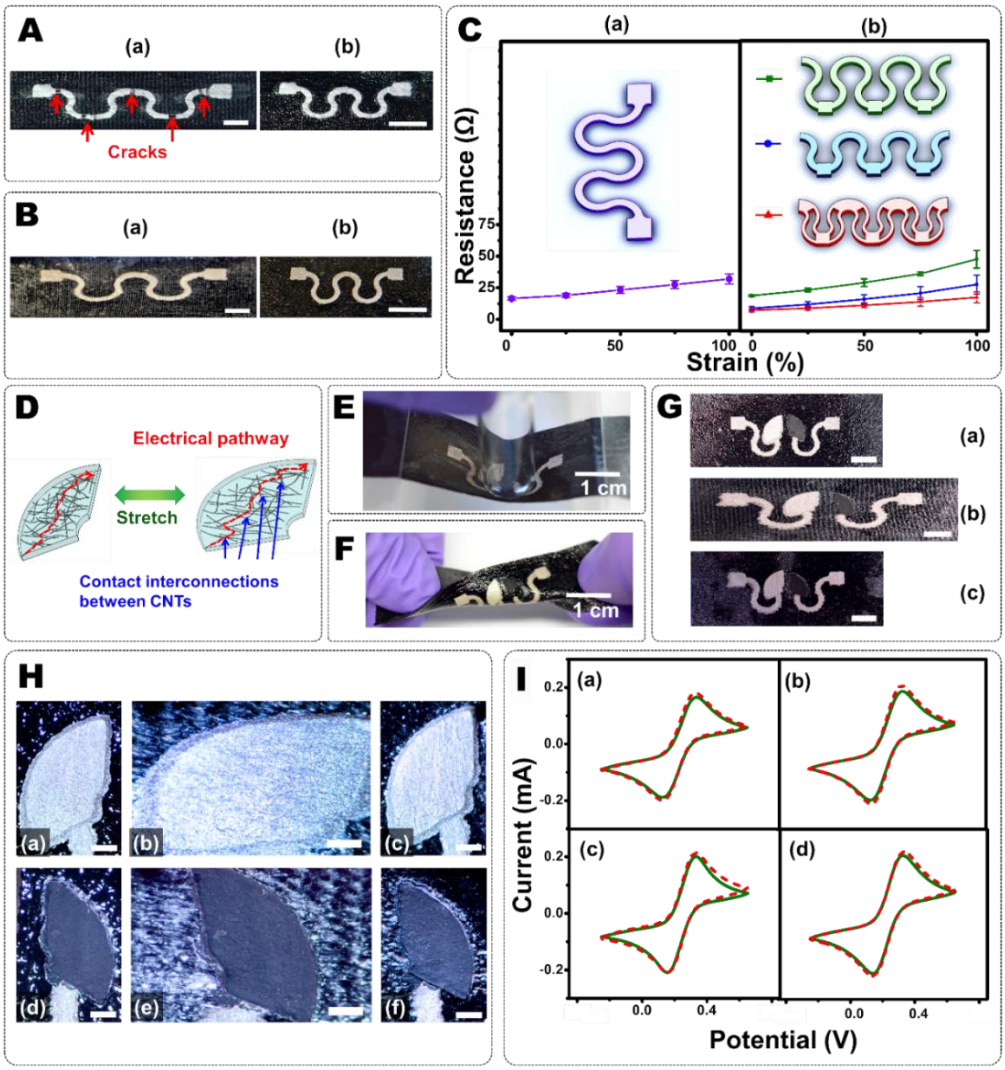

Figure 2.2 Mechanical stretching study performed on the serpentine patterns printed by using (A) pristine and (B) modified Ag/AgCl inks with 10% (wt) Ecoflex®. During stretching at 100% (a) and after stretching (b). Scale bar: 5 mm. (C) Resistance study of the printed serpentine patterns. Legends show pictorial representation of the serpentine interconnect designs. Corresponding details of the designs are shown in Figure 2.3 and Figure 2.4. (D) Illustration showing the percolation structure of the electrode with the nanofiller of CNTs embedded within an elastomeric matrix offering stretchability. Photographs of the stretchable device showing the mechanical robustness: (E) 5 mm indention; (F) 180° twisting; (G) (a) before stretching, (b) during stretching and maintaining at 100% strain and (c) after repeated stretching at 100% strain for 100 times. Scale bar: 5 mm. (H) Microscopic images from the cathode (before (a), during 100% strain (b), and after 100 repeated 100% strain cycles (c)), and from the anode (before (d), during 100% stretching (e), and after 100 repeated 100% stretching cycles (f)). Scale bar: 1 mm. (I) CVs recorded before (green solid lines) and after (red dash lines) (a) applying increasing levels of strain from 0 to 100% with increments of 25%; (b) applying 100% stretching cycles for a total of 100 iterations; (c) indentations (5 mm) for a total of 100 repetitions; (d) 180° twisting cycles for a total of 100 iterations. Complementary CVs are shown in Figure 2.5. Adapted with permission.[27] Copyright 2016, The Royal Society of Chemistry.

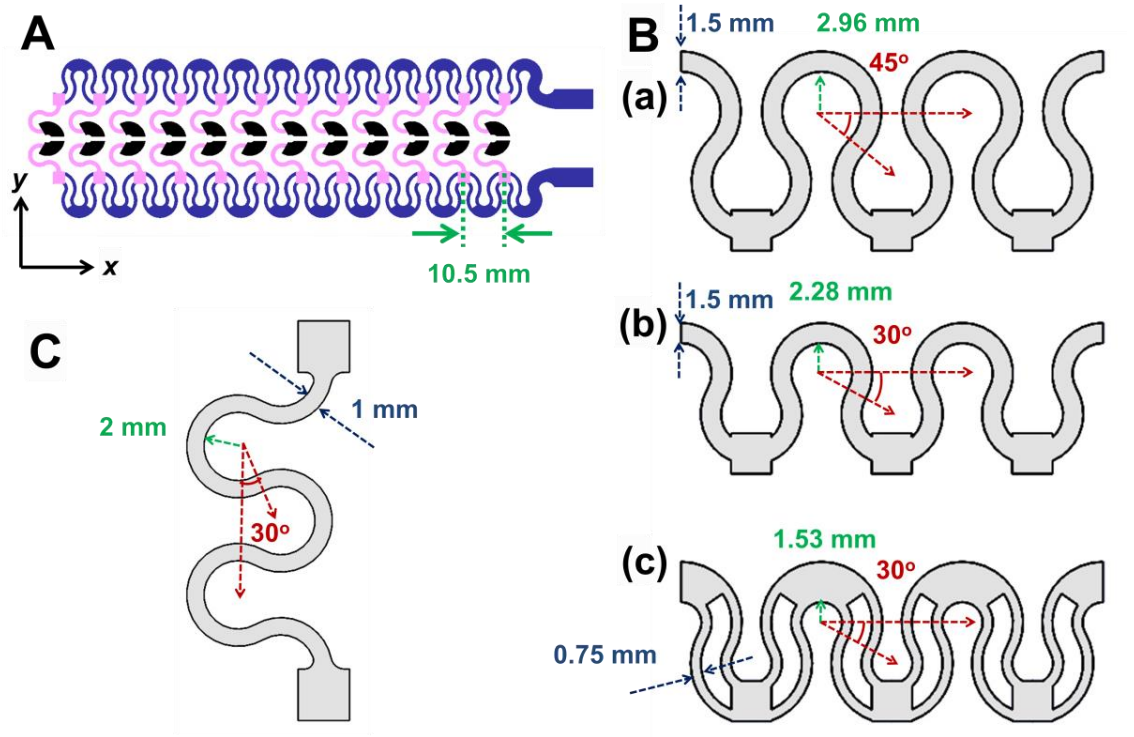

Figure 2.3 Illustration of the designs. (A) An example of designed pattern for stretchable BFC array. This design is for accommodating multi-directions of external strains: x-direction (blue) and y-direction (pink). (B) Designed patterns for accommodating external strain in x-direction: (a) 45-degree design (45°); (b) 30-degree design (30°); and (c) separated trace design. (C) Designed patterns for accommodating external strain in y-direction. Adapted with permission.[27] Copyright 2016, The Royal Society of Chemistry.

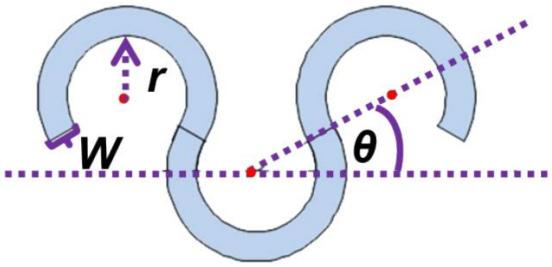

Figure 2.4 Definition of parameters for the arc of the serpentine interconnects. The parameters are connecting angle (θ), width (W), and inner radius (r). Adapted with permission.[27] Copyright 2016, The Royal Society of Chemistry.

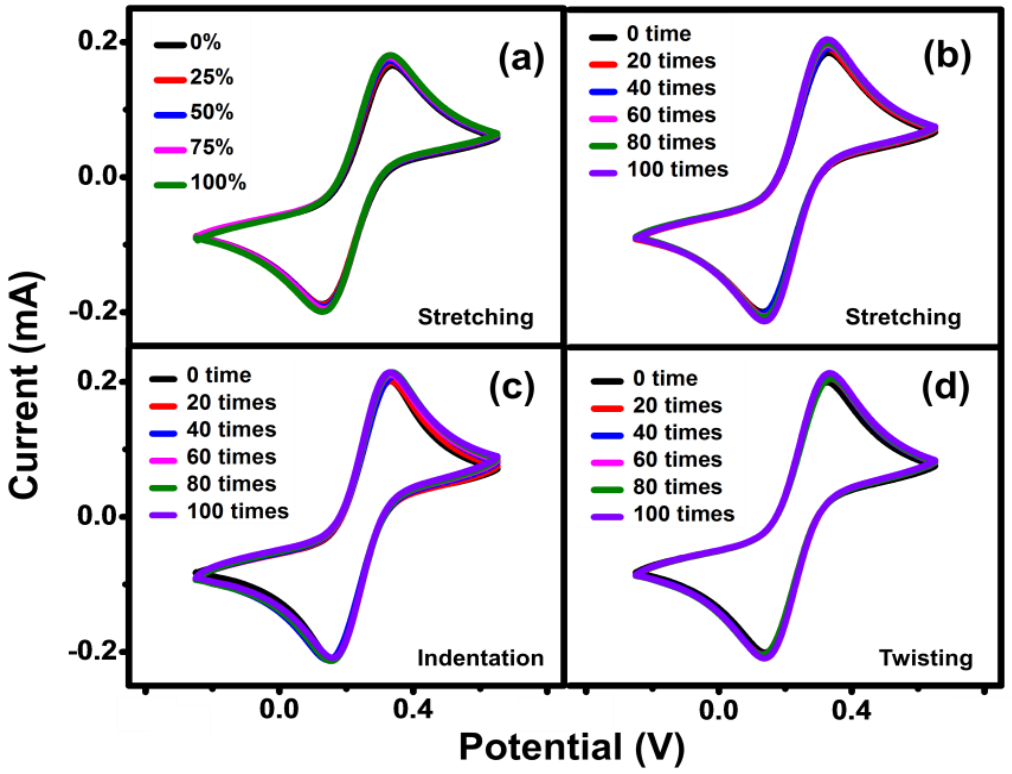

Figure 2.5 CVs recorded when (a) applying increasing levels of strain (repeated 20 cycles for each) from 0 to 100% with increments of 25%. (b) applying 20 repeated 100% stretching cycles for a total of 100 iterations (c) 20 repeated indentations (5 mm) for a total of 100 repetitions (d) 20 torsional 180º twisting cycles for a total of 100 iterations. The working electrode is the stretchable CNT-based electrode. Adapted with permission.[27] Copyright 2016, The Royal Society of Chemistry.

2.3 Results and Discussion

2.3.1 Fabrication of the Stretchable BFC Self-Powered sensors

The dissertation author and the team demonstrated a scalable, facile, and low-cost method to fabricate highly stretchable textile-based BFC devices by utilizing the screen-printing process, based on stretchable tailored inks, along with the customized stencil and electrode design (Figure 2.1A). The membrane-less BFC was employed to obtain the

wearable stretchable textile-based device (Figure 2.1B). The bioanode was functionalized with a single enzyme (*i.e.* GOx or LOx) and NQ as a redox mediator for the biocatalytic oxidation of biofuels and increase of power density, respectively[140] (Figure 2.1B(a)). A silver(I) oxide/silver (Ag_2O/Ag) redox couple electrode was chosen as the cathode because of several advantages, such as integration as the cathode for the BFC under anaerobic conditions[93] (Figure 2.1B(b)). Upon adding a biofuel (*e.g.*, glucose or lactate), the biochemical fuel is enzymatically oxidized on the anode and releases electrons. On the cathode compartment, silver oxide accepts those electrons to complete the power circuit. Therefore, this BFC does not rely on the oxygen reduction reaction (ORR) and can thus operate on human-body sweat to harvest energy or provide a self-powered response without errors associated with the limited or fluctuated oxygen concentrations. With this approach, we could obtain a printable electronic array on stretchable fabrics, such as socks, that can be worn comfortably on human bodies, *e.g.*, a foot, as shown in Figure 2.1C and D. Compared with other fabrication methods, this approach guarantees mechanical resilience, accommodating stress such as multiaxial stretching, bending, wrinkling, stretching (Figure 2.1E), besides being simple, scalable, and free from complex transferring steps, vacuum, clean room, high temperature, and time-consuming processes.[136-137]

2.3.2 Substrate Modification, Rationale for the Stretchable Connection Design and Engineering of Stretchable Inks

As a solely straight pattern cannot endure high strains, we had to employ a serpentine shaped pattern for printing the stretch-enduring traces.[141] Hence, preliminary efforts relied on our reported design to print the conductive traces. Additionally, the textile substrate was modified by printing elastomers in order to ensure mechanical robustness of the devices and smooth down the fabric hair in order to achieve decent printing quality (Figure 2.6). The modification was carried out by a simple low-cost process. First, a layer of highly stretchable Ecoflex® was printed on the fabric surface, filling the empty spaces of the textile's mash, offering an improvement in the fabric stretchability and also generating a smooth surface by trapping down the textile hair. As the engineered inks are typically hydrophilic in order to obtain desirable electrochemical characteristics, they are not compatible with the elastomeric under layer. Thus, in the second step, an interface layer of PU was printed over the Ecoflex® in order to overcome the ink compatibility issue with the substrate. 15% (wt/vol) polyurethane in DMF was the optimum composition to ensure printability, stretchability, and compatibility with ink materials (Table 2.1). After printing the PU layer, the substrate was cured at 60 °C for 20 minutes, this process allows time for the PU to anchor into the Ecoflex® layer, promoting good adhesion.

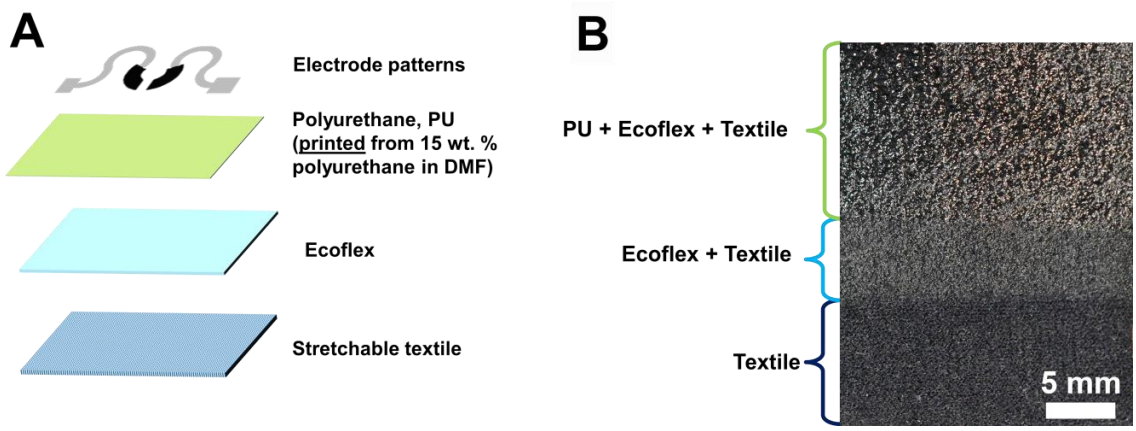

Figure 2.6 The fabrication process of the stretchable BFC device. (A) The process starts by delaminating the Ecoflex and PU layers on the stretchable Nylon- Spandex textile and then screen-printing the designed pattern onto the modified surface. (B) Optical image shows the surface of the pristine textile and modified layers. Adapted with permission.[27] Copyright 2016, The Royal Society of Chemistry.

Table 2.1 Optimization of polyurethane (PU) layer for surface modification. †T_b of THF = 66°C; ‡T_b of DMF = 153°C. Adapted with permission.[27] Copyright 2016, The Royal Society of Chemistry.

	Printability	Mechanical Properties
10.0% PU in THF†	Hard to print, low viscosity, fast evaporation of solvent	Poor, thickness not enough to stress applied
12.5% PU in THF	Easy to print, good viscosity	Poor, thickness not enough to stress applied
15.0% PU in THF	Printable, fast evaporation (bubbles) when cured under temperature higher than 50 ºC.	Good, enough thickness to stress applied even when stretched over 100%
15.0% PU in DMF‡	Easy to print, can be cured at higher temperature, less curing time, no bubbles over 50 ºC	Good, enough thickness to stress applied even when stretched over 100%

Conductive Ag/AgCl patterns were printed on the modified textiles. Ag/AgCl ink was used to demonstrate the stretchable conductive ink as it is compatible with the elastomer and can be further integrated with electrochemical sensors as pseudo-reference[130] or iontophoretic[142] electrodes. Figure 2.2A and B show optical images comparing the pristine and modified Ag/AgCl inks with 10% (wt) Ecoflex®. Figure 2.2A shows the poor interfacial adhesion and cracking problems of the normal commercial ink, when it was printed on the modified textile. These issues have been addressed by adding an elastomer into the pristine ink. Note that adding Ecoflex® leads to a decreased conductivity and hence requires careful tuning of the ink composition. The optimum

composition that ensures both favorable stretchability and conductive properties of the engineered ink was found to be 90% (wt) Ag/AgCl ink : 10% (wt) Ecoflex®. Compared with the pristine ink pattern in Figure 2.2A at 0% strain, the Ecoflex® addition resulted in an increased electrical resistance of ~14 Ω (*vs.* the 2.5 Ω original resistance of the pristine ink). As shown in Figure 2.2B, it is evident that this approach enabled us to achieve a stretch-enduring ink that was compatible with the mechanically stretchable textile. No fractures were found under microscopic observation. Accordingly, these optimum conditions were applied for realization of the connection design.

Recently, we described a design that induces additional stretchability.[24]The change in electrical resistance from this pattern (Figure 2.2C(a)) indicates that this printed serpentine remained a good conductor (~32 Ω) even under 100% strain. The resistance increased slightly with increasing 100% tensile strain. To further explore and accomplish superior patterns, we systematically designed a new stencil and elucidated different printed patterns (Figure 2.3 and Figure 2.4). The combination patterns are also designed to accommodate the bidirections of external strains. In order to obtain the same device size, the array-to-array distance was fixed at 10.5 mm. The important parameters including the connecting angle (θ), width (W), and inner radius (r) are defined in Figure 2.4. As we proved in the previous report, a wider angle θ is preferable. Therefore, we focused on θ = 30° and 45°. Three new different patterns were designed, and their stretchable silver patterns were printed on the textiles to explore the best pattern. From a mechanical point of view, W should be decreased, while r should be wider to reduce an actual maximum strain on serpentine structures.[141, 143] On the other hand, Pouillet's

law suggests that the resistance of interconnects will also unwillingly increase with the length and increase with decreasing *W*. Hence, we demonstrated the designs by keeping *W* constant (at 1.5 mm). One approach to reduce *W* is by splitting the curvature, whereas the overall size of *W* is still the same. The connecting lines between the small separated traces were intended to ensure lower resistance. The details are illustrated in Figure 2.3. When comparing the effect of the applied strain on the electrical resistance (Figure 2.2C(b)) and performing two-way analysis of variance (ANOVA), we find that the designs are statistically different with 95% confidence. The separated traces exhibited superior durability and conductivity than 30° and 45° designs, respectively. This separated trace design showed that applying 100% tensile strain causes a slight increase in the resistance by less than 10 Ω. With this separated trace design and aforementioned reasons, this stretchable interconnect can withstand the applied stress better. This attractive ability to relax the stresses is supported by earlier simulations.[143-144] The experimental results fulfill the stretch-enduring electronics realization, because the consequences of two real parameters (*i.e.* conductivity and stress) were evaluated.

Regarding the BFC, more special materials are required for the anode and the cathode. The developed CNT-based ink was used in the printed anode since the CNTs provide favorable conductivity properties and play an important role in the bioelectronic processes. In addition, the high surface area of CNT leads to high and stable adsorption of the enzyme and mediator. We observed that the maximum ratio of CNT–mineral oil composite : PU was 65 : 35 (wt/wt) to achieve a highly porous surface, favorable electrochemical properties and mechanical durability.

Moreover, regarding the cathode, the Ag_2O/Ag couple was used in order to improve the performance of the BFC and mitigate the effect from environmental oxygen fluctuations. It is shown that the Ag_2O cathode has superior advantages over the common Pt, laccase, or bilirubin oxidase cathodes. Most of the existing BFCs rely on precious metals or enzymes to catalyze the ORR at the cathode. Besides high cost (*e.g.*, Pt) and instability (*e.g.*, enzymes), these BFCs have a relatively low power output, because they are limited by the low concentration of dissolved oxygen and sluggish kinetics.[67, 145-146] In this work we achieved a significantly higher power density using the Ag_2O-based cathode, compared with the Pt-based one (Figure 2.7 and Table 2.2). However, our preliminary effort on using anodization synthesis of Ag_2O merely obtained from a scarified silver ink showed a significant loss of conductivity of the electrode.[147-148] Therefore, COOH-CNTs were added to the ink in order to enhance the conductivity and further improve its mechanical properties. This high-aspect-ratio (~1300) CNT filler promotes sufficient percolation within the ink matrix (Figure 2.2D). We suggest that dispersed CNT percolation is useful to facilitate the electron transport and the reduction on the Ag_2O cathode, as well as to enhance the mechanical resilience.[149-151] The nanometer-scale of the CNT filler enables sufficient pathways to allow electrons to complete the electrochemical reaction. It should be noted that the simple addition of CNTs resulted in the significantly inferior mechanical performance of the cathode due to the limited binder content for holding the CNT filler. This stretchable issue could be overcome by carefully tailoring the amount of CNTs and adding an elastomeric binder. Here, highly stretchable Ecoflex®, plasticized at a mild curing process, was used to offer mechanical compliance.

After having CNTs, Ecoflex®, and electrochemically generating Ag_2O, the desirable electrochemical performance was obtained. Nevertheless, considering the trade-off of three critical factors: mechanical, electrical, and chemical properties, we had to judiciously optimize the mixing ratio of the three components, namely CNTs, Ecoflex®, and silver. The optimum weight percentage was observed using 3 : 10 : 87 (COOH-CNTs/Ecoflex®/pristine silver ink). While the electrode potential was controlled at +0.2 V in the anodization process, the outermost silver layer was first oxidized. Immediately, under alkaline aqueous solution (pH ~ 13), the generated silver ions reacted with hydroxide ions to form Ag_2O.[152-153]The nanometer-scale of the CNT filler allows favorable electrical transport during such electrochemical synthesis as well as favorable power generation processes. Advantageously, the stretchable Ag_2O material offers potential applications in diverse energy-related applications, *e.g.*, catalytic reactions,[154-155] fuel cells,[156] batteries,[157] and photovoltaic cells.[158]

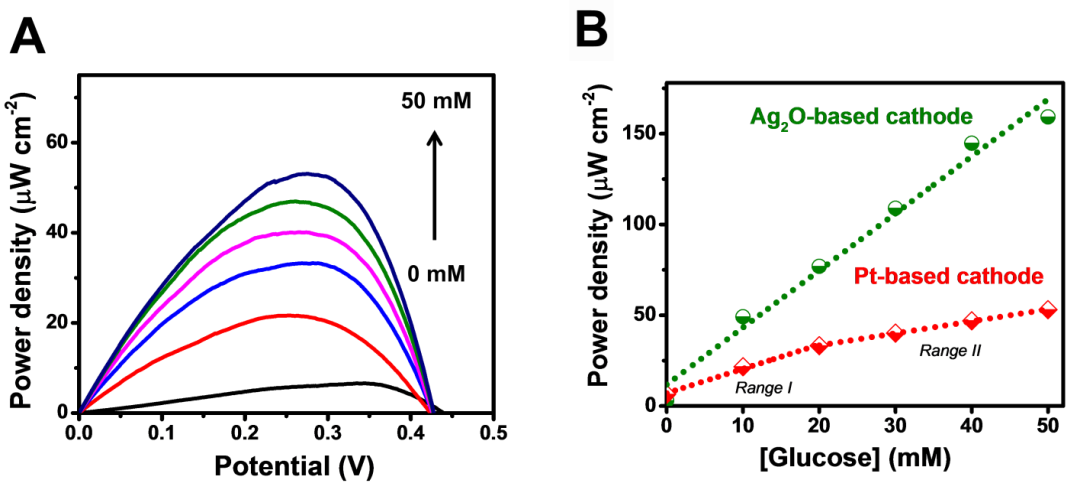

Figure 2.7 (A) Plot of power density vs potential plots of the assembled GOx bioanode/Pt-based cathode BFC when varying glucose concentrations (0–50 mM) in 0.1 M PBS (pH 7.0). (B) Corresponding power–concentration calibrations obtained from glucose BFCs with different cathodes: Ag_2O-based cathode (green circle) and Pt-based cathode (red square). Preparation of Pt-based cathode: Stretchable CNT ink was used as underline layer of cathode. After printed and dried, the cathode was modified by drop casting solution of 5 μL of 5 mg mL^{-1} OH-CNTs dispersed in 10 mg mL^{-1} of Platinum black ethanol solution. Then, 2 μL of 0.5% Nafion® solution was dropped after overnight. Adapted with permission.[27] Copyright 2016, The Royal Society of Chemistry.

Table 2.2 BFC performance obtained from Ag_2O-based and Pt-based cathodes. Adapted with permission.[27] Copyright 2016, The Royal Society of Chemistry.

Cathode	Sensitivity (μW cm^{-2} mM^{-1})	R^2
Ag_2O-based cathode	3.14 ± 0.20	0.980
Pt-based cathode	Range I: 1.34 ± 0.10	0.988
	Range II: 0.66 ± 0.01	0.999

2.3.3 Mechanical Resiliency Study

The integration of the BFCs with wearable textiles requires resilience to harsh mechanical deformations. Therefore, mechanical resiliency was extensively tested. Figure 2.2E–G shows the photographs of the poked, twisted and stretched devices. The highly stretchable serpentine interconnect helps in distributing the applied strain, reducing the actual strain on the BFC part.[24, 130] After performing these multiple deformations, we observed that the devices were mechanically rugged and maintained good adhesion with the textile substrate. Moreover, the active surface morphology of the device was also analyzed by light microscopy in reflection mode. The resulting images in Figure 2.2H reveal no major cracks or major effect on the surface even though the device was stretched repeatedly for 100 times at 100% stretching. Cyclic voltammetry (CV) was used

to examine the electrochemical characteristic and mechanical resiliency of the active electrode surface. First, a series of increasing strains was applied repeatedly. CVs were recorded with successive increments of tensile strain from 0 to 100% (repeated 20 times for each), as shown in Figure 2.2I(a). We observed reversible CVs, as the ratio of cathodic (I_{pc}) to anodic peak (I_{pa}) currents is unity. The device maintained good functionality even under this repeated stretching, as the peak separation (ΔE_p) and peak currents were negligibly affected by such deformations (indicated from RSD for ΔE_p = 2.53%; for I_{pc}/I_{pa} = 1.31%). Furthermore, to emulate the intermittent strains of a large stretching level, the device was stretched repeatedly at strain as extremely high as 100% for 100 times. The CVs in Figure 2.2I(b) confirms again the robustness of the printed device (RSD for ΔE_p = 3.93%; for I_{pc}/I_{pa} = 1.50%). Other types of strains can be anticipated for on-body applications. For instance, indentation force of 5 mm depth was applied repeatedly for 100 times. No obvious variation in the electrochemical functionalities was observed in Figure 2.2I(c) (RSD for ΔE_p = 4.96%; for I_{pc}/I_{pa} = 2.61%). Additionally, as the wearable device may wrinkle, repeated torsional twisting was also emulated and tested. After applying a torque to cause 180° twisting for 100 repetitions, there was a minimal effect on the electrochemical performance (RSD for ΔE_p = 4.20%; for I_{pc}/I_{pa} = 0.76%), as shown in Figure 2.2I(d). For clarity, only the first and the last CVs are displayed in Figure 2.2I. The corresponding midway CVs are shown in Figure 2.5.

SEM was also used to characterize the microscopic morphology (Figure 2.8). The SEM images reveal that the printed-CNT electrode possesses homogeneous distribution and high density of CNTs within the matrix, showing good nanoscale percolation networks

with numerous contact connections between CNTs, which result in excellent electrical pathways. Furthermore, the porosity exposes an internal surface area toward enhanced electrochemical properties. SEM images that were obtained after applying a large strain at 100% for 100 cycles to the device indicate a negligible effect of these mechanical deformations (Figure 2.8B), indicating an outstanding mechanical resiliency of the printed device.

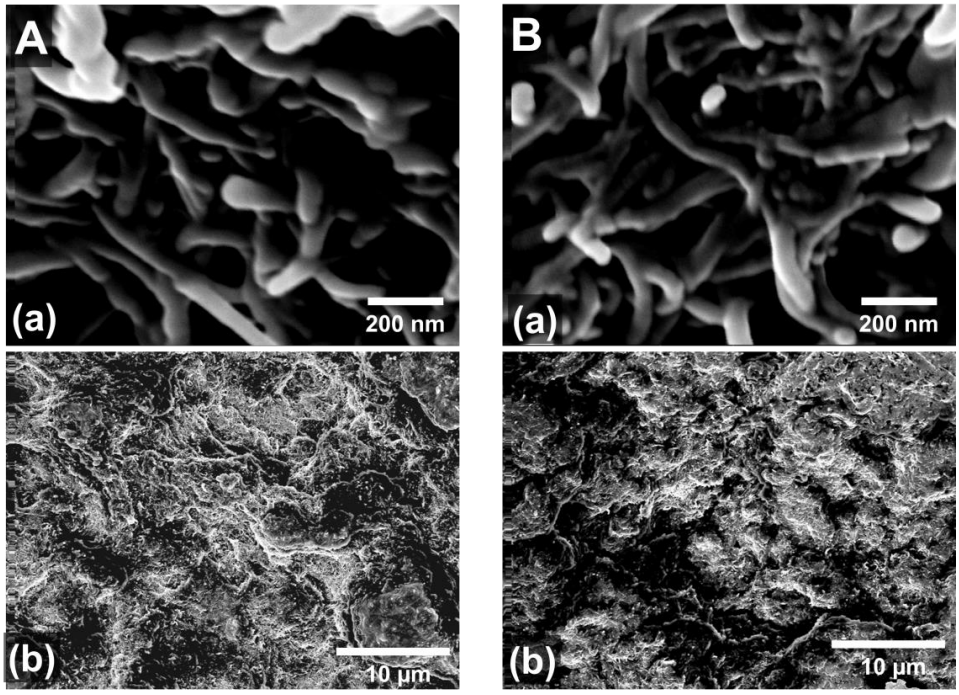

Figure 2.8 SEM image of stretchable CNT-based anode (A) before and (B) after repeated stretching at 100% strain for 100 times. (a) High magnification and (b) low magnification SEM images. Adapted with permission.[27] Copyright 2016, The Royal Society of Chemistry.

The remarkable mechanical durability of the textile-based devices toward extreme external strains is observed. A variety of severe strains were demonstrated, ranging from linear and biaxial stretching, twisting, bending, and indentation. These data indicate that the new textile-based printed BFC devices can accommodate extremely large, multiaxial and repeated multi-forms of strains. These observations suggest that the textile-printed devices allow several degrees of freedom relevant to the wearer's movement, and the devices can be conformably utilized in diverse real-life situations.

2.3.4 BFC Power and Stretchability

The power from the textile-based glucose BFC was primarily tested using different glucose concentrations. Figure 2.9A shows that the power density increases proportionally with the glucose concentration. The maximum power density achieved was 160 μW cm^{-2} with potential showing maximum power around 0.3 V and an open circuit voltage of 0.44 V. The high power density was achieved due to the attractive conductive properties of CNTs in the tailored inks, which facilitate the electron flow from the anode to the cathode.[159] The power density increases linearly with the glucose concentration in the 0–50 mM range, with good sensitivity (3.14 ± 0.20 μW cm^{-2} mM^{-1}) and correlation coefficient (R^2 = 0.980), as displayed in Figure 2.9B. Deviation from linearity was observed when concentrations were higher than 50 mM. Such behavior indicates that the textile BFC holds considerable promise as a self-powered biosensor.

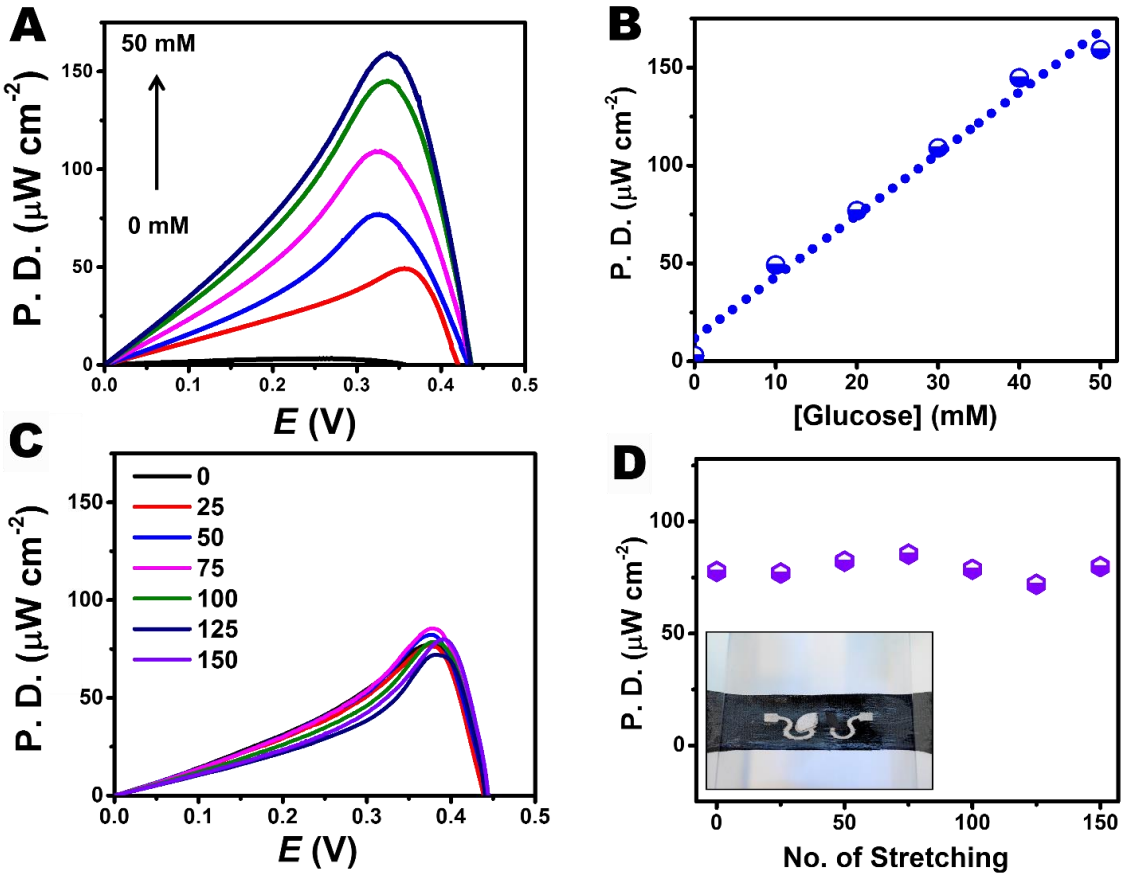

Figure 2.9 (A) Power density vs. potential plots of the stretchable glucose BFC when varying the glucose concentration (0, 10, 20, 30, 40, and 50 mM) in 0.1 M PBS (pH 7.0). (B) Corresponding power–concentration calibration plot. (C) Power density vs. potential plots obtained from 20 mM glucose after every 25 cycles of 100% stretching for a total of 100 iterations. (D) Stability of the power output during these 100 stretching iterations. Inset: photograph of the stretchable BFC under 100% strain. Adapted with permission.[27] Copyright 2016, The Royal Society of Chemistry.

The stability and efficiency of the prepared BFC toward real on-body applications were examined using stretching deformation tests. For example, the durability of the generated power was monitored while applying repeated cycles of 100% stretching for many times. As shown in Figure 2.9C and Figure 2.9D, no significant variation was observed in the shape and power density after every 25 cycles of 100% stretching up to 150 iterations, with high stability (RSD = 5.37%) even after these iterations of harsh

deformations. Such results illustrate the attractive performance after stretching of the present textile-based BFC against any other stretchable BFCs reported.[67] One of the keys for the high stretchability is our customized stretchable inks used to print the cathode and anode arrays. For the cathode, the stretchable character of the ink was improved *via* elastomeric properties of Ecoflex® and the high-aspect-ratio CNT nanofiller. For the anode, the stretchable feature of the ink was achieved through the PU elastomeric properties and the good interfacial formation of hydrogen bonds between carboxyl groups on CNTs and functional groups of PU. Besides, the layers of elastomers used as a supporting layer onto textile are essential to maintain the BFC device firmly attached to the fabric, preventing cracks on the printed array and enabling favorable stretchability to the bioelectronic printed device. This route for fabricating mechanically robust and power-efficient devices is thus attractive for creating a variety of wearable textile-based electrochemical devices.

2.3.5 Demonstration of Wearable BFC Energy Harvesting and Self-Powered Biosensing During On-Body Applications

We demonstrated the versatility of our approach by patterning arrays on several commercially available flexible and stretchable substrates, as shown in Figure 2.10. This route can meet the demands of printing electronic technology for the commercial viability, as general substrates should be manufactured only under a mild processing temperature and in a scalable, rapid and inexpensive fashion. This approach, thereby, enables mass

fabrication and commercialization. To illustrate the potential practical green-energy applications in personalized medicine, we fabricated the BFC devices on mechanically soft substrates of commercial accessories, such as socks, underwear, textile straps, and flexible watches that ensure the appropriate conformability between the sensor and the wearer. Six BFCs were printed on a sock (inner bottom) and connected in series to demonstrate the direct powering of six LEDs (Figure 2.11A), and illustrate its potential as a feasible wearable power source.

Figure 2.10 The fully integrated system for wearable lactate biosensing showing the "scavenge-sense-display" concept. The stretchable BFC arrays were printed on (A) the wearable underwear textile and (B) the stretchable strap. (C) Illustration of a 'green' model and photographs of wearable energy harvesting system and self-powered BFC array printed on conventional textiles and different body-worn accessories, such as stretchable headbands, straps and socks. Adapted with permission.[27] Copyright 2016, The Royal Society of Chemistry.

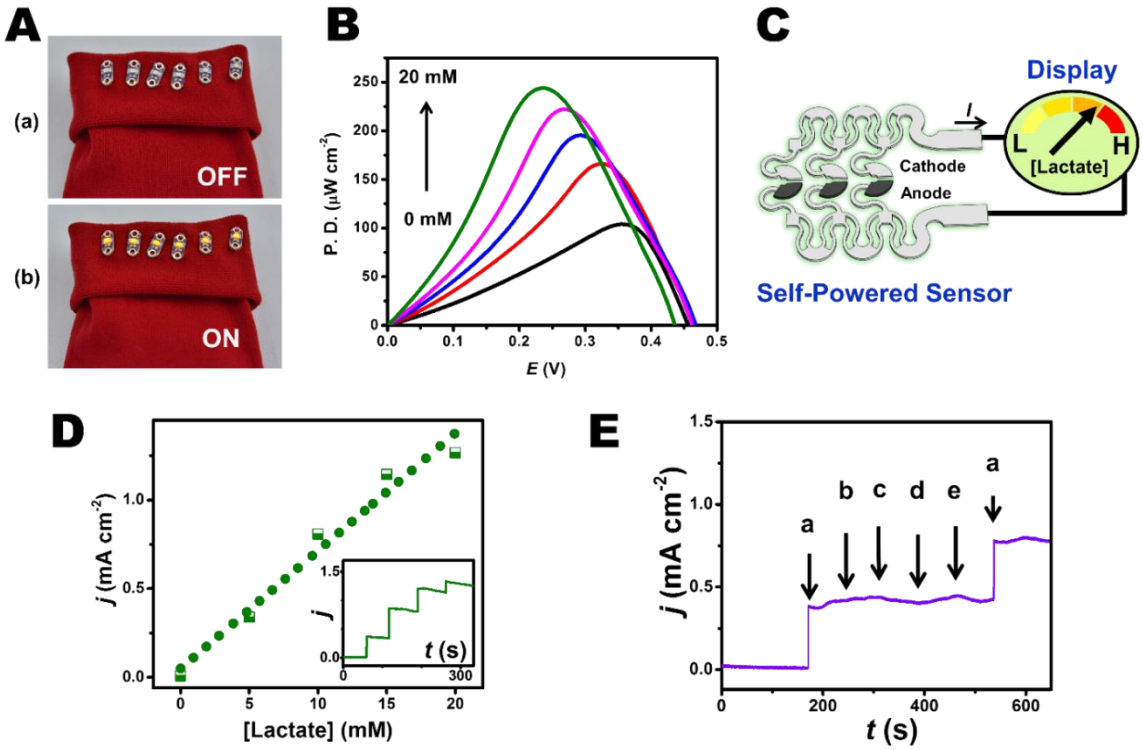

Figure 2.11 (A) Photographs demonstrating the operation of six LEDs powered by six equivalent textile BFCs that were connected in series in a 14 mM lactate solution. (B) Power density *vs.* potential plots of the stretchable nylon–spandex textile-based lactate BFC at varying lactate concentrations (0, 5, 10, 15, and 20 mM). (C) Schematic diagram of the integrated "scavenge-sense-display" system. (D) The self-generated current response, obtained from the stretchable lactate BFC, is plotted against the concentration of lactate, with no applied potential. The inset depicts the current response upon increasing the lactate concentrations (0, 5, 10, 15, and 20 mM). (E) Response of the stretchable self-powered BFC sensor to (a) 5 mM lactate, (b) 84 μM creatinine, (c) 10 μM ascorbic acid, (d) 0.17 mM glucose, and (e) 59 μM uric acid, with no applied potential. Adapted with permission.[27] Copyright 2016, The Royal Society of Chemistry.

Herein, we introduce the Stretchable Textile-based Autonomous Sensor ("STAS") where the electrical power is extracted for probing sensing events. Lactate, as a health indicator of pressure ischaemia, physiological metabolism, or pathological disorders, was selected for demonstration.[160-162] As illustrated in Figure 2.11B, the LOx bioanode/Ag_2O cathode BFC displays well defined lactate power signals in the presence of different lactate concentrations. The open circuit voltage of the cell is assessed to be 0.46 V. The maximum power density of 250 μW cm^{-2} was obtained in the presence of 20 mM lactate. Such a

power density is sufficient to power electronic devices.[163] We also found a linear relationship between the power output and the lactate concentration up to 20 mM (R^2 = 0.974) with the sensitivity of 6.71 ± 0.90 μW cm^{-2} mM^{-1}. The potential shift for the power curve upon increasing fuel concentration is slightly larger for the lactate BFC (Figure 2.11B) compared with the glucose one (Figure 2.11A). The slightly different behavior may be attributed to the enzymatic reaction of LOx, which has much smaller Michaelis constant (K_m). Apparently, LOx has a higher affinity for lactate, with smaller amounts of the biofuel needed to saturate the active sites of the enzyme, leading to common performance losses in BFCs.[30, 164-165] To demonstrate the fully autonomous sensing system in the mechanically compliant wearable platform, short circuit current responses, generated by the sensor itself, were recorded when no voltage was applied (Figure 2.11C and D). This approach proves that our wearable self-powered sensor can display a real-time signal of lactate levels without any amplification, filtering, and applied energy from external energy sources, to greatly simplify such lab-on-a-textile operation (inset of Figure 2.11D). The calibration curve of the autonomous signals in Figure 2.11D shows good linearity (R^2 = 0.985) up to 20 mM lactate and a limit of detection of 0.3 mM (3 × SD/sensitivity) with enhanced sensitivity (66.5 ± 6.8 μA cm^{-2} mM^{-1}), compared to early lactate sensors.[166-167] The high sensitivity, along with mechanical stretchability, reflects the combination of several factors, including the customized nanomaterial-based inks, the effective single-enzyme immobilization and electron shuttle, and the electrical communication associated with the simplified BFC configuration.[30] The selectivity was examined in the presence of common interference at physiological levels expected in real sweat.[95] As illustrated

in Figure 2.11E, the STAS offers high selectivity in the presence of common co-existing interference. Such an analytical selectivity of the self-power sensor is attractive compared with traditional amperometric biosensors that are subjected to interference from these co-existing electroactive species. The STAS thus enables monitoring of the analyte (fuel) in the real complex matrix without interference.[106, 110]

Figure 2.11C and Figure 2.10 demonstrate the "scavenge-sense-display" concept using the totally integrated system in connection with the biosensing of lactate. The system consists of the stretchable biofuel cell and the analog ammeter display, without any external power sources. The current signal from the sensor is extracted by the BFC (an energy bio-harvester that converts biochemical inputs into electricity), and is quantitatively monitored by the dial display due to the relationship of magnetic and electric fields in the ammeter. This results in a quantitative response as the electricity generated by the BFC is proportional to the biofuel concentration. As shown in Figure 2.10, the device has been printed on a variety of textiles, ranging from stretchable headbands, straps and socks. The real-time change in the autonomous current output upon increasing the lactate concentration is clearly observed. Electronic supplementary information including the video of the demonstration is also available (See DOI: 10.1039/c6ta08358g). This concept involves scavenging bio-energy from human perspiration while simultaneously monitoring the health status by the autonomous power output and using this energy itself to show the response. In order to further demonstrate the on-body performance of the new stretchable self-powered biosensing concept and obtain the real-time data, we adapted the compact wireless device to record the lactate signal on a smart phone. The system includes a STAS,

a resistor as a load, the compact wireless device, and a smart phone. The voltage output between the cathode and anode was measured by the compact device and transmitted to the smart phone *via* Bluetooth (Figure 2.13). The response of this wireless system compares favorably with that of a bench-top equipment (Figure 2.12A). Our STAS can eliminate concerns about external applied potentials as well as bulky and complex instrumentation, as illustrated in Figure 2.12B for integrating it with the sock-based biosensor and applying them on the volunteer's foot. Placing the sock-based STAT on the foot involves extreme mechanical strain. In order to monitor the real-time lactate concentration for the on-body test, the STAS was calibrated at 37 °C, reflecting the enzyme's activity in the physiological temperature. The volunteer wearing the sock-based STAT was asked to cycle at a constant level and the real-time voltage output was recorded during the cycling exercise (Figure 2.12D, left *y*-axis). The corresponding lactate concentration was obtained from the correlated calibration (Figure 2.12D, right *y*-axis). The output of the LOx-immobilized (purple plot) and the control "LOx-free" (black plot) of the sock-based STASs is shown for comparison. The real-time signal that was self-generated from the LOx-immobilized STAS clearly indicates the well-defined lactate response (different from the control one). Such a negligible background signal represents an attractive feature of the self-powered biosensing system, compared to common controlled-potential amperometric measurements. From the real-time lactate profile, no self-generated output is detected during the first stage of cycling. After the subject secreted the lactate-containing sweat, the self-generated signal output can be observed due to the power harvested from the lactate biofuel in the wearer's sweat. After operating the device

under physiological conditions for 50 minutes, the device was successfully rechecked to evaluate the operational stability, which indicated that it was still functional. This proof-of-concept demonstration can be further developed as a self-powered logic for manipulating biocomputing systems and could greatly simplify the design of intelligent miniaturized wearable electronics wherein mechanical compliance is also mandatory.[135, 168-169]

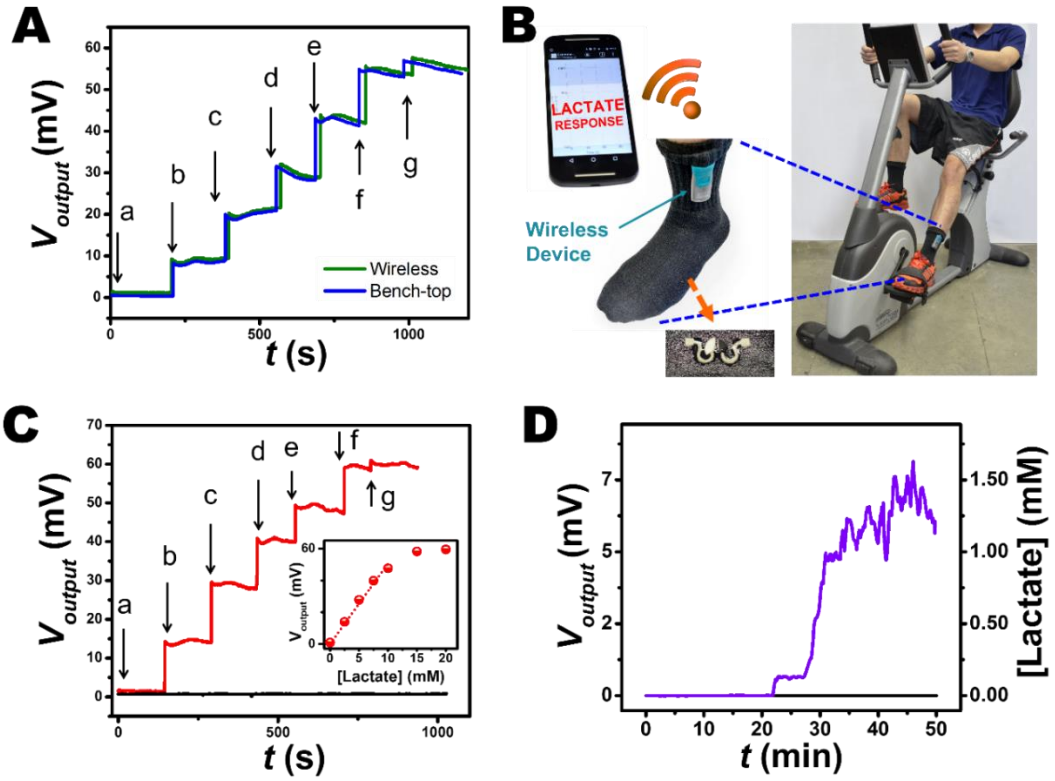

Figure 2.12 Self-powered lactate sensing. (A) Comparison of calibration obtained from a bench-top multimeter (blue plot) and a compact wireless device (green plot). (a–g: 0, 2.5, 5.0, 7.5, 10, 15, and 20 mM). No potential was applied. (B) The lactate STAS on the sock applied to a volunteer's foot. (The device was printed inside the sock.) The self-generated real-time signal obtained from the sock-based biosensor can be read and recorded wirelessly using a smartphone and a compact wireless device. The corresponding circuit is shown in Figure 2.13. (C) Self-generated voltage output obtained from the lactate STAS and a compact wireless device at 37 °C (a–g: 0, 2.5, 5.0, 7.5, 10, 15, and 20 mM). Response of the LOx- (red plot) and enzyme-free (black plot) sensors. No potential was applied. Inset: corresponding *in vitro* calibration curve of the lactate STAS at 37 °C, autonomous response to different lactate concentrations up to 20 mM. (D) Real-time lactate response obtained from the on-body test during the cycling exercise. The subject maintained a constant cycling rate for 50 min. Response of the LOx- (purple plot) and enzyme-free (black plot) STASs on the sock, with no applied potential. Adapted with permission.[27] Copyright 2016, The Royal Society of Chemistry.

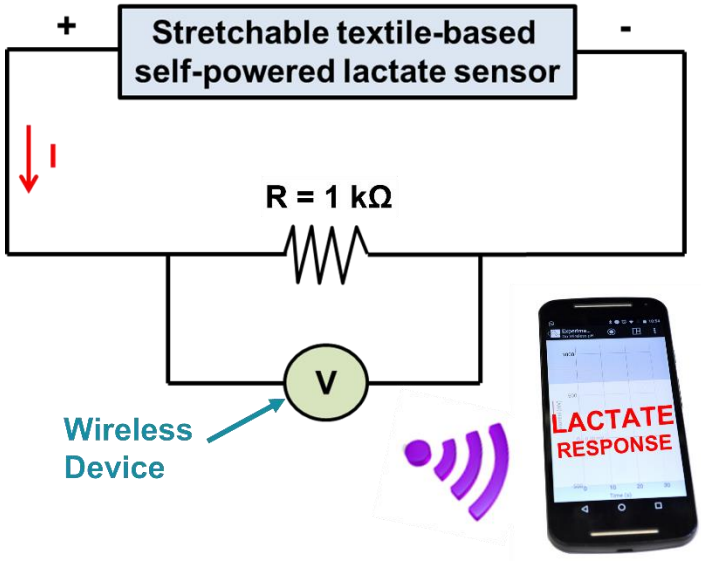

Figure 2.13 The scheme shows the circuit system for lactate monitoring. This allows reading and real-time wireless recording by using a smartphone and a compact wireless device. The compact wireless device with an integrated rechargeable battery was used to perform on-body measurements. Adapted with permission.[27] Copyright 2016, The Royal Society of Chemistry.

2.4 Conclusions

We demonstrated the fabrication and operation of stretchable textile-based printed biochemical energy harvesters and self-powered sensors. Tailored stretch-enduring inks and judicious design patterns were used for screen-printing these bioelectronic devices onto the corresponding textile substrates. Nanocomposite materials were carefully engineered to enhance the electrical, electrochemical, and mechanical properties. The resulting devices displayed remarkable mechanical resiliency without compromising their functionalities. To advance further understanding of the system behavior, future work will focus on strain distribution analysis to evaluate the combinational effects on the devices from intrinsic and design-induced stretchability using strain mapping analysis and theoretical mechanical

simulations. By addressing the limitations of traditional textile-based electrochemical devices, the new devices can readily conform to the body and are thus ideal for epidermal energy harvesting in diverse real-life situations. These capabilities offer considerable promise toward potential on-body, non-invasive self-powered sensing and energy-harvesting operations. The versatile fabrication approach could be applied to a wide range of soft commercial garments. The new bioelectronic socks can incorporate additional sensors (*e.g.*, pressure sensors for monitoring the foot pressure for athletes or diabetics) and can be integrated with mobility sport tracking devices to collect vital-sign data *via* wireless communication. The new textile-based stretchable devices thus hold considerable promise for next-generation of smart clothes for monitoring personal health and performance.

2.5 Acknowledgements

This work is supported by the NIH (Award R21EB019698) and DTRA (HDTRA1-16-1-0013). Itthipon Jeerapan, J. R. S, and A. P. acknowledge support from the Thai Development and Promotion of Science and Technology Talents Project (DPST), National Council for Scientific and Technological Development (CNPq-216981/2014-0), and FAPESP-BEPE (2015/08033-0), respectively.

Chapter 2 is based, in part, on the material as it appears in Journal of Materials Chemistry A, 2016, by Itthipon Jeerapan, Juliane R. Sempionatto, Adriana Pavinatto, Jung-Min You, and Joseph Wang. The dissertation author was the primary investigator and author of this paper.

Chapter 3 Fully Edible Biofuel Cells Toward Ingestible Biosensors and Bioelectronics

3.1 Introduction

Food-based electronics has recently opened a new chapter of biocompatible and safe medical devices with considerable diagnostic and therapeutic potential.[170] Such edible electronics can be coupled with ingestible devices to enable direct access to internal body systems, ranging from the mouth to the whole gastrointestinal (GI) tract, leading to biomedical operations which are impossible using traditional non-ingestible technology. The ability of edible devices to be digested makes them attractive candidates for monitoring the GI tract. Silk-based antenna sensors for *in situ* monitoring of food quality have been reported recently.[171] We demonstrated food-based electrochemical sensors that could monitor ascorbic acid and dopamine,[84] while Keller *et al.* reported edible hydrogel pressure sensors.[172] In addition to the biocompatibility issue, such ingestible electronic devices require adequate energy supply, regardless of their applications. While most commercially available ingestibles currently rely on coin batteries and many other energy storage devices have been reported, they are usually composed of toxic components and are subject to health and safety issues that hinder routine biomedical operations. To date, there are few reports on highly biocompatible energy-storage systems, and this has stimulated researchers to develop biosafe energy supply devices. Energy storage devices,

such as biologically derived batteries[173-174] and ingestible supercapacitors,[175] have thus been developed recently. Realizing alternative approaches for food-based energy harvesting and storage devices remains of tremendous interest. The biomedical impact of ingestible electronics could thus be greatly enhanced by expanding the spectrum of biocompatible energy-supplying devices.

This work demonstrates the first example of fully edible biofuel cells (BFCs) based solely on natural and processed food materials. BFCs using enzymes as catalysts can generate electricity from fuels such as sugars or alcohols.[13] Such devices represent 'green' alternative solutions for diverse energy harvesting applications, ranging from implantable power sources to energy sources for electronic and medical devices, self-powered sensors, and bioelectrocatalytic logic gates.[176-177] Such BFCs harvest electrical energy from chemicals present in biofluids, and can act as self-powered sensors for monitoring the fuel analyte concentration. The majority of common BFCs rely on biocatalytic reactions of the pure enzymes, along with mediators and common electrode materials (*e.g.*, Pt, C and Au). Microbial BFCs based on biofilms, using bacterium electrodes, have also been developed.[178] Despite the attractive advantages of BFCs and ingestible devices, there are no early reports on fully edible BFCs. Utilizing biocatalysts present in plant tissues[179-180] is potentially useful for BFC biocatalytic reactions, similar to tissue-based electrochemical sensors.[180] Gu *et al.* reported a tissue-based glucose/O_2 BFC in connection to different bioanode and biocathode paste electrodes.[181] However, it still required the use of carbon nanotubes, Meldola's blue mediator, and mineral oil, which are not food ingredients or highly biocompatible, and hence represent a major hurdle to

practical ingestible devices. Eliminating the need for additional reagents, such as redox mediators, commonly leads to a poor power performance, since mediators are crucial for shuttling electrons between enzymes and the electrode towards efficient power generation. In the following sections, the dissertation author and the team demonstrate a 'green' approach to address these issues by creating fully edible BFCs that offer environmentally-sustainable non-toxic energy-converting devices. The new BFC relies on food-based electrode materials along with biocatalytically-rich plant tissues containing the necessary anode and cathode enzymes and the corresponding co-factors. Such development of fully edible BFCs obviates the need for costly isolated enzymes, synthetic catalysts or mediators, and offers high biocompatibility, efficient, and environmentally eco-friendly energy harvesting routes towards meeting the power requirements of ingestible biomedical devices.

In the present study, membrane-less ethanol/air BFCs, without any additional chemical mediators, were introduced for implementing completely edible low-cost energy-harvesting platforms and self-powered biosensing in connection to carbon-paste bioanode and cathode matrices, as illustrated in Figure 3.1. Carbon paste BFCs are commonly prepared by dispersing graphite powder (along with the enzyme and mediator) within a water-immiscible non-conducting pasting liquid.[182] The present ethanol BFCs rely on two biocatalytic edible charcoal-based electrodes. These fully edible catalytic anode and cathode pastes were packed within hollow food supports, such as almond. For example, the present anode contains an ethanol-oxidizing alcohol oxidase (AOx) biocatalyst, present in an edible mushroom extract, while the cathode containing polyphenol oxidase (PPO)

along with phenolic compounds is present in apple tissue. In the present study, we evaluated and compared a variety of food-based materials for preparing biocatalytic-active pastes for the fabrication of biologically friendly BFCs. Such alcohol-based edible BFCs can be readily constructed without the requirement of a separator membrane and can serve as self-powered ethanol sensor. Such ingestible ethanol-based BFCs and sensors could facilitate the study of alcohol related effects, *e.g.*, dose dumping and dynamic effects on drugs.[183] Edible BFCs, fabricated entirely from food materials, can thus serve as a viable green strategy for on-body energy generation and self-powered biosensing.

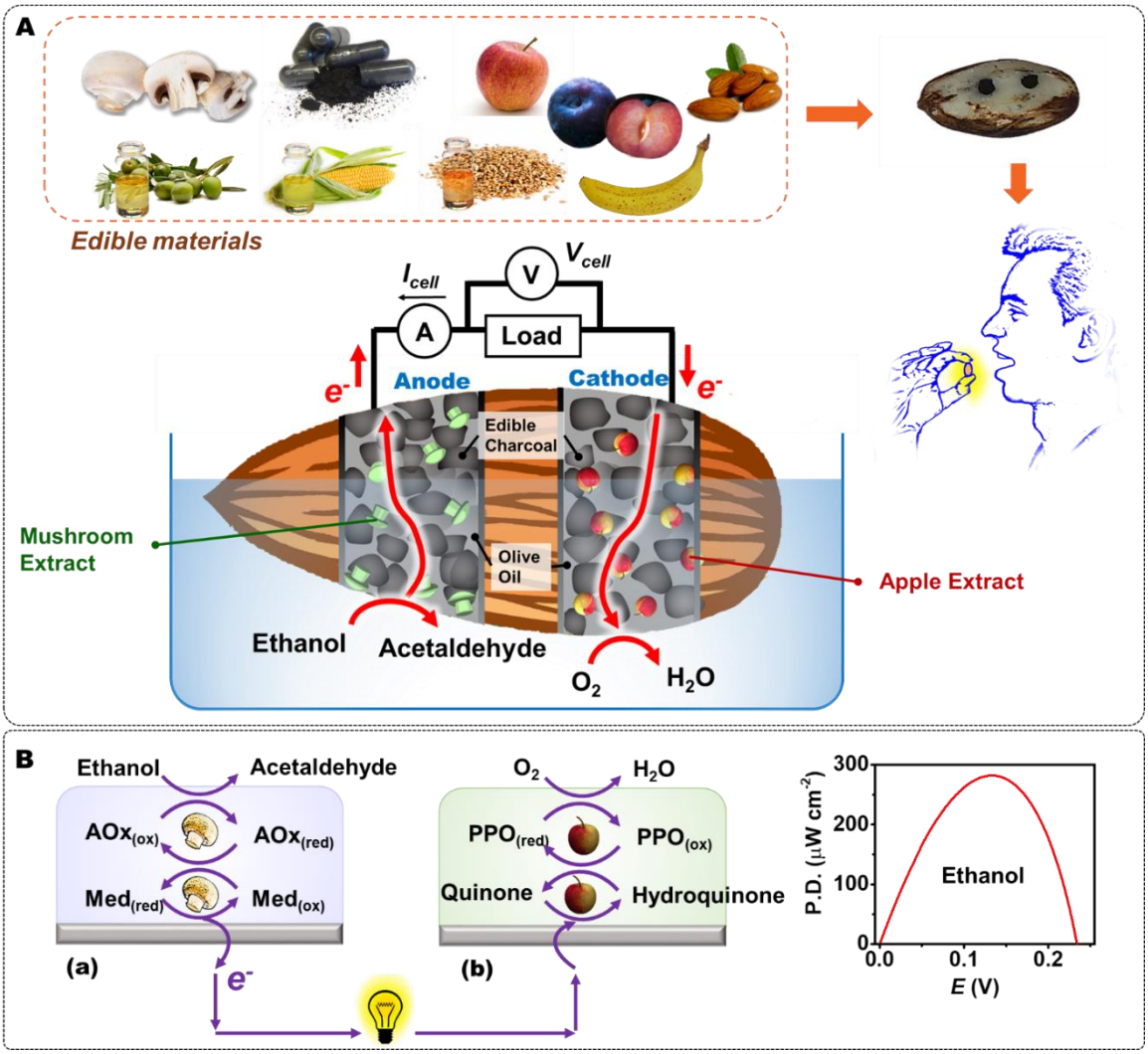

Figure 3.1 Fully edible energy-harvesting BFCs. (A) Scheme of edible material-based electrodes, consisting of a variety of food-based materials, and of the BFC configuration. (B) Schematic configuration of the edible membrane-free ethanol BFCs and the redox reactions that occur on the anode (a) and cathode (b). AOx and Med refer for the alcohol oxidase biocatalyst and the natural mediator present in the edible mushroom, respectively. PPO is polyphenol oxidase present in the apple. Adapted with permission.[72] Copyright 2018, The Royal Society of Chemistry.

3.2 Experimental Section

3.2.1 Materials and Reagents

The edible activated charcoal (Nature's Way Products, Inc., USA), white Crimini mushroom (*Agaricus bisporous*) , Fuji apple (*Malus pumila*), Black Amber plum (*Prunus domestica*), Cavendish banana (*Musa acuminata*) , extra virgin olive oil (Kroger, USA), corn oil (Mazola, USA), sesame oil (Kadoya, Japan), and almond (Wonderful, Lost Hills, CA) were purchased from a local grocery store. Graphite powder was purchased from ACROS Organics. Alcohol oxidase (AOx, from *Pichia pastoris*, 10–40 units per mg protein), mineral oil, tetrathiafulvalene (TTF), potassium phosphate dibasic (K_2HPO_4), and potassium phosphate monobasic (KH_2PO_4) were purchased from Sigma-Aldrich. Ethanol was purchased from Koptec, USA. All chemicals were of analytical grade and were used without further purification. Ultra-pure deionized water (18.2 MΩ cm) was used for preparing all of the aqueous electrolyte solutions.

3.2.2 Electrode Preparation

Various edible electrodes were prepared by mixing dietary charcoal with vegetable oils, along with natural plant/mushroom-based biocatalyst materials directly obtained from vegetables and fruits. The mushroom and other food materials were cut, crushed, and then squeezed to obtain the pulp. The water content in the pulp was evaporated under a

N_2 bubbling atmosphere until the pulp was preconcentrated eight times by volume. The mushroom/olive oil bioanode was prepared by thoroughly grinding 250 mg of edible charcoal, 250 mg of the preconcentrated mushroom extract, and 67 μL of olive oil in an agate mortar. Similarly, the apple/olive oil biocathode was prepared by thoroughly mixing 250 mg of edible charcoal, 250 mg of the preconcentrated apple extract, and 67 μL of olive oil. The resulting pastes were packed firmly into the cavity of food materials (*e.g.*, almond). Afterward, the electrode surface was smoothed on clean weighing paper. The surface could be refreshed by pushing an excess amount of the paste out of the holder and polishing the electrode surface. Different extracts and electrodes were prepared in a similar process. The paste compositions are summarized in the following section. To perform the characterization of the BFCs and record the data, a conventional potentiostat was connected to the edible compartments *via* metal wires. Such characterization and connection involved a 0.9 mm diameter stainless steel wire placed into the inner ends of the two electrodes.

3.2.3 Electrode Compositions

3.2.3.1 Edible Electrodes

The edible mushroom/olive oil/charcoal bioanode was prepared by thoroughly grinding 250 mg of preconcentrated mushroom solution, 67 μL of olive oil, and 250 mg of dietary charcoal in an agate mortar. The resulting homogenous paste was packed into the support cavity to obtain a workable electrode. Similarly, edible mushroom/corn oil/charcoal and mushroom/sesame oil/charcoal anodes were prepared, but the olive oil

was replaced by corn and sesame oils, respectively. In addition, the edible apple/olive oil/charcoal biocathode was prepared by thoroughly mixing 250 mg of preconcentrated apple solution, 67 µL of olive oil, and 250 mg of dietary charcoal in an agate mortar. Similarly, the edible apple/corn oil/charcoal and apple/sesame oil/charcoal cathodes were prepared, but the olive oil was replaced by corn and sesame oils, respectively. The edible plum/olive oil/charcoal and banana/olive oil/charcoal cathodes were also prepared in a similar process, but the apple solution was replaced by plum and banana solutions, respectively. Moreover, the control edible electrode without extracts was prepared in a similar process by using the homogeneous paste consisting of 250 mg of dietary charcoal and 200 µL of olive oil.

3.2.3.2 Non-Edible Electrodes

The non-edible alcohol oxidase (AOx)/tetrathiafulvalene (TTF)/mineral oil/graphite anode was prepared by thoroughly mixing 80 µL of five-fold-diluted AOx solution, 40 mg of TTF, 150 µL of mineral oil, and 250 mg of graphite in an agate mortar. The resulting homogenous paste was then packed into the support cavity to obtain a workable electrode. The non-edible AOx/mineral oil/graphite without TTF was also prepared in a similar process, but TTF was not added. In addition, the non-edible Ag_2O/Nafion®/graphite cathode was prepared by the following. Graphite/Ag_2O mixture was prepared by thoroughly grinding graphite with Ag_2O powder (2:3 wt. ratio) in an agate mortar. The cathode paste was obtained by mixing 250 mg graphite/Ag_2O composite with 900 µL of a 2 wt% Nafion in ethanol to obtain a homogeneous composite material. The

homogenous paste was then packed into the support to obtain the non-edible Ag_2O/Nafion®/graphite cathode.

3.2.4 Electrochemical Study

The electrode resistance was measured using an Agilent multimeter (6½ digit model 34411A). The resistance of these packed electrode composites was measured and calculated from two-probe resistance data using the equation: resistivity = RA/L, where R, A, and L are the resistance (Ω), cross sectional area (cm^2), and length (cm), respectively. The resistivity of edible electrodes with different compositions is summarized in Table 3.1.

Table 3.1 Resistivity of different compositions of the edible electrodes. Adapted with permission.[72] Copyright 2018, The Royal Society of Chemistry.

Electrodes	Extracts	Oils	Resistivity (Ω cm)
Anode	Mushroom	Olive oil	15
		Corn oil	16
		Sesame oil	10
Cathode	Apple	Olive oil	5
		Corn oil	5
		Sesame oil	4
	Plum	Olive oil	6
	Banana	Olive oil	17

BFCs were investigated at room temperature in a single chamber without any separating membrane. Batch experiments were performed. Electrochemical experiments were carried out using a μAutolab Type II controlled by the NOVA software (version 1.11). The power curves were obtained by scanning the voltage between the open circuit voltage (OCV) of the BFC and 0 V at a constant scan rate of 5 mV s^{-1}. The geometrical area of each compartment (~0.06 cm^2) was used to calculate the areal power density. A 0.5 M phosphate buffer solution (PBS, pH 7.4) was used as a supporting electrolyte. Electrodes were immersed in the test solution for 45 min at room temperature prior to the electrochemical characterization.

3.2.5 Electrode Storage and the Stability Test

After careful packing of the electrodes, they were stored in a dry container in a fridge. Therefore, both the anode (based on the mushroom extract) and the cathode (based on the apple extract) maintained their biocatalytic activity, ready to be reused. Before the tests, the electrodes were removed from the fridge and allowed to reach room temperature. The electrode surface was gently smoothed on weighing paper, with a fresh electrode layer exposed to the ethanol solution. During the stability test, the packed BFCs were stored (between each power curve) in a 0.5 M PBS (pH 7.4) solution containing 500 mM ethanol at room temperature.

3.3 Results and Discussion

3.3.1 BFC Configurations

The new concept of fully edible BFCs as highly biocompatible energy-harvesting devices is based only on materials found in common diets, without any additional chemicals. Daily food materials and products were fully transformed into edible electrodes. The resulting ingestible energy-harvesting devices rely on the biocatalytic conversion of ethanol into electricity and consist of two key compartments: an edible anode and cathode, packed in a supporting almond sleeve holder (Figure 3.1 (A)). Dietary activated carbon, mixed thoroughly and homogeneously with olive oil, served as an edible conductive paste

support. Extracts obtained directly from mushroom and apple are used as the biocatalytic systems of the anode and cathode, respectively. As shown in Figure 3.1A (bottom), the complete BFC was assembled by using the edible anode and cathode. The current–voltage behavior of the BFC in a closed circuit at different external loads was investigated by using a potentiostat. Therefore, the power output was obtained using the $P = IV$ relationship, where P, I, and V are the power output, current output, and voltage of the BFC, respectively. As illustrated in Figure 3.1B, the ethanol fuel can be oxidized and generates electrons on the anode, assisted by the biocatalytic system present naturally in the mushroom extract component of the bioanode. On the cathode compartment, electron accepting reactions completing the energy-converting circuitry rely on the oxygen-reducing PPO enzyme coupled with the phenolic constituents of the apple extract. Traditionally, the membrane separating cathode and anode compartments of BFCs are used to isolate the reaction compartments and control the permeability and transport across the two compartments, leading to a major drawback of BFCs.[184] Advantageously, a favorable selective reaction of biocatalysts (*e.g.*, from mushroom and apple) offers an attractive behavior, obviating the need for such a membrane, and simplifying the BFC assembly in connection to low cost edible food sources.

The ethanol oxidation at the bioanode is based on the biocatalytic ability of its mushroom tissue component.[179] The homogenized mushroom extract provides the biocatalytic activity necessary to catalyze the ethanol oxidation reaction.[181] Effective electronic communication with the co-existing natural mediators offers a safe alternative to common redox mediators. Despite the absence of additional mediators, a favorable

power generation performance has thus been obtained from the fully edible mushroom-based BFCs. Such BFC performance is indicated from the OCV and power output of Figure 3.1B. Considering the tremendous interest of studying and exploiting the presence of alcohol in the small intestine,[185] where the pH is around 7,[186] the test electrolyte solution for the present proof-of-the-concept had a pH of 7.4.

The biocathode carries redox biocatalysts containing polyphenol oxidase (PPO), catalyzing two different oxygen-involved reactions, including the hydroxylation of monophenols to *o*-diphenols and the oxidation of *o*-diphenols to *o*-quinones.[181, 187] Different sources of oxygen-involved cathodic biocatalysts, including extracts from apple,[188] plum,[189] and banana,[190-191] were investigated. On these cathodes, PPO was employed to assist in the oxygen reduction reaction to water. For instance, the dissolved O_2 is electroreduced to water at the apple-based cathode, which can be catalyzed by the PPO enzyme obtained from the apple extract. PPO also quickly oxidizes phenolic compounds (naturally existing in the apple tissue) to quinones. This process will accept the electrons generated by the anode, eventually completing the power circuit. The resulting power performances are shown in Figure 3.2A. Similar processes also occur at the plum- and banana-based cathodes. The resistivity of different cathode compositions consisting of apple, plum, and banana extracts was 5, 6, and 17 Ω cm, respectively. The apple/olive paste composition had comparable but slightly better conductivity than the plum-based one. The BFCs using apple-, plum-, and banana-based cathodes displayed maximum power outputs of 282, 182, and 63 μW cm^{-2}, respectively. The fully edible BFC using the apple-based cathode provided the highest power performance, reflecting its high conductivity, efficient

electron transfer and catalytic activity. The banana/olive cathode yielded a low electrical conductivity, leading to a low power output.

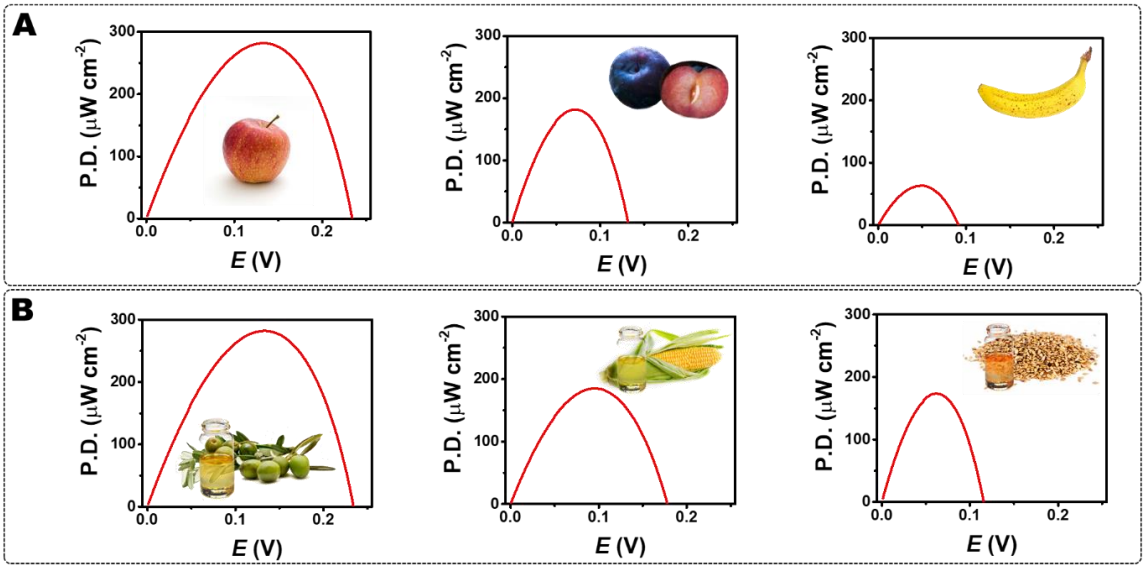

Figure 3.2 Power density *vs.* potential plots obtained from different fully edible BFCs based on (A) different plant extracts and on (B) different edible oils in 0.5 M PBS (pH 7.4) containing 500 mM ethanol. (A) Study of different tissue extracts for the cathodes: apple, plum, and banana (from left to right, respectively) as biocatalytic electron-accepting systems, along with an olive oil-based mushroom anode. The results are obtained from different cathodes containing apple, plum, and banana (from left to right, respectively). (B) Study of different edible oils. Results obtained from different mushroom/apple-based BFCs based on different oil binders: olive, corn, and sesame oils (from left to right, respectively). Adapted with permission.[72] Copyright 2018, The Royal Society of Chemistry.

Conventional carbon paste BFC devices commonly rely on water-immiscible (non-edible) mineral oil non-conducting pasting liquid binders. The selection of an appropriate food binder plays an important role in developing effective BFC anodes and cathodes. Such an oil binder prevents leaching of the paste constituents. The creation of an edible BFC requires replacement of the non-edible mineral oil. A variety of paste materials based on different edible binders (oil pasting liquids), such as olive oil, corn oil, and sesame oil, were thus examined for preparing the edible paste electrodes. The resistivity of mushroom

bioanode compositions using different oils (olive, corn, and sesame oils) was 15, 16, and 10 Ω cm, respectively. The resistivity of the apple cathodes using different oils (olive, corn, and sesame oils) was 5, 5, and 4 Ω cm, respectively. The resulting power performances of these different oil-based mushroom/apple-based BFCs are compared in Figure 3.2B. The edible olive-oil based BFC provided a higher power density compared to the corn oil-based BFC, with the maximum-power density outputs of 282 and 185 μW cm^{-2}, respectively, along with the OCVs of 0.24 and 0.18 V. Using the sesame-oil binder, the edible BFC displayed a low power performance with an OCV of 0.12 V and a peak power density of 173 μW cm^{-2}.

3.3.2 Conceptual Studies

The new edible BFC concept was studied systematically. Initially, we recorded the power curve of a BFC consisting of the mushroom-based bioanode coupled with an apple-based cathode, in the presence of an ethanol fuel solution (Figure 3.3A). This BFC performed well, displaying an OCV of 0.34 V and power in the region of 280 μW cm^{-2}. In contrast, keeping the same apple-based cathode while removing the mushroom component from the anode resulted in a greatly diminished power curve, down to the nW cm^{-2} range, as expected without the ethanol oxidation reaction (Figure 3.3B). Such a dramatic decrease in the power output reflects the significant role of the mushroom biocatalytic reaction in the bioanode. Similarly, on the opposite side, we investigated a BFC based on the use of a workable mushroom anode along with the control cathode (without apple materials). The resulting power curve, plotted in Figure 3.3C, displays an extremely low power (in the nW

cm^{-2} range), reflecting the absence of biocatalytic activity at the cathode, despite the presence of the ethanol fuel and the edible mushroom-based biocatalytic anode.

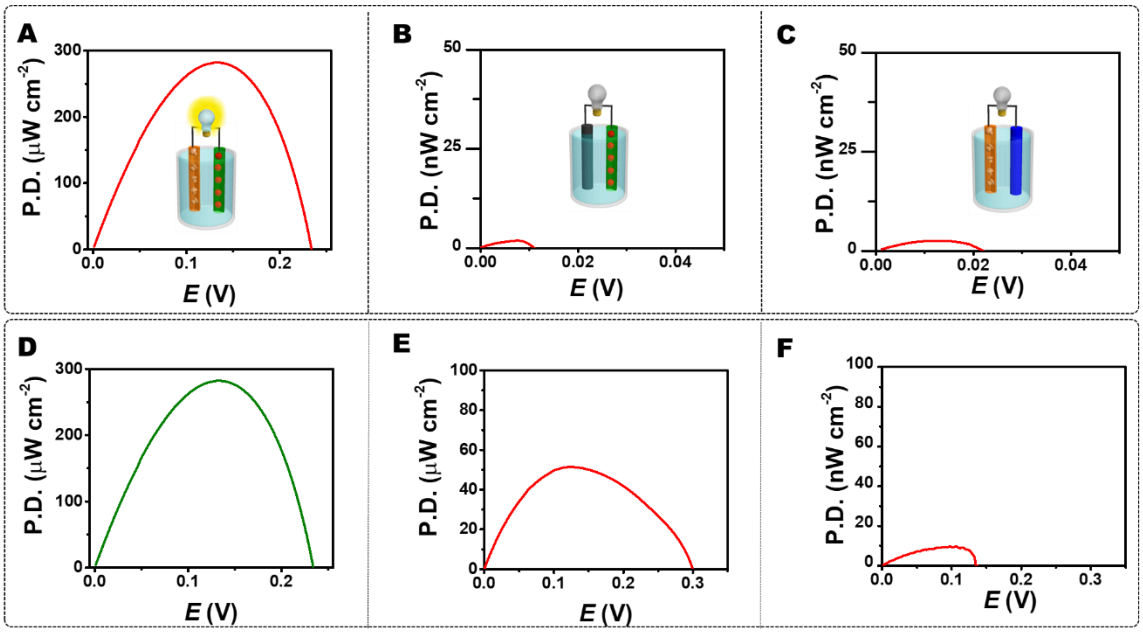

Figure 3.3 Conceptual studies of (A–C) edible anodes and cathodes, and (D–F) power curves of edible *versus* non-edible electrodes. (A–C) Power density *vs.* potential plots obtained from fully edible BFCs acquired with (A) the BFC consisting of a mushroom-based anode coupled with an apple-based cathode, (B) a BFC consisting of a control anode (without the mushroom) coupled with an apple-based cathode, and (C) a mushroom-based anode coupled with a control cathode (without apple materials). (D–F) Power density *vs.* potential plots obtained from (D) the fully edible BFC and (E and F) non-edible BFCs: (D) the fully edible BFC, consisting of a mushroom/charcoal/olive oil anode and an apple/charcoal/olive oil cathode; (E and F) non-edible BFCs consisting of an AOx/graphite/mineral oil anode (E) with and (F) without the TTF mediator, respectively, along with an Ag_2O/graphite/Nafion cathode. Power density *vs.* potential plots showing the performance obtained in 0.5 M PBS (pH 7.4) containing 500 mM ethanol. Adapted with permission.[72] Copyright 2018, The Royal Society of Chemistry.

For most enzymes, the shuttling of electrons between the enzymes and electrode surfaces is inherently inefficient. AOx is an enzyme that catalyzes the alcohol oxidation. Characteristically, in the absence of mediating molecules, the direct electrochemical transfer of electrons is problematic, since the active center flavin adenine dinucleotide (FAD) is deeply located in a protein shield.[192] Accordingly, establishing electrical

communication between the biocatalysts and electrodes is essential for the development of biosensors and BFCs.[41, 193] It is crucial to employ additional mediators or specific electrochemical surfaces to establish efficient electron transfer from enzymes to electrodes. Even though redox mediators facilitate electron transfer, they have limitations, in particular in biomedical applications.[13, 194] For example, mediators may leak out during on-body operation and cause toxicity. Importantly, for engineering edible devices, a critical criterion is that all components must be harmless to the user. Numerous attempts have thus been devoted to eliminating mediators by using nanomaterials, such as carbon nanotubes.[68, 195] In the present work, the limitations of mediators for fabricating edible devices have been addressed by relying on the built-in mediator-pathways present in the tissue extracts. The ethanol BFC can thus be prepared without any extra mediators by employing the mushroom extract which leads to an efficient anodic bioelectrocatalytic reaction (Figure 3.3D). The food-based materials used to fabricate the BFC are highly biocompatible, allowing the user to safely consume all components.

The fully edible BFC was compared to non-edible BFCs based on commercial AOx from *Pichia pastoris* for the anode, along with Ag_2O as a cathode. This non-edible BFC carbon-paste relies on mixing graphite powder with the common mineral oil pasting liquid. The organosulfur TTF mediator was used to promote the efficiency of the BFCs.[196-197] The power performance obtained from the non-edible BFCs, consisting of the AOx/TTF/graphite/mineral oil anode and the Ag_2O/graphite/Nafion cathode, is shown in Figure 3.3E. In the presence of the TTF mediator, the alcohol fuel is oxidized by AOx with electrons transferred to the conducting carbon supports *via* the mediated electron

transfer system, and eventually flowing through the load to the cathodic side. This BFC yields an OCV of 0.30 V with a peak power density of 52 μW cm^{-2} (at 0.13 V). Upon removing the mediator, the non-edible BFCs consisting of the AOx/graphite/mineral oil anode and the Ag_2O/graphite/Nafion cathode displayed a very low power output, with an extremely small OCV of 0.06 V and a maximum power density of 9 nW cm^{-2} (Figure 3.3F). Compared with the mediated non-edible system (from Figure 3.3E), the power performance of the non-mediated system (Figure 3.3F) dropped dramatically (~5800 times), reflecting the difficulty of shuttling electrons without the electron-transfer mediator.

3.3.3 Edible Self-Powered Ethanol Biosensing

One of the attractive applications of BFCs is self-powered biosensing.[18, 27, 135] Such self-powered devices simplify the assembly and operation of biosensors and minimize interferences from co-existing electroactive species compared to common amperometric biosensing devices.[18, 27] The anode can thus act as a working fuel-sensitive sensing electrode. Ethanol, as a biofuel undergoing oxidation by the mushroom biocatalytic AOx, can thus lead to a power output that is proportional to the fuel analyte concentration. As shown in Figure 3.4A, the generated power intensity increased with ethanol concentration, clearly suggesting that the ethanol oxidation process is catalyzed by the mushroom-containing biocatalyst. The resulting calibration plots of the edible self-powered electrochemical ethanol biosensor are shown in Figure 3.4B. The maximum power and OCV responses of the edible BFC-based sensor devices at variable ethanol

concentrations are shown in Figure 3.4B (left and right *y*-axes, respectively). Both the peak power and OCV outputs increase linearly upon adding the ethanol analyte (fuel), leading to calibration plots with a good correlation (R^2 = 0.99) with the concentration. The sensitivity of the maximum power and the OCV ethanol response correspond to 0.24 μW mM^{-1} cm^{-2} and 0.15 mV mM^{-1}, respectively. These analytical data indicate that the edible ethanol BFC is promising for operation as an edible self-powered sensing device.

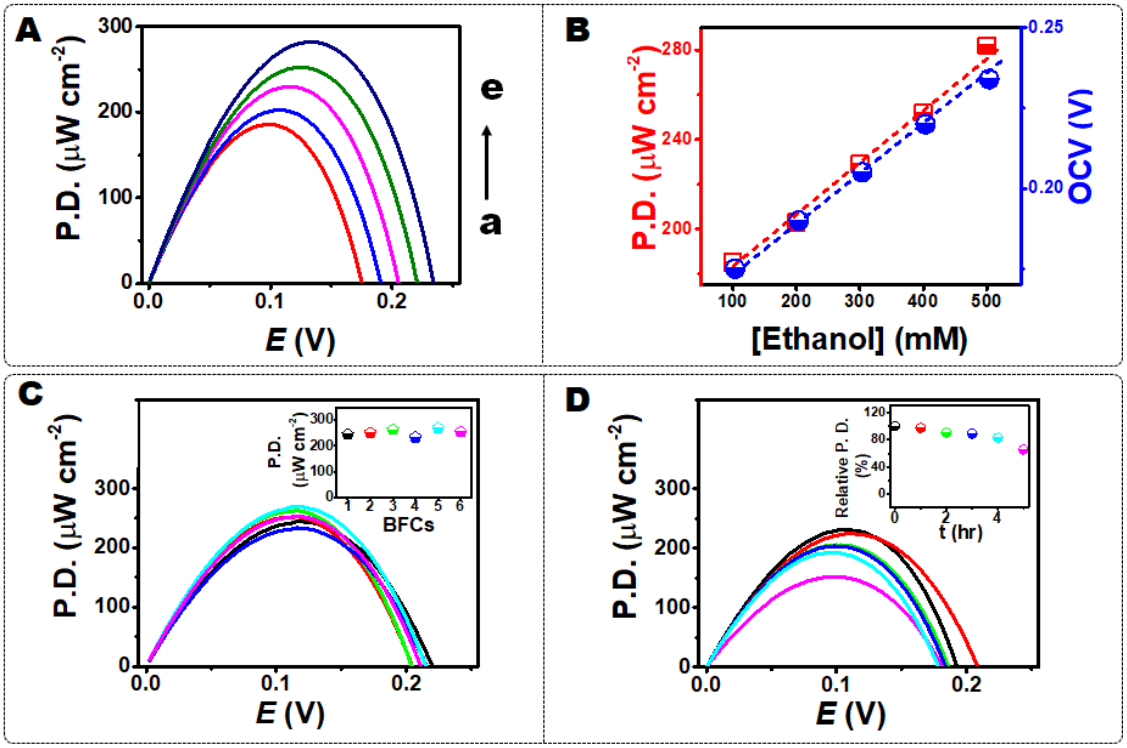

Figure 3.4 (A and B) Self-powered ethanol biosensors and (C and D) reproducibility and stability studies. (A) Power density vs. potential plots of the BFCs at various ethanol concentrations ((a–e) 100, 200, 300, 400, and 500 mM) in 0.5 M PBS (pH 7.4). (B) Corresponding ethanol responses obtained from the BFCs, showing their (red square plots) maximum power output and (blue circle plots) open circuit voltage (OCV) vs. ethanol concentration. (C) Reproducibility test obtained from different edible BFCs. The inset shows the corresponding maximum power outputs. (D) Stability test for edible BFCs. The inset shows the relative power density outputs. The power performance was obtained in 0.5 M PBS (pH 7.4) containing 500 mM ethanol. Adapted with permission.[72] Copyright 2018, The Royal Society of Chemistry.

3.3.4 Reproducibility and Stability

Plant/mushroom tissues offer increased stability to their enzymes by maintaining them in their natural environment.[198] The reproducibility and stability of the edible ethanol/O_2 BFCs, based on the mushroom anode and the apple cathode, were investigated using a 500 mM ethanol fuel concentration (Figure 3.4C). The power density for a series of 6 repetitive power curves had a relative standard deviation of 5.5%. This indicates good reproducibility using such a simple low-cost fabrication process. In addition, the stability of the food material-based BFCs was investigated by measuring their power harvesting over an extended period. For example, Figure 3.4D shows the output of the edible BFC during a five-hour period using 500 mM ethanol fuel. These data indicate that the BFC remains operational during this long period, maintaining 80% of its initial power over the first four hours, with further decrease to 65% of the initial output after five hours.

3.4 Conclusions

We have demonstrated the first example of fully edible BFCs with ingestible electrode composites based solely on food materials. Different food materials were evaluated as components of edible anodes and cathodes, including dietary activated charcoal, mushroom, apple, and vegetable oils, leading to an attractive BFC performance. The resulting energy harvesting devices are extremely attractive owing to the fully biodegradable, ingestible, and edible properties of their food-materials constituents. The

power harvesting efficiencies of such food-based edible paste composites have been compared for selecting the most effective materials for creating ethanol-based BFCs. The edible ethanol/O_2 BFC anode and cathode were composed of different natural extracts, vegetable oil and charcoal. The ethanol fuel oxidation at the bioanode relies on the biocatalytic activity of the AOx constituent of its mushroom component. The cathode is based on an oxygen-reducing PPO enzyme along with phenolic compounds present in its apple component. The remarkable natural and selective biocatalytic pathways available in such plant extracts address the limitations of toxic chemical mediators and obviate the need for a membrane separating the anode and the cathode. The resulting devices displayed favorable power performance, with output approaching 300 μW cm^{-2}. Moreover, the mushroom/apple-based BFC displayed power and OCV outputs which increased linearly with the ethanol fuel concentration towards the realization of ingestible self-powered biosensors. The edible BFCs thus represent an attractive route for edible energy harvesting devices and could be coupled with edible energy storage devices. Such food-material based BFCs could eventually supply the power necessary for operating ingestible capsules along the gastrointestinal tract. Such an edible energy-conversion system thus indicates considerable promise for diverse biomedical applications, involving *in vivo* diagnostics and treatment of patients. The rich enzymatic activity of plant tissues (with the presence of multiple enzymes) could facilitate wider energy-harvesting applications, with the multiple biochemicals present in the GI tract serving as potential fuels. The effect of the source and season of the natural tissue upon the biocatalytic activity, and hence the resulting power, will be examined in future studies, along with further insights into the biocatalytic activity

of these tissue extracts. Such future efforts will also assess the performance of the new edible BFC in the relevant biological media (*i.e.*, GI tract fluids). Studies in such complex media will require an additional permselective protective layer to prevent biofouling and extend the BFC lifetime. Swallowable devices, integrating the edible BFC with sealed miniaturized electronics, will be the subject of future efforts. Ultimately, food-based electronics could be realized for a fully edible microsystem.

3.5 Acknowledgements

This work was supported by the Defense Threat Reduction Agency Joint Science and Technology Office for Chemical and Biological Defense (HDTRA1-16-1-0013). Itthipon Jeerapan and B. C. acknowledge support from the Thai Development and Promotion of Science and Technology Talents Project (DPST) and from a Fulbright grant and UMF Cluj-Napoca, Romania (Grant no. 7690/24/15.04.2016), respectively.

Chapter 3 is based, in part, on the material as it appears in Journal of Materials Chemistry B, 2018, by Itthipon Jeerapan, Bianca Ciui, Ian Martin, Cecilia Cristea, Robert Sandulescu, and Joseph Wang. The dissertation author was the primary investigator and author of this paper.

Chapter 4 Challenges of Oxygen Reduction Reaction in the Cathode of Biofuel Cells

4.1 Introduction

Tremendous research efforts have been devoted to the development of enzyme-based biofuel cells (BFCs) for a variety of applications,[13] such as energy-harvesting devices,[199-200] self-powered sensors,[27, 110] and biocomputers.[201] In particular, oxidase-based BFC based on metabolite fuels, such as glucose,[202] lactate,[27] cholesterol,[110] or ethanol,[203] have been developed for a variety of biomedical and biotechnological applications. Particular attention has been given to the development of bioenergy devices[199-200] as a source of renewable and sustainable power. Such BFCs offer considerable promise for harvesting usable electrical energy from metabolites present in biofluids. The most commonly described BFC consists of a glucose oxidization anode and an oxygen-reducing cathode.[204] Oxygen is widely used in the cathode compartment because it is a readily available good oxidant that leads to harmless products. The four-electron reduction of oxygen to water, used in most fuel cell cathodes,[205] is one of the most widely studied electrochemical reactions. The performance and power of metabolite/oxygen BFC, thus, strongly depend on the oxygen concentration. This leads to a tremendous challenge to the development of effective oxygen-based BFCs, especially in anaerobic circumstances, such as wearable and

implantable BFCs devices, or for other harvesting applications involving oxygen-deficit conditions.

One approach toward the design of an implantable, membrane-less, and biocompatible BFC consists of catalyzing the oxidation of glucose at the anode using glucose oxidase or glucose dehydrogenase, coupled to oxygen reduction at the cathode by an oxygen-reducing enzyme (*e.g.,* laccase) or platinum nanoparticles supported on carbon. Unfortunately, oxygen fluctuations can cause a considerable change in the BFC performance of these glucose BFCs. Fluctuating and low oxygen levels can be expected in various realistic scenarios, ranging from the low concentration of O_2 in certain biofluids (on skin, mouth, or blood) to biological processes involving anaerobic respiration that occur under low oxygen levels.[206] These oxygen limitations are generally attributed to the BFC cathode. Therefore, it is essential to develop an effective bioenergy-harvesting approach that alleviates the severe oxygen limitations during the long and short operations of implantable and wearable BFC, respectively.

Various efforts have been devoted for satisfying the oxygen requirement of the BFC cathode reaction. One route to address the oxygen limitation involves designing BFCs based on additional oxidant materials, *e.g.*, silver oxide (Ag_2O)[93] and tri-iodide (I_3^-).[207] While these alternative cathodes can accept electrons, oxidants (*i.e.*, Ag_2O or I_3^-) are inherently not natural fuel sources, and unlike oxygen, require an extra regeneration step. For example, Dong's group demonstrated a BFC based on a glucose dehydrogenase anode and a silver oxide/silver (Ag_2O/Ag) cathode. The solid-state Ag_2O cathode accepts

electrons and forms the Ag product, generating the power, but it requires back-conversion of Ag into Ag_2O in harsh basic conditions,[93] hence limiting long-term operations, *e.g.*, of implantable or continuous monitoring devices. As a result, researchers have continued to focus on oxygen-based cathodes. The use of air-breathing gas cathodes has been proposed.[208] Although these devices can assist in supplying oxygen *via* the gaseous phase, assembling such BFC devices introduces major technological challenges. Hence, there are considerable needs for developing self-sustaining metabolite/oxygen BFCs, operating under severe oxygen depletion or fluctuations. To the best of our knowledge, no studies have been reported on the operation of glucose/oxygen BFC (using O_2 as the renewable fuel) under oxygen-deficit conditions, including the absence of oxygen. Oxygen-rich cathodes have been described,[209-210] but not in connection to BFCs or oxygen deficiency. Despite these continuing efforts, there are no reports on glucose/oxygen BFCs that can function under fully anaerobic situations.

This chapter demonstrates, for the first time, an effective glucose/oxygen BFC – utilizing glucose-based bioanode and oxygen-reducing cathode – that can operate successfully under severe oxygen-deficit conditions, including complete anaerobic conditions. The new oxygen-independent enzymatic BFC relies on a glucose oxidase-mediated composite bioanode and an oxygen-rich polychlorotrifluoroethylene (PCTFE)-based platinized carbon cathode that satisfies the oxygen requirement for the cathode reaction even in oxygen-free solutions with 90% of the initial power for ~ 10 h. The internal flux of oxygen, associated with the high oxygen solubility in the PCTFE fluorocarbon binder of the cathode nanocomposite,[211] thus facilitates the oxygen

reduction cathode reaction under severe oxygen-deficit conditions. Such remarkable oxygen-storage capacity of the composite cathode electrode enables the new BFC to operate continuously under O_2 fluctuating and anaerobic conditions (N_2-saturated atmosphere) over extended time periods. Oxygen-rich electrode binders have been used previously for oxidase-based amperometric biosensors,[211] but not in connection to energy harvesting BFCs. The new oxygen-rich cathode strategy is thus promising for enhancing bioenergy conversion systems by supplying oxygen internally when oxygen levels are low or fluctuating by using other catalysts for advanced biosensing applications in anaerobic systems.

4.2 Experimental Section

4.2.1 Chemicals and Reagents

Carboxylic acid functionalized multi-walled carbon nanotubes (CNTs) (purity >95%, diameter = 10–20 nm, length = 10–30 μm) were purchased from Cheap Tubes Inc. Glucose oxidase (GOx) from *Aspergillus niger*, Type X-S (EC 1.1.3.4), catalase from bovine liver, mineral oil (MO), D (+)-glucose, tetrathiafulvalene (TTF), 1-butyl-3-methylimidazolium hexafluorophosphate (ionic liquid, IL), platinum black particles (≤ 20 μm), potassium phosphate dibasic (K_2HPO_4), and potassium phosphate monobasic (KH_2PO_4) were purchased from Sigma-Aldrich. Kel-F (PCTFE) oil was purchased from Ohio Valley Specialty Chemical (USA).

All chemicals were of analytical grade and were used without further purification. Ultra-pure deionized water (18.2 MΩ cm) was used for all of the aqueous electrolyte solutions. Glucose stock solution was allowed to mutarotate for at least 24 h prior to use and stored at 4 °C.

4.2.2 Preparation of the Glucose Bioanode

The enzymatic bioanode was prepared by thoroughly grinding 10 mg CNTs, 12.5 mg GOx, 5.1 mg TTF, 27 μL MO, and 12.5 mg catalase in an agate mortar. Grinding proceeded for about 20 min with a pestle. The resulting paste was filled compactly into the cavity of a plastic tube (2.8 mm inner diameter and 8 mm depth). Subsequently, the electrode surface was smoothed on a weighing paper. Only the tip of the carbon-paste tube was exposed to the test solution. Electrical contact was made by using a 0.8 mm diameter conductive stainless-steel wire.

4.2.3 Preparation of the Cathode

The oxygen-rich PCTFE/IL-based cathode was prepared in a similar way by mixing 10 mg CNTs, 5 mg Pt, 25 μL PCTFE oil and 25 μL IL. The conventional (MO-based) carbon paste cathode, used as a control, was prepared by mixing 10 mg CNTs, 5 mg Pt and 50 μL MO. The pastes were used in similar process as the anode.

4.2.4 Electrochemical Measurements

All experiments were carried out at room temperature in a single batch chamber. Electrochemical experiments were performed using a μAutolab Type II controlled by NOVA software (version 1.11). The power curves were obtained by scanning the voltage between the open circuit voltage (OCV) of the BFC to 0 V at a constant scan rate of 5 mV s^{-1}. This scan rate was maintained during all the experiments. A lower scan rate can be used to minimize the charging effect, contributing to the power density profiles. The geometric area of each compartment (~0.06 cm^2) was used to calculate the areal power density. Oxygen removal was accomplished by purging N_2 gas, with N_2 atmosphere subsequently maintained over the solution. Half-cell characterizations were carried out in a three-electrode system. For half-cell studies, the anode or cathode were set as working electrodes, with an external Ag/AgCl and Pt wire electrodes (used as reference and counter electrodes, respectively). A 0.1 M phosphate buffer solution (PBS, pH 7.0) was used as the supporting electrolyte, unless otherwise indicated.

4.3 Results and Discussion

4.3.1 BFC Configurations

The dissertation author and the team demonstrate a new strategy for designing glucose/oxygen-driven BFCs that can operate in oxygen-free conditions. Carbon-

paste electrodes, commonly used for preparing glucose biosensors,[22, 182] were employed to fabricate the bioanode and cathode of the BFCs. Both compartments, *i.e.*, bioanode and cathode, relied on carbon nanotubes (CNTs), thus offering favorable electrochemical properties and high surface area for confining the enzymes and composite materials such as catalysts and mediators.[212]

For the glucose bioanode, GOx, which is highly specific to β-D-glucose,[213] was used to catalyze the biofuel. GOx does not require additional cofactors (*e.g.*, nicotinamide adenine dinucleotide (NAD^+ or NADH), compared with glucose dehydrogenase-based BFCs which commonly require external or built-in cofactors.[93, 214] Consequently, the attractive biocatalytic capability and the BFC design used here enable simplification of BFC configurations for miniaturized devices as they obviate the needs for separating membrane between anodic and cathodic chambers. Moreover, the heterocyclic electron-shuttling mediator TTF enhances the electron transfer from the GOx-FAD redox center to the nanocomposite supports. Notably, a secondary competing reaction at the anode can cause the reduction of oxygen to H_2O_2. The H_2O_2 byproduct can inhibit the GOx activity, decreasing the BFC performance.[215-216] Hence, catalase was added to the bioanode to decompose the generated H_2O_2.

Pt black served for enhancing the catalytic oxygen reduction, along with CNTs, and hence to lower the onset potential of oxygen reduction reaction (ORR) and increase the ORR cathodic current.[217] Ionic liquids (IL) were added in order to improve ionic conductivity and catalytic reactions while providing a large potential window, good

viscosity, and high thermal stability to the electrode paste composites.[218] However, the concentration of dissolved oxygen in the operating solutions is governed by the temperature, pressure, or metabolic processes (in case of biological systems). Fluctuations in the oxygen levels at the cathode-electrolyte interface can thus diminish the BFC performance.[46, 208] In order to address the decreased BFCs performance under anaerobic or oxygen-fluctuations conditions, an oxygen-rich polychlorotrifluoroethylene (PCTFE) was employed as the pasting liquid of the cathode composite electrode, replacing the widely used mineral oil (MO) binder. Adding this chlorofluorocarbon polymer to the nanocomposite cathode results in an internal oxygen reservoir, that effectively meets the ORR demand (compared to the MO binder). The key cathodic reaction in the oxygen-rich PCTFE/IL cathode is illustrated in Figure 4.1C.

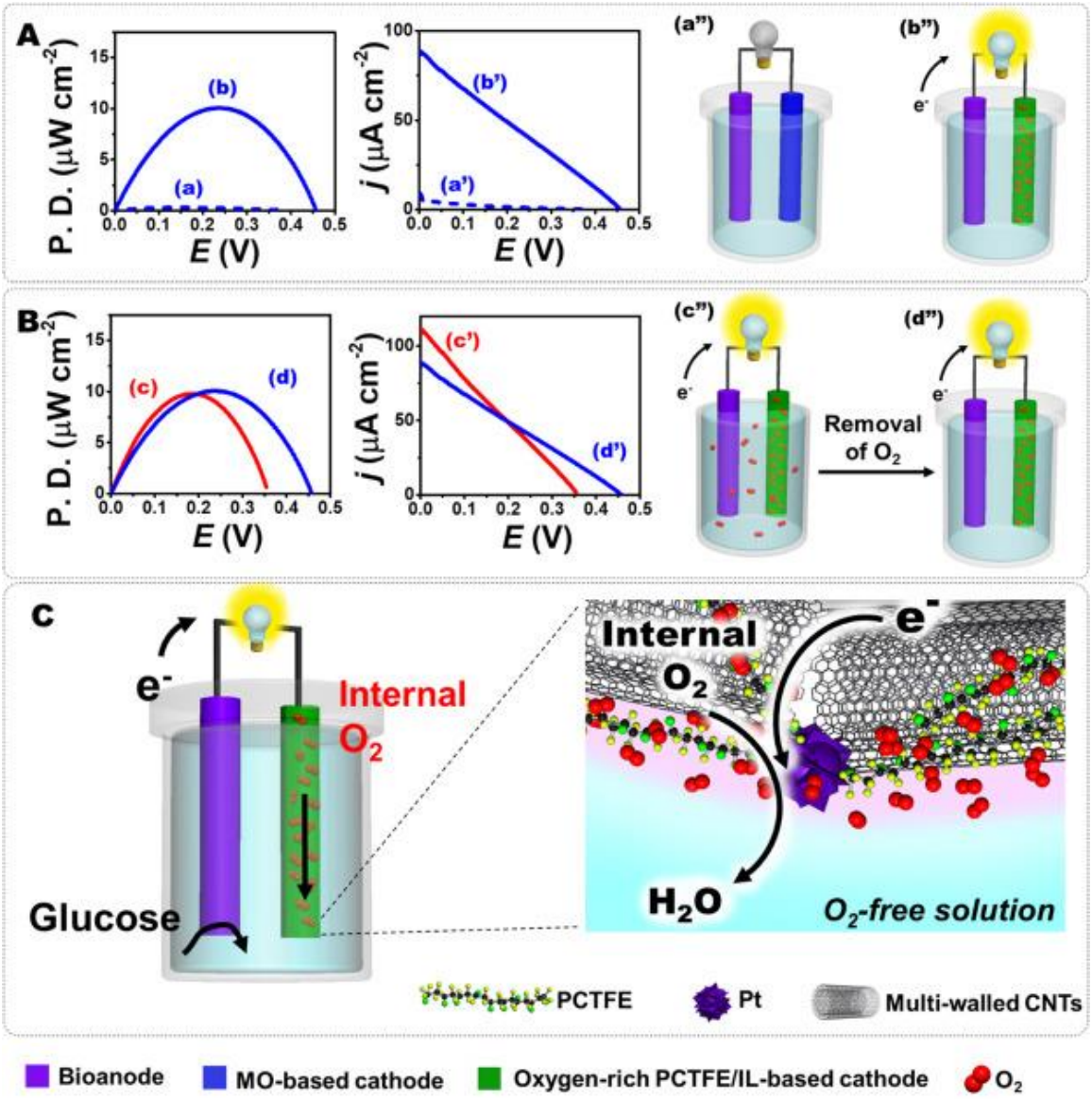

Figure 4.1 (A) Comparison of the power outputs of BFCs operated with (a) MO-based and (b) PCTFE/IL-based cathodes in 5 mM glucose in 0.1 M PBS (pH 7.0) solution under anaerobic conditions Corresponding (a′ and b′) polarization curves and (a″ and b″) schematic illustrations. (B) Power performances obtained from BFCs based on a PCTFE/IL-based cathode operating in the solution containing 5 mM glucose in 0.1 M PBS, pH 7.0 under (c) aerobic and (d) anaerobic conditions. Corresponding (c′ and d′) polarization curves and (c″ and d″) schematic illustrations. (C) Schematic illustration of the glucose/oxygen BFC, operating under severe oxygen-deficit conditions. The inset shows the main cathodic reaction in the oxygen-rich PCTFE/IL cathode. The corresponding BFC reactions are shown in Figure 4.2. Adapted with permission.[75] Copyright 2018, Elsevier.

The new BFC concept was examined extensively under both ambient aerobic and anaerobic solutions. Figure 4.1A compares power curves obtained from BFCs consisting of MO-based (a) and PCTFE/IL-based (b) cathodes in an oxygen-free 5 mM glucose solution. While the same anode was used, the resulting power curves (a and b) are largely different, reflecting the effect of the different BFC cathode materials and reactions (Figure 4.2), and hence the corresponding oxygen dependence. In a N_2-saturated atmosphere, the glucose fuel is catalytically oxidized by GOx and the shuttled electrons are transferred to the cathode compartment. Subsequently, the internal oxygen held by the PCTFE 'tank' accepts the electrons generated at the anode side to complete the circuit. Apparently, the oxygen-rich chlorofluorocarbon cathode performs well in N_2-saturated atmosphere, leading to an OCV of 0.46 V (Figure 4.1A (b)). In contrast, no apparent power is generated at the conventional MO-based cathode system (Figure 4.1A (a)), reflecting the complete oxygen deficiency. The polarization curve of the assembled BFC consisting of PCTFE/IL-based cathode (Figure 4.1A (b′)) indicates a closed-circuit current density of 89 μA cm^{-2}, compared to the negligible current observed for the BFC consisting of the MO-based cathode (Figure 4.1A (a′)). The latter reflects the poor performance of the MO-based cathode under oxygen deficiency (as supported by Figure 4.3 (a′)). It also illustrates that in the presence of the 5 mM glucose fuel under anaerobic conditions, the oxygen-rich cathode-based BFC can generate a current output of 43 μA cm^{-2} at an optimum operating voltage of 0.23 V, which provides the maximum power output. The concept is depicted also in the schematics (of Figure 4.1A, a″ and b″).

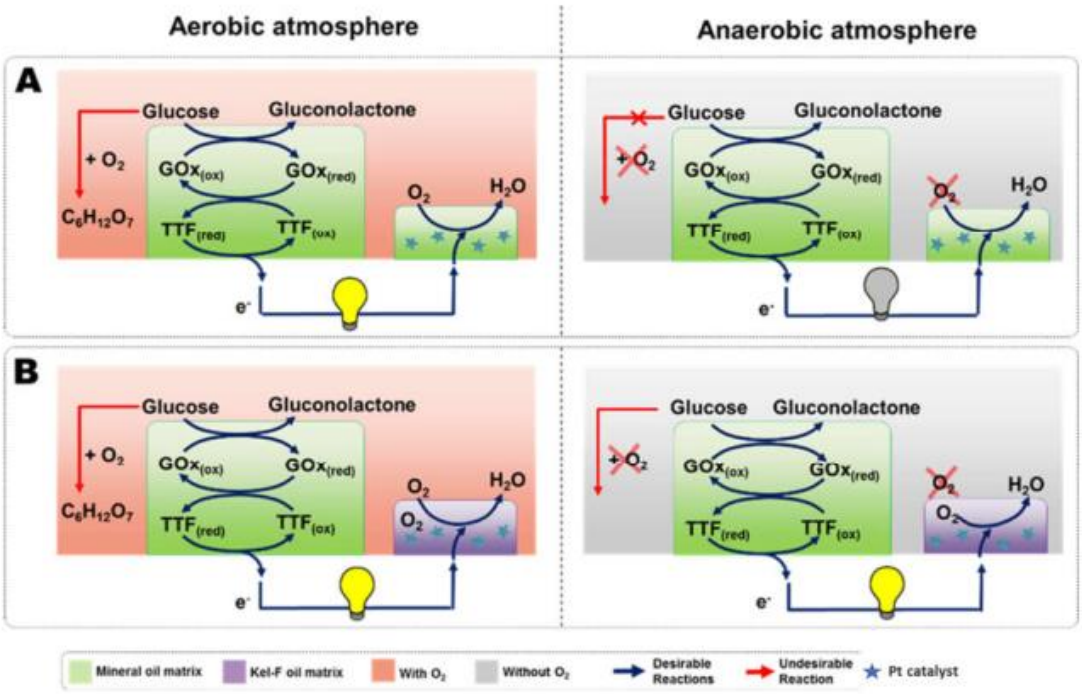

Figure 4.2 Schematic illustrations showing reactions occuring in BFCs. The BFCs are operated with (A) MO-based and (B) PCTFE/IL-based cathodes under (left column) aerobic and (right column) anaerobic atmospheres. Adapted with permission.[75] Copyright 2018, Elsevier.

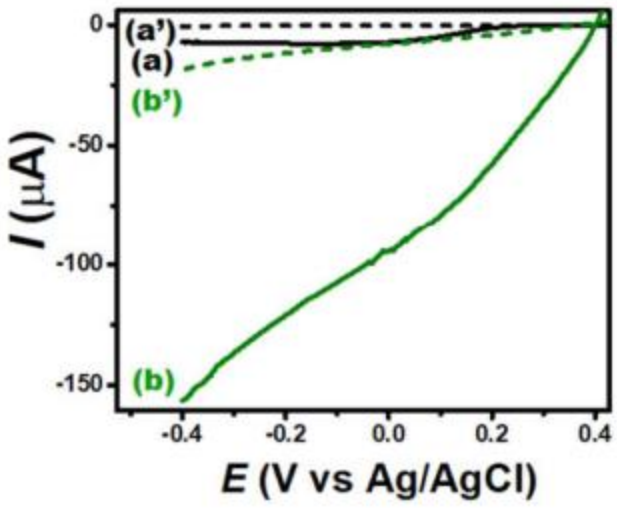

Figure 4.3 Linear sweep voltammograms of the different cathodes including (a, a') MO-based cathode and (b, b') PCTFE/IL-based cathode. The measurements were carried out under (a, b solid plots) ambient oxygen atmosphere and (a', b' dash plots) saturated-N2 atmosphere. Scan rate: 5 mV s^{-1}. Adapted with permission.[75] Copyright 2018, Elsevier.

Figure 4.4(A) indicates that the ORR processes at the MO-based electrode display two reaction steps, indicating a hydrogen peroxide formation pathway. On the other hand, the PCTFE-based nanocomposite electrode shows efficient oxygen reduction processes based on a four-electron pathway (Figure 4.4 (B)). Notice also the larger reduction current at the PCTFE electrode. Advantageously, by relying on the natural electron acceptor (*i.e.*, oxygen), this strategy does not require any additional oxidant materials (such as Ag_2O) to regenerate the reducing agent on the cathode, offering practical use with the oxygen re-supplied spontaneously from the cathode interior.

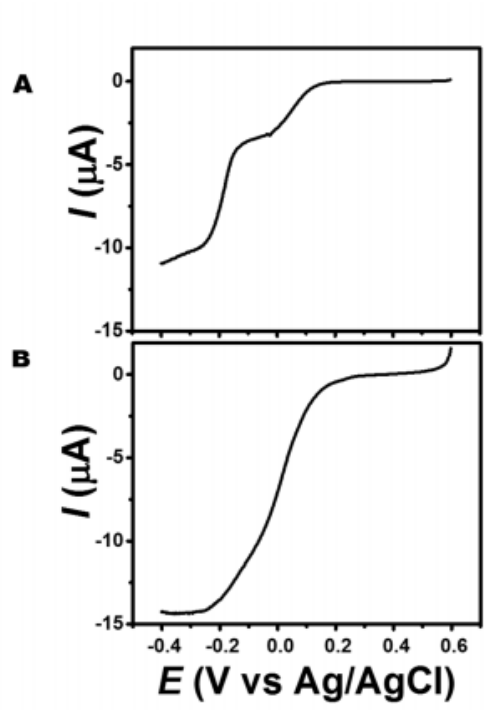

Figure 4.4 Linear sweep voltammograms of the different cathodes with low loadings catalytic nanomaterials of including (A) MO-based† and (B) PCTFE-based‡ cathodes. The measurements were carried out under ambient atmosphere. Electrolyte: 0.1 M potassium phosphate buffer solution, pH 7.0. Scan rate: 5 mV s-1. Electrodes Preparations, †(A): 10 mg of 20/80 (% w. ratio) CNTs/graphite, 10 µL Mineral oil, and 1 mg Pt black. ‡(B): 10 mg of 20/80 (% w. ratio) CNTs/graphite, 10 µL PCTFE oil, and 1 mg Pt black. Adapted with permission.[75] Copyright 2018, Elsevier.

For comparison of the new system, the BFC was assembled by the same bioanode and using the oxygen-rich PCTFE/IL-based cathode (Figure 4.1B). The performance of this BFC was evaluated under ambient aerobic and anaerobic solutions in order to demonstrate the mitigation of oxygen effects from the external surrounding. Using aerobic conditions (Figure 4.1B (c)) resulted in a typical power curve. The system thus generated the maximum power density of 9.8 µW cm^{-2} with the OCV of 0.36 V, with relative standard deviations of 5.9% and 2.7%, respectively. The BFC was evaluated again after removing oxygen. The result of Figure 4.1B (d) illustrates that the PCTFE/IL-based

cathode satisfies the power output performance by mitigating the oxygen-dependent effect. In addition, we observed a slightly higher power density and an increase of the OCV to 0.46 V. This suggests that the system shows the evidence of secondary reaction of oxygen electroreduction at the bioanode. Such enhanced OCV behavior of mediator-based BFC bioanode in the absence of O_2 was reported earlier.[219-220] Such operation under N_2-saturated atmosphere minimizes the presence of oxygen at the anode surface and related competing reaction, leading to increased electron generation from the anode along with improved output voltage. Notably, removal of oxygen from the whole BFC chamber can decrease the current loss at the bioanode by suppressing the following GOx reaction (as shown below in Equation 4.1). The BFC reactions are also shown in Figure 4.2 (B).

$$C_6H_{12}O_6 + O_2 + H_2O \xrightarrow{GOx} C_6H_{12}O_7 + H_2O_2 \qquad \textbf{Equation 4.1}$$

Furthermore, as shown in Figure 4.1B (c′ and d′), the polarization curves display the mitigation of performance loss in the absence of oxygen when using the BFC assembled with the oxygen-rich cathode. Upon removing O_2, the decrease of closed-circuit current density from 110 to 90 μA cm^{-2} (c′ to d′, respectively) corresponds to the lower amount of external O_2 at the cathode (as supported by Figure 4.3 (b and b′)). In the presence of 5 mM glucose fuel under anaerobic conditions, the oxygen-rich cathode-based BFC can still generate a current output of 40 μA cm^{-2} at an optimum operating voltage of 0.24 V (Figure 4.1A (c′ and d′))

As expected, the ORR cathode performance is diminished using conventional cathode materials (Figure 4.3 (a′)). In contrast, the oxygen-rich PCTFE/IL-based cathode

can still support the BFC reactions internally through the internal flux of oxygen under severe oxygen-deficit conditions (as shown in Figure 4.3 (b′), hence maintaining an effective cathode capability. Overall, the whole system successfully addresses severe oxygen limitations, even under complete anaerobic environments. The detailed reactions are also shown in Figure 4.2.

4.3.2 Design of an Oxygen-Rich Nanocomposite Electrode for BFCs (a Triphase Interface System)

On the cathode compartment, in general, the oxygen transport from distant locations to catalytic surface sites is the restrictive factor for electrocatalytic ORR, which requires judicious engineering of specific cathode designs. In this work, as shown in Figure 4.1C, the cathode matrix includes Pt, CNTs, PCTFE, and IL, leading to a microscopic triphase system within the oxygen-rich PCTFE/IL cathode. Catalytic Pt particles were dispersed as ORR center within the cathode matrix. The microscopic oxygen-rich 'tank' established in the PCTFE/IL cathode plays a crucial role as an internal oxygen source, particularly when the BFC is operated under severe oxygen-deficit conditions. In addition, PCTFE, which has large chlorine atoms, compared to fluorine atoms of polytetrafluoroethylene, makes relatively weak intermolecular interaction. This provides a liquid oil state, enabling the facile fabrication of uniform cathode composites. The engineered tri-phase interface enables an interfacial assembly, joining a communication of gaseous, liquid, and solid phases, respectively.[221-222] This interface can

be sustained for long periods, as demonstrated below. Furthermore, the numerous 'docking' locations of the PCTFE/IL nanocomposites maximize the numbers of reactive centers at the catalytic conducting solid-oxygen-electrolyte interphase. The important phases are the following.

First, PCTFE traps oxygen, developing the air phase. The distribution of the oxygen captured in PCTFE cathode allows the effective diffusion of oxygen to active catalytic centers within a short distance. Besides, the high internal oxygen flux is expected to extend the operating period under oxygen-free situations. In addition, the hydrophobicity of this phase – which also has high oxygen concentration – offers a favorable cathodic reaction reservoir because it can repel the water product from ORR. According to Le Châtelier's principle, the elimination of water 'flooding' causes improved mass transport and the shift of equilibrium position, thus enhancing the electron accepting processes in the cathode. This function is supported also by the IL immiscible with the water region.[223] Second, the solid phase including conducting nanomaterials and catalytic Pt particles is also crucial.[224-225] The high surface area of CNTs serving as the conductive base for dispersing the Pt catalytic sites offers attractive electrocatalytic performance toward ORR. Moreover, intrinsic properties of IL can enhance the conductivity and surface reactivity.[226] Third, in addition to oxygen and solid phases, the phase consisting of protons controls the catalytic performance of the BFC. Protons are important to supply reaction centers. Carboxylic groups on CNTs can serve as effective proton exchange sources to the reaction zones. As a result, establishing such triphase within the nanocomposite

cathode is expected to improve the catalytic performance, and to lead to an attractive BFC performance under oxygen-deficit conditions.

4.3.3 Comparison of Enzymatic Glucose/Oxygen BFCs

The power harvesting performance of the two different BFCs consisting of MO-based and PCTFE/IL-based carbon-paste cathodes were compared. As the total power output strongly depends on both anode and cathode compartments, the effect of different levels of glucose on the power output were studied up to 12.5 mM glucose level. The data in Figure 4.5A-B show the power performance of the BFC with MO-based cathode under aerobic (red plots) and anaerobic (blue plots) conditions. In contrast, Figure 4.5C-D displays the results obtained when using the same bioanode but replacing the cathode with the oxygen-rich PCTFE/IL-based electrode. The power curves were obtained also under aerobic (red plots) and anaerobic (blue plots) conditions. Using the MO-based cathode under aerobic conditions, the power output increases with the fuel concentration up to 10 mM and levels off at higher glucose concentrations. However, after completely removing the external oxygen, the power output was very low, indicating that the cathode reaction is a power-limiting factor. In contrast, using the oxygen-rich PCTFE/IL-based cathode, the BFC performs effectively under both aerobic and anaerobic conditions (Figure 4.5C-D and Figure 4.6 (B)). The power output under aerobic surrounding is proportional to the glucose concentration. Furthermore, in the absence of external oxygen in the glucose solution, the BFC output provided a significantly larger OCV, owing to suppression of secondary reaction of oxygen electroreduction at the bioanode (as discussed earlier).[219,

[227] The power density is also enhanced under glucose levels below ~5 mM due to the elimination of the oxygen competition reaction on the bioanode mediated reaction. The largest power improvements (vs the aerobic data) is observed at the lowest (2.5 mM) glucose level. However, at higher concentration of glucose, a slight increment of power output was observed, suggesting a saturation at elevated glucose levels. Considering the relative concentrations of the glucose and oxygen fuels in biologically relevant media, the oxygen level is generally lower than glucose. Under anaerobic surrounding, in particular, the limited oxygen may indicate that the cathode will be the power-determining compartment. Moreover, Figure 4.6 compares polarization curves of BFCs based on the MO-based cathode and the PCTFE/IL oxygen-rich cathode. These data indicate that when using the oxygen-rich cathode under anaerobic conditions (Figure 4.6 (B)), the effect of oxygen-deficit conditions can be mitigated as closed-circuit current outputs display small changes, particularly at low glucose levels. This is in contrast to the data observed using the MO-based cathode (Figure 4.6 (A)), confirming the importance of cathodes with internal oxygen reservoir.

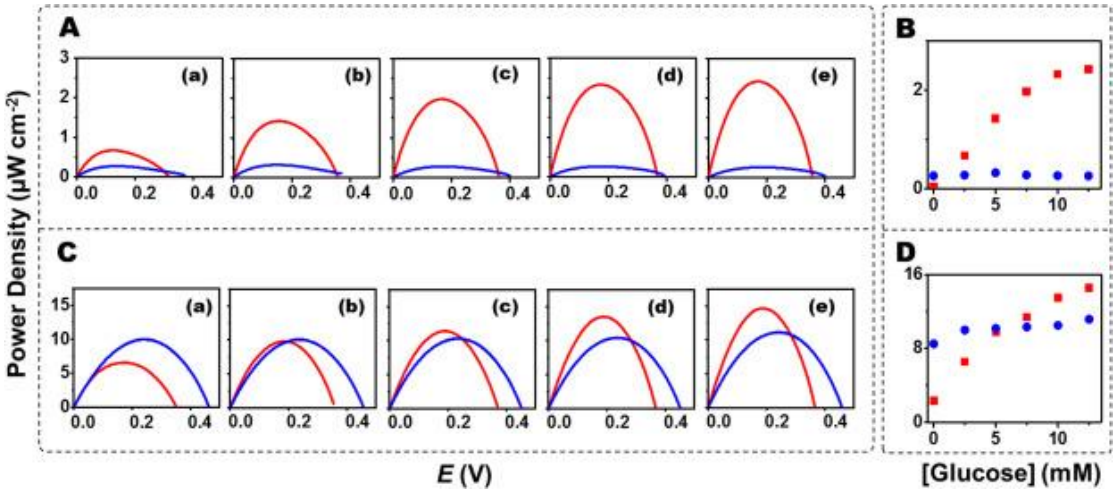

Figure 4.5 The power output performance of (A, B) MO cathode-based BFC and (C, D) PCTFE/IL cathode-based BFC using different levels of the glucose fuel. ((a-e) 2.5, 5.0, 7.5, 10.0, and 12.5 mM glucose) in 0.1 M PBS, pH 7.0, under (red plots) aerobic and (blue plots) anaerobic conditions. The corresponding curves of maximum power output vs glucose concentration for the MO cathode-based and PCTFE/IL cathode-based BFCs are shown in (B) and (D), respectively. The corresponding polarization curves are shown in Figure 4.6. Adapted with permission.[75] Copyright 2018, Elsevier.

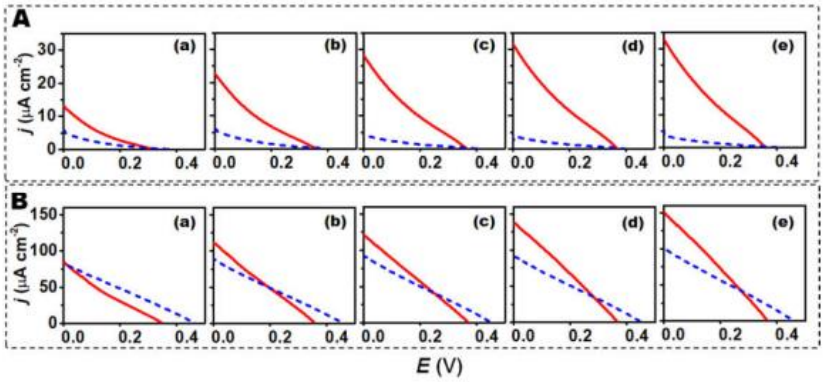

Figure 4.6 The polarization curves of (A) MO cathode-based BFC and (B) PCTFE/IL cathodebased BFC using different levels of the glucose fuel. ((a-e) 2.5, 5.0, 7.5, 10.0, and 12.5 mM glucose) in 0.1 M PBS, pH 7.0, under (red solid plots) aerobic and (blue dash plots) anaerobic conditions. Adapted with permission.[75] Copyright 2018, Elsevier.

In addition, harvesting energy from natural glucose and oxygen fuels was tested successfully in the artificial interstitial fluid, as indicated in Figure 4.7. These data suggest potential applications related to metabolism processes in biological systems, such as fluctuating oxygen in the interstitial fluid for minimally invasive microneedle applications.

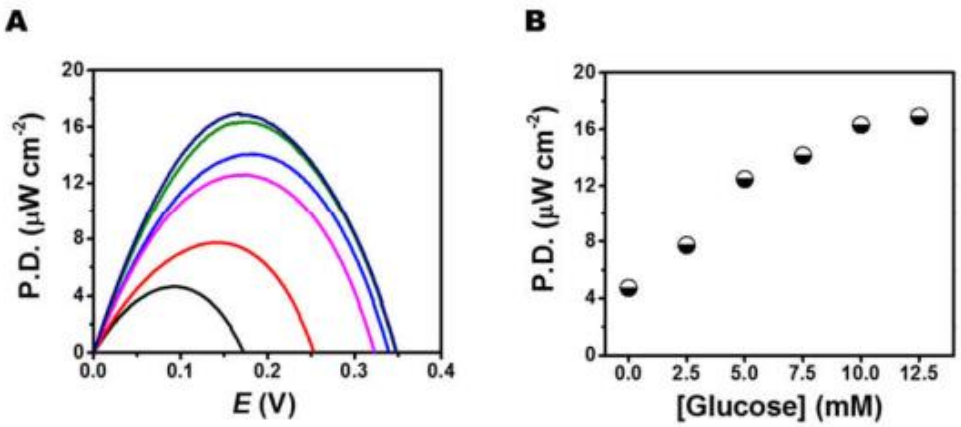

Figure 4.7 (A) Plots of power density vs potential for the bioanode/oxygen-rich PCTFE/IL cathode BFC when varying glucose concentrations (0–12.5 mM) in artificial interstitial fluid. (B) Corresponding power–concentration calibrations. The artificial interstitial fluid contains 107 mM NaCl, 3.48 mM KCl, 1.53 mM $CaCl_2$, 0.69 mM $MgSO_4$, 26.2 mM $NaHCO_3$, 1.67 mM NaH_2PO_4, 9.64 mM sodium gluconate, and 7.6 mM sucrose. Adapted with permission.[75] Copyright 2018, Elsevier.

This proof-of-concept demonstration can be further applied as a self-powered biosensor and can simplify the architecture of miniaturized bioelectronics when severe oxygen-deficit conditions are involved.

4.3.4 Prolonged Operation under Anaerobic Conditions

The high oxygen storage capacity of the PCTFE/IL-based cathode permits prolonged power generation in oxygen-free solutions. Such extended power generation

under completely anaerobic conditions will depend on the internal oxygen storage capacity of the new cathode. It is thus important to investigate the power output during prolonged operation in oxygen-free solutions. Such evaluation was carried out by monitoring the stability of BFC performance continuously in a N_2-saturated atmosphere. The BFC consisting of the oxygen-rich PCTFE/IL-based cathode was discharged at a current density of 5 μA cm^{-2} in an oxygen-free 10 mM glucose solution. Its performance was compared to a BFC consisting of the same bioanode, but using a MO-based cathode, which served as the control. The results, displayed in Figure 4.8, show the output of the conventional (A) and oxygen-rich (B) BFC during a prolonged (~24 h) operation in the deoxygenated 10 mM glucose solution.

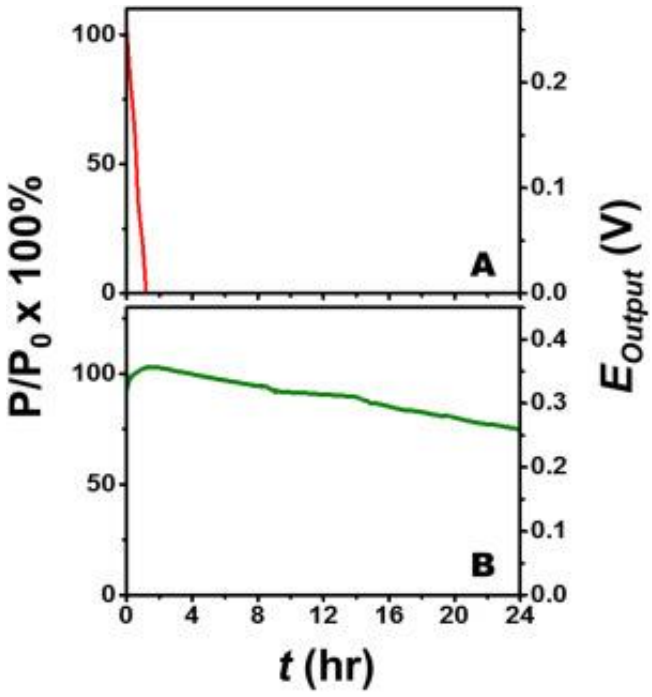

Figure 4.8 Prolonged BFC operations under oxygen-free (N_2 -saturated atmosphere) conditions of carbon-paste cathodes based on (A) MO and (B) PCTFE/IL binders. The outputs are shown in (left y-axis) as relative power and (right y-axis) voltage output. The experiments were performed continuously in 0.1 M PBS (pH 7.0) containing 10 mM glucose under a N_2-saturated atmosphere. Adapted with permission.[75] Copyright 2018, Elsevier.

As expected, the power output obtained from the common MO-based cathode BFC displayed a dramatic loss of the power performance, rapidly approaching zero within less than 1.5 h (Figure 4.8A). Such fast power decay reflects the negligible oxygen solubility of MO. Such fast oxygen depletion is characteristic challenge to common BFC under oxygen fluctuation conditions.[208] In contrast, the oxygen-rich PCTFE/IL-based cathode results in effective power generation throughout the entire 24 h operation owing to its effective internal flux of oxygen (Figure 4.8B). Only a slow decrease of the power output is observed with the system maintaining 95%, 90%, and 70% of its power output following 5, 10, and 24 h, respectively. Note the enhanced power observed during the initial 3 h, that may reflect the secondary oxygen competition reaction on the bioanode. Note also the remarkable

voltage output obtained in the oxygen-rich PCTFE/IL cathode-based BFC during such prolonged operation. Such performance in anaerobic (oxygen-free) media indicates that the high oxygen storage capacity of the oxygen-rich cathode is maintained over prolonged operations in oxygen-free solutions. These data suggest very slow depletion of the internal oxygen supply from the nanocomposite paste electrode over extended periods, to allow continuous operation of the oxygen-rich cathode when the oxygen surrounding is the limiting factor. Such internal oxygen supply thus supports the oxygen requirement for the cathode reaction over a prolonged operation in oxygen-free solutions. Note that such BFC operation in the absence of oxygen over a very long period is an extreme case used here to clearly demonstrate the new concept. In practical scenarios, some oxygen enters and re-supplied into the BFC system, inherently recovering the BFC performance. Consequently, this approach offers self-sustaining energy-conversion systems because the natural oxygen can simply re-supply internally. Note that the surface of carbon pastes can be readily renewed for extending this power generation ability in oxygen-free solutions to several days.

4.4 Conclusions

In summary, we have demonstrated a glucose/O_2 driven BFC that can operate efficiently even in the absence of oxygen in the fuel solution. The new BFC relies on an oxygen-rich PCTFE/IL-based carbon/Pt paste cathode that acts as an internal source of oxygen to provide an efficient oxygen supply, satisfying the oxygen reduction

reaction (ORR) internally. The stable power obtained in anaerobic (oxygen-free) media over prolonged operations (*e.g.,* maintaining over 90% of its initial power during continuous 10-h operation) indicates that the internal oxygen supply is not depleted during extended periods in oxygen-free solutions. This contrasts with the results observed using cathodes based on the common mineral-oil carbon-paste binder that exhibited a severe oxygen dependence. The new oxygen-rich cathode approach can be tailored for BFC based on biocatalysts, such as bilirubin oxidase and laccase, or other ORR inorganic catalysts. The use of such oxygen reducing enzymes can lead fully enzymatic BFCs. By successfully operating under anaerobic conditions, the internal oxygen-rich BFC design addresses the major oxygen-deficit limitation of metabolite/oxygen BFCs and allows effective operation in conditions of fluctuating oxygen concentrations, such as in wearable and implantable devices. Remaining challenges, including the requirement for a mediator, limited power and voltage outputs, and limited oxygen capacity, should be addressed in future studies. Kinetic and transport limitations related to scan-rate effect can be further investigated for gaining fundamental insights. We anticipate that the new power-generating BFC approach can meet the demands of a wide range of practical energy-harvesting scenarios involving low or fluctuating oxygen levels.

4.5 Acknowledgments

This work is supported by Defense Threat Reduction Agency Joint Science and Technology Office for Chemical and Biological Defense (HDTRA 1–16-1–0013). Itthipon

Jeerapan and J.R.S. acknowledge fellowships from the Thai Development and Promotion of Science and Technology Talents Project (DPST), Thailand, and CNPq (number 216981/2014-0), Brazil, respectively. The authors thank Aidan Kennedy and Paul Warren for assistance in the sample preparation.

Chapter 4 is based, in part, on the material as it appears in Biosensors and Bioelectronics, 2018, by Itthipon Jeerapan, Juliane R. Sempionatto, Jung-Min You, and Joseph Wang. The dissertation author was the primary investigator and author of this paper.

Chapter 5 Conclusions and Prospects

The studies of the present doctoral dissertation have devoted to address some of the challenges in biofuel cell (BFCs) when BFC-based devices are applied in a variety of applications, such as wearable and ingestible applications and toward implantable scenarios. For example, advanced wearable devices with additional capability of biosensing or electrochemical sensing can screen biomarkers (such as in sweat, interstitial fluid, tear, and saliva),[20, 228] while swallowable bioelectronics can sense biomarkers and track in vivo physiological parameters with exclusive possibilities to provide an access to the location of gastrointestinal tracts when the swallowable sensors go through the gastrointestinal tract inside the body.[170]

BFCs, able to harvest the bioenergy from biological systems, have received considerable attention and have observed significant research efforts.[30, 39] Enzymatic BFCs, which is a big class of fuel cells or energy-conversion devices, could be employed to yield electrical energy from green biofuels (such as naturally available glucose and lactate) by applying the advantages of biocatalysts. Despite many attractive benefits and wonderful opportunities of BFCs, the foremost challenge of low power output and stability of the bioelectrode still presents in this research domain. Moreover, as discuss some key challenges in Chapter 1, many challenges also include the power output of BFCs, stability, working conditions, mechanical robustness and compliance of BFC devices, and environmental effects (e.g., oxygen, pH, temperature) on BFC performances. Therefore,

the opportunities and difficulties have stimulated a variety of research efforts, which are discussed and reported in this dissertation. Powering bioelectronics for biomedical applications in different platforms (e.g., wearable, ingestible, and implantable systems) denotes grand challenges, impeding the realization and clinical and practical applications of overall biosensors and bioelectronic devices. Many biosensors and bioelectronic devices used in state-of-the-art biomedical fields require viable power sources to power the biodevices and operating units (Figure 5.1). Considering some opportunities and limitations, the dissertation author has attempted to addresses some challenges and demonstrated example directions to efficient powering of biosensors and bioelectronics.

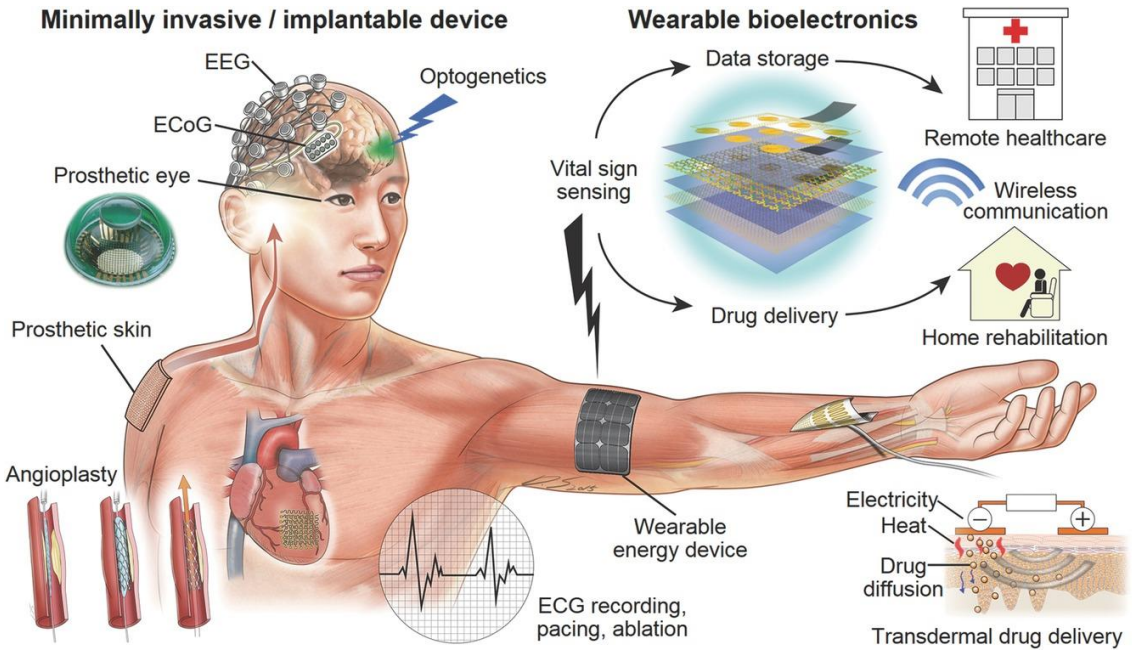

Figure 5.1 Some examples of various wearable, minimally invasive, and implantable biomedical devices. Various biodevices require the power sources to support their multifunctions. Adapted with permission.[229] Copyright 2016, Wiley-VCH.

In order to demonstrate a strategy to address the key challenge pertaining to the mechanical stability of BFCs, the dissertation author and the team have devoted to developing a stretchable and wearable BFCs. Highly stretchable textile-based BFCs, acting as effective self-powered sensors, have been fabricated using screen-printing of customized stress-enduring inks. The first example of self-sustainable biosensors on wearable platforms is described in Chapter 2. Due to the synergistic effects of nanomaterial-based engineered inks and the serpentine designs, these printable bioelectronic devices endure severe mechanical deformations, e.g., stretching, indentation, or torsional twisting. Glucose and lactate BFCs with single-enzyme and membrane-free configurations generated the maximum power densities of 160 and 250 μW cm^{-2} with the open circuit voltages of 0.44 and 0.46 V, respectively. The textile-BFCs were able to withstand repeated severe mechanical deformations with minimal impact on its structural integrity, as was indicated from their stable power output after 100 cycles of 100% stretching. By providing power signals proportional to the sweat fuel concentration, these stretchable devices act as highly selective and stable self-powered textile sensors. Their applicability to sock-based BFCs and self-powered biosensors and mechanically compliant operations was demonstrated on human subjects. These stretchable skin-worn "scavenge-sense-display" devices are expected to contribute to the development of skin-worn energy harvesting systems, advanced non-invasive self-powered sensors and wearable electronics on a stretchable garment.

Ingestible bioelectronics is one of the most exciting classes of emerging technologies, opening opportunities for advanced and modern biomedical

investigations.[170, 230-233] However, to fabricate such an ingestible device requires careful attention to the biocompatibility of materials and all components. These challenges could be solved by using fully edible materials. Considerable effort has been invested in the expansion of advanced materials for support ingestible applications.[234] The first example of a fully edible biofuel cell (BFC), based solely on highly biocompatible food materials without any additional external mediators, is described in Chapter 3 in this dissertation. The new BFC energy-harvesting approach relies on a variety of edible plant/mushroom extract/vegetable oil/charcoal paste biocatalytic electrodes and represents an attractive route for energy harvesting towards ingestible biomedical devices. The edible BFC anode and cathode paste materials consist of biocatalytic rich mushroom, apple, plum, and banana plant tissues, along with dietary activated charcoal and water-immiscible olive oil, corn oil, and sesame oil for creating the paste matrix. The ethanol/O_2 BFC relies on a bioanode, based on ethanol oxidation induced by the intrinsic biocatalytic activity of its mushroom component, along with a biocathode based on oxygen-reducing apple extract containing polyphenol-oxidase and phenolic compounds. The integrated natural catalytic system and selective biocatalytic activity of the natural extracts offer the successful operation of BFCs without any extra mediators or membrane separating the anode and the cathode. The mushroom/apple/olive oil-based BFC displays a favorable power density of 282 μW cm^{-2} with an open circuit-voltage (OCV) of 0.24 V. The power and OCV signals are linearly proportional to ethanol levels and indicate promise for self-powered alcohol sensing. The food-based BFCs were reproducible and able to maintain a power performance of over 80% of their initial output for four hours. These edible energy-

harvesting BFCs hold great promise for the next-generation of ingestible devices and smart self-powered biosensors for monitoring the health and the digestive system.

To satisfy long-term use in very dynamic biosystems, the engineering design is vital to prolonging the lifetime of the biodevice. Paramount to such trials has been shown by developing composite materials and strategies of enzyme immobilization.[30, 235-238] As discussed in the dissertation, oxygen is a key factor as it is vital for common cathodes, employed in various BFC systems. A glucose/oxygen biofuel cell (BFC) that can operate continuously under oxygen-free conditions is described in Chapter 4. The oxygen-deficit limitations of metabolite/oxygen enzymatic BFCs have been addressed by using an oxygen-rich cathode binder material, polychlorotrifluoroethylene (PCTFE), which provides an internal oxygen supply for the BFC reduction reaction. This oxygen-rich cathode component mitigates the potential power loss in oxygen-free medium or during external oxygen fluctuations through internal supply of oxygen, while the bioanode employs glucose oxidase-mediated reactions. The internal oxygen supply leads to a prolonged energy-harvesting in oxygen-free solutions, e.g., maintaining over 90% and 70% of its initial power during 10- and 24-h operations, respectively, in the absence of oxygen. The new strategy holds considerable promise for energy-harvesting and self-powered biosensing applications in oxygen-deficient conditions. Other parameters such as the variation of temperature, pH, and electrolytes in dynamic physiological systems are interesting keywords for future research.

An idealistic goal on the attractive applications of BFCs is to provide self-sustainable systems for biosensors and bioelectronics. In other words, the integrated device should be working without any extra rechargeable batteries or complicated supportive electronics. This is expected to support the paradigm shift toward the possibility to achieve an autonomous 'sense-act-treat' feedback loop.[169, 239] For instance, this concept would enhance the modern capability to autonomously diagnose and manage the health of users (such as wearers or users who have implanted BFCs, ingestible BFC-based devices, and/or integrated bioelectronics). The example of the integrated system of artificially maintaining glycemic control, involving mechanisms of sensing and treating systems, is shown in Figure 5.2.

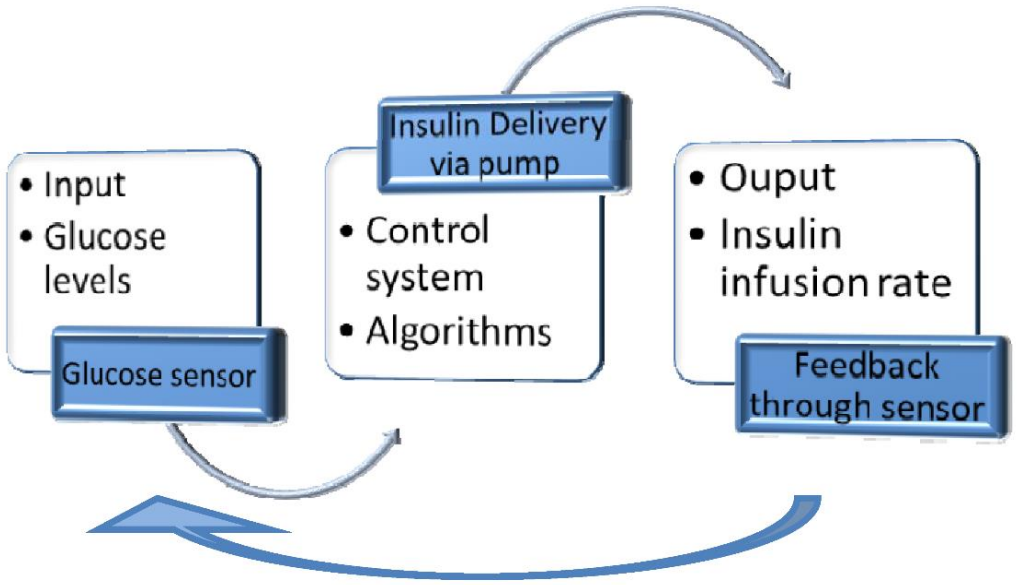

Figure 5.2 Principles of control systems applied to glycemic control. Adapted under the terms and conditions of the Creative Commons Attribution license CC BY 3.0.[240] Copyright 2009, the authors, published by Molecular Diversity Preservation International, Basel, Switzerland.

The demonstrated self-powered biosensors and self-sustainable bioelectronics in this dissertation represent a new strategic approach for addressing the need of both biosensors and energy to power bioelectronics. This can be seen by following up work that has revealed BFCs for various autonomous applications.[29] The integration of BFCs for personalized biosensors and bioelectronics have been outlined in this dissertation. Future work will endeavor to apply the BFCs for many platforms, including ingestible and implantable devices. Such new and unique capabilities will open exciting potential to basic science and broad applied physiological and medical domains. From this perspective, with continuous research, the BFC technology and related integrated modules of biosensors and bioelectronics are moving forward toward many modern biomedical applications, ranging from diagnostic and therapeutic purposes.

5.1 Acknowledgements

Chapter 5 is based, in part, on the materials as they appear in Journal of Materials Chemistry A, 2016, by Itthipon Jeerapan, Juliane R. Sempionatto, Adriana Pavinatto, Jung-Min You, and Joseph Wang; Journal of Materials Chemistry B, 2018, by Itthipon Jeerapan, Bianca Ciui, Ian Martin, Cecilia Cristea, Robert Sandulescu, and Joseph Wang; in Biosensors and Bioelectronics, 2018, by Itthipon Jeerapan, Juliane R. Sempionatto, Jung-Min You, and Joseph Wang. The dissertation author was the primary investigator and author of these papers.

Index

Bibliography

[1] Willner, I.; Katz, E., *Bioelectronics – An Introduction*. Wiley-VCH Verlag GmbH & Co. KGaA: 2005.

[2] Zhang, A.; Lieber, C. M., Nano-Bioelectronics. *Chem. Rev.* **2016,** *116* (1), 215-257.

[3] Ray, T. R.; Choi, J.; Bandodkar, A. J.; Krishnan, S.; Gutruf, P.; Tian, L.; Ghaffari, R.; Rogers, J. A., Bio-Integrated Wearable Systems: A Comprehensive Review. *Chem. Rev.* **2019,** *119* (8), 5461-5533.

[4] Kim, J.; Jeerapan, I.; Sempionatto, J. R.; Barfidokht, A.; Mishra, R. K.; Campbell, A. S.; Hubble, L. J.; Wang, J., Wearable Bioelectronics: Enzyme-Based Body-Worn Electronic Devices. *Acc. Chem. Res.* **2018,** *51* (11), 2820-2828.

[5] Gao, W.; Emaminejad, S.; Nyein, H. Y. Y.; Challa, S.; Chen, K.; Peck, A.; Fahad, H. M.; Ota, H.; Shiraki, H.; Kiriya, D.; Lien, D.-H.; Brooks, G. A.; Davis, R. W.; Javey, A., Fully integrated wearable sensor arrays for multiplexed in situ perspiration analysis. *Nature* **2016,** *529* (7587), 509-514.

[6] Kim, J.; Campbell, A. S.; de Ávila, B. E.-F.; Wang, J., Wearable biosensors for healthcare monitoring. *Nat. Biotechnol.* **2019,** *37* (4), 389-406.

[7] Yu, Y.; Nyein, H. Y. Y.; Gao, W.; Javey, A., Flexible Electrochemical Bioelectronics: The Rise of In Situ Bioanalysis. *Adv. Mater.* **2019**, 10.1002/adma.201902083.

[8] Gao, W.; Ota, H.; Kiriya, D.; Takei, K.; Javey, A., Flexible Electronics toward Wearable Sensing. *Acc. Chem. Res.* **2019,** *52* (3), 523-533.

[9] Liu, Y.; Pharr, M.; Salvatore, G. A., Lab-on-Skin: A Review of Flexible and Stretchable Electronics for Wearable Health Monitoring. *Acs Nano* **2017,** *11* (10), 9614-9635.

[10] Dubal, D. P.; Chodankar, N. R.; Kim, D.-H.; Gomez-Romero, P., Towards flexible solid-state supercapacitors for smart and wearable electronics. *Chem. Soc. Rev.* **2018,** *47* (6), 2065-2129.

[11] Bandodkar, A. J.; Jeerapan, I.; Wang, J., Wearable Chemical Sensors: Present Challenges and Future Prospects. *ACS Sens.* **2016,** *1* (5), 464-482.

[12] Katz, E.; MacVittie, K., Implanted biofuel cells operating in vivo – methods, applications and perspectives – feature article. *Energy Environ. Sci.* **2013,** *6* (10), 2791-2803.

[13] Bandodkar, A. J.; Wang, J., Wearable Biofuel Cells: A Review. *Electroanalysis* **2016,** *28* (6), 1188-1200.

[14] Xiao, X.; Xia, H.-q.; Wu, R.; Bai, L.; Yan, L.; Magner, E.; Cosnier, S.; Lojou, E.; Zhu, Z.; Liu, A., Tackling the Challenges of Enzymatic (Bio)Fuel Cells. *Chem. Rev.* **2019**, 10.1021/acs.chemrev.9b00115.

[15] Moehlenbrock, M. J.; Minteer, S. D., Extended lifetime biofuel cells. *Chem. Soc. Rev.* **2008,** *37* (6), 1188-1196.

[16] Aston, W. J.; Turner, A. P. F., Biosensors and Biofuel Cells. *Biotechnology and Genetic Engineering Reviews* **1984,** *1* (1), 89-120.

[17] Kim, J.; Jia, H.; Wang, P., Challenges in biocatalysis for enzyme-based biofuel cells. *Biotechnol. Adv.* **2006,** *24* (3), 296-308.

[18] Grattieri, M.; Minteer, S. D., Self-Powered Biosensors. *ACS Sens.* **2018,** *3* (1), 44-53.

[19] Fu, L.; Liu, J.; Hu, Z.; Zhou, M., Recent Advances in the Construction of Biofuel Cells Based Self-powered Electrochemical Biosensors: A Review. *Electroanalysis* **2018,** *30* (11), 2535-2550.

[20] Jeerapan, I.; Sempionatto, J. R.; Wang, J., On-Body Bioelectronics: Wearable Biofuel Cells for Bioenergy Harvesting and Self-Powered Biosensing. *Adv. Funct. Mater.* **2019,** *0* (0), 1906243.

[21] Jia, W.; Valdés-Ramírez, G.; Bandodkar, A. J.; Windmiller, J. R.; Wang, J., Epidermal Biofuel Cells: Energy Harvesting from Human Perspiration. *Angew. Chem. Int. Ed.* **2013,** *52* (28), 7233-7236.

[22] Valdés-Ramírez, G.; Li, Y.-C.; Kim, J.; Jia, W.; Bandodkar, A. J.; Nuñez-Flores, R.; Miller, P. R.; Wu, S.-Y.; Narayan, R.; Windmiller, J. R.; Polsky, R.; Wang, J., Microneedle-based self-powered glucose sensor. *Electrochem. Commun.* **2014,** *47*, 58-62.

[23] Ogawa, Y.; Kato, K.; Miyake, T.; Nagamine, K.; Ofuji, T.; Yoshino, S.; Nishizawa, M., Organic Transdermal Iontophoresis Patch with Built-in Biofuel Cell. *Adv. Healthcare Mater.* **2015,** *4* (4), 506-510.

[24] Bandodkar, A. J.; Jeerapan, I.; You, J.-M.; Nuñez-Flores, R.; Wang, J., Highly Stretchable Fully-Printed CNT-Based Electrochemical Sensors and Biofuel Cells: Combining Intrinsic and Design-Induced Stretchability. *Nano Lett.* **2016,** *16* (1), 721-727.

[25] Falk, M.; Andoralov, V.; Blum, Z.; Sotres, J.; Suyatin, D. B.; Ruzgas, T.; Arnebrant, T.; Shleev, S., Biofuel cell as a power source for electronic contact lenses. *Biosens. Bioelectron.* **2012,** *37* (1), 38-45.

[26] Kwon, C. H.; Lee, S.-H.; Choi, Y.-B.; Lee, J. A.; Kim, S. H.; Kim, H.-H.; Spinks, G. M.; Wallace, G. G.; Lima, M. D.; Kozlov, M. E.; Baughman, R. H.; Kim, S. J., High-power biofuel cell textiles from woven biscrolled carbon nanotube yarns. *Nat. Commun.* **2014,** *5*, 3928.

[27] Jeerapan, I.; Sempionatto, J. R.; Pavinatto, A.; You, J.-M.; Wang, J., Stretchable biofuel cells as wearable textile-based self-powered sensors. *J. Mater. Chem. A* **2016,** *4* (47), 18342-18353.

[28] Bandodkar, A. J.; You, J.-M.; Kim, N.-H.; Gu, Y.; Kumar, R.; Mohan, A. M. V.; Kurniawan, J.; Imani, S.; Nakagawa, T.; Parish, B.; Parthasarathy, M.; Mercier, P. P.; Xu, S.; Wang, J., Soft, stretchable, high power density electronic skin-based biofuel cells for scavenging energy from human sweat. *Energy Environ. Sci.* **2017,** *10* (7), 1581-1589.

[29] Bandodkar, A. J.; Gutruf, P.; Choi, J.; Lee, K.; Sekine, Y.; Reeder, J. T.; Jeang, W. J.; Aranyosi, A. J.; Lee, S. P.; Model, J. B.; Ghaffari, R.; Su, C.-J.; Leshock, J. P.; Ray, T.; Verrillo, A.; Thomas, K.; Krishnamurthi, V.; Han, S.; Kim, J.; Krishnan, S.; Hang, T.; Rogers, J. A., Battery-free, skin-interfaced microfluidic/electronic systems for simultaneous electrochemical, colorimetric, and volumetric analysis of sweat. *Sci. Adv.* **2019,** *5* (1), eaav3294.

[30] Rasmussen, M.; Abdellaoui, S.; Minteer, S. D., Enzymatic biofuel cells: 30 years of critical advancements. *Biosens. Bioelectron.* **2016,** *76*, 91-102.

[31] Matousek, J. L.; Campbell, K. L., A comparative review of cutaneous pH. *Veterinary Dermatology* **2002,** *13* (6), 293-300.

[32] Abelson, M. B.; Udell, I. J.; Weston, J. H., Normal Human Tear pH by Direct Measurement. *JAMA Ophthalmology* **1981,** *99* (2), 301-301.

[33] Cinquin, P.; Gondran, C.; Giroud, F.; Mazabrard, S.; Pellissier, A.; Boucher, F.; Alcaraz, J.-P.; Gorgy, K.; Lenouvel, F.; Mathé, S.; Porcu, P.; Cosnier, S., A Glucose BioFuel Cell Implanted in Rats. *PLOS ONE* **2010,** *5* (5), e10476.

[34] Rantonen, P. J. F.; Meurman, J. H., Viscosity of whole saliva. *Acta Odontologica Scandinavica* **1998,** *56* (4), 210-214.

[35] Zhang, H.; Chiao, M., Anti-fouling coatings of poly (dimethylsiloxane) devices for biological and biomedical applications. *Journal of medical and biological engineering* **2015,** *35* (2), 143-155.

[36] Wisniewski, N.; Moussy, F.; Reichert, W. M., Characterization of implantable biosensor membrane biofouling. *Fresenius' Journal of Analytical Chemistry* **2000,** *366* (6), 611-621.

[37] Bandodkar, A. J., Review—Wearable Biofuel Cells: Past, Present and Future. *J. Electrochem. Soc.* **2017,** *164* (3), H3007-H3014.

[38] Gonzalez-Solino, C.; Lorenzo, D. M., Enzymatic Fuel Cells: Towards Self-Powered Implantable and Wearable Diagnostics. *Biosensors* **2018,** *8* (1).

[39] Huang, X.; Zhang, L.; Zhang, Z.; Guo, S.; Shang, H.; Li, Y.; Liu, J., Wearable biofuel cells based on the classification of enzyme for high power outputs and lifetimes. *Biosens. Bioelectron.* **2019,** *124-125*, 40-52.

[40] Yahiro, A. T.; Lee, S. M.; Kimble, D. O., Bioelectrochemistry: I. Enzyme utilizing bio-fuel cell studies. *Biochimica et Biophysica Acta (BBA) - Specialized Section on Biophysical Subjects* **1964,** *88* (2), 375-383.

[41] Katz, E.; Willner, I.; Kotlyar, A. B., A non-compartmentalized glucose | O2 biofuel cell by bioengineered electrode surfaces. *J. Electroanal. Chem.* **1999,** *479* (1), 64-68.

[42] Mano, N.; Heller, A., A Miniature Membraneless Biofuel Cell Operating at 0.36 V under Physiological Conditions. *J. Electrochem. Soc.* **2003,** *150* (8), A1136-A1138.

[43] Chen, T.; Barton, S. C.; Binyamin, G.; Gao, Z.; Zhang, Y.; Kim, H.-H.; Heller, A., A Miniature Biofuel Cell. *J. Am. Chem. Soc.* **2001,** *123* (35), 8630-8631.

[44] Katz, E., Implantable Biofuel Cells Operating In Vivo—Potential Power Sources for Bioelectronic Devices. *Bioelectronic Medicine* **2015,** *2* (1), 1-12.

[45] Bartlett, P. N.; Al-Lolage, F. A., There is no evidence to support literature claims of direct electron transfer (DET) for native glucose oxidase (GOx) at carbon nanotubes or graphene. *J. Electroanal. Chem.* **2018,** *819*, 26-37.

[46] Zebda, A.; Gondran, C.; Le Goff, A.; Holzinger, M.; Cinquin, P.; Cosnier, S., Mediatorless high-power glucose biofuel cells based on compressed carbon nanotube-enzyme electrodes. *Nat. Commun.* **2011,** *2*, 370.

[47] Ivnitski, D.; Branch, B.; Atanassov, P.; Apblett, C., Glucose oxidase anode for biofuel cell based on direct electron transfer. *Electrochem. Commun.* **2006,** *8* (8), 1204-1210.

[48] Wang, X.; Falk, M.; Ortiz, R.; Matsumura, H.; Bobacka, J.; Ludwig, R.; Bergelin, M.; Gorton, L.; Shleev, S., Mediatorless sugar/oxygen enzymatic fuel cells based on gold nanoparticle-modified electrodes. *Biosens. Bioelectron.* **2012,** *31* (1), 219-225.

[49] Coman, V.; Vaz-Domínguez, C.; Ludwig, R.; Harreither, W.; Haltrich, D.; De Lacey, A. L.; Ruzgas, T.; Gorton, L.; Shleev, S., A membrane-, mediator-, cofactor-less glucose/oxygen biofuel cell. *Phys. Chem. Chem. Phys.* **2008,** *10* (40), 6093-6096.

[50] Falk, M.; Blum, Z.; Shleev, S., Direct electron transfer based enzymatic fuel cells. *Electrochim. Acta* **2012,** *82*, 191-202.

[51] Gross, A. J.; Holzinger, M.; Cosnier, S., Buckypaper bioelectrodes: emerging materials for implantable and wearable biofuel cells. *Energy Environ. Sci.* **2018,** *11* (7), 1670-1687.

[52] Drake, R.; Kusserow, B.; Messinger, S.; Matsuda, S., A tissue implantable fuel cell power supply. *ASAIO Journal* **1970,** *16* (1), 199-205.

[53] Malachesky, P.; Holleck, G.; McGovern, F.; Devarakonda, R. In *Parametric studies of implantable fuel cell*, Proceedings of the 7th Intersociety Energy Conversion Engineering Conference, 1972; pp 727-732.

[54] Schwefel, J.; Ritzmann, R. E.; Lee, I. N.; Pollack, A.; Weeman, W.; Garverick, S.; Willis, M.; Rasmussen, M.; Scherson, D., Wireless Communication by an Autonomous Self-Powered Cyborg Insect. *J. Electrochem. Soc.* **2015,** *161* (13), H3113-H3116.

[55] Rasmussen, M.; Ritzmann, R. E.; Lee, I.; Pollack, A. J.; Scherson, D., An Implantable Biofuel Cell for a Live Insect. *J. Am. Chem. Soc.* **2012,** *134* (3), 1458-1460.

[56] Halámková, L.; Halámek, J.; Bocharova, V.; Szczupak, A.; Alfonta, L.; Katz, E., Implanted Biofuel Cell Operating in a Living Snail. *J. Am. Chem. Soc.* **2012,** *134* (11), 5040-5043.

[57] Szczupak, A.; Halámek, J.; Halámková, L.; Bocharova, V.; Alfonta, L.; Katz, E., Living battery – biofuel cells operating in vivo in clams. *Energy Environ. Sci.* **2012,** *5* (10), 8891-8895.

[58] El Ichi-Ribault, S.; Alcaraz, J.-P.; Boucher, F.; Boutaud, B.; Dalmolin, R.; Boutonnat, J.; Cinquin, P.; Zebda, A.; Martin, D. K., Remote wireless control of an enzymatic biofuel cell implanted in a rabbit for 2 months. *Electrochim. Acta* **2018,** *269*, 360-366.

[59] Miyake, T.; Haneda, K.; Nagai, N.; Yatagawa, Y.; Onami, H.; Yoshino, S.; Abe, T.; Nishizawa, M., Enzymatic biofuel cells designed for direct power generation from biofluids in living organisms. *Energy Environ. Sci.* **2011,** *4* (12), 5008-5012.

[60] Katz, E., *Implantable Bioelectronics* John Wiley & Sons: 2014, 10.1002/9783527673148.ch1.

[61] Bazaka, K.; Jacob, M. V., Implantable Devices: Issues and Challenges. *Electronics* **2013,** *2* (1), 1-34.

[62] Hannan, M. A.; Mutashar, S.; Samad, S. A.; Hussain, A., Energy harvesting for the implantable biomedical devices: issues and challenges. *BioMedical Engineering OnLine* **2014,** *13* (1), 79.

[63] Onuki, Y.; Bhardwaj, U.; Papadimitrakopoulos, F.; Burgess, D. J., A Review of the Biocompatibility of Implantable Devices: Current Challenges to Overcome Foreign Body Response. *Journal of Diabetes Science and Technology* **2008,** *2* (6), 1003-1015.

[64] Rogers, J. A.; Ghaffari, R.; Kim, D.-H., *Stretchable Bioelectronics for Medical Devices and Systems*. Springer: 2016.

[65] Fujimagari, Y.; Fukushi, Y.; Nishioka, Y., Stretchable Biofuel Cells with Silver Nanowiring on a Polydimethylsiloxane Substrate. *J. Photopolym. Sci. Technol.* **2015,** *28* (3), 357-361.

[66] Lv, J.; Jeerapan, I.; Tehrani, F.; Yin, L.; Silva-Lopez, C. A.; Jang, J.-H.; Joshuia, D.; Shah, R.; Liang, Y.; Xie, L.; Soto, F.; Chen, C.; Karshalev, E.; Kong, C.; Yang, Z.; Wang, J., Sweat-based wearable energy harvesting-storage hybrid textile devices. *Energy Environ. Sci.* **2018,** *11* (12), 3431-3442.

[67] Ogawa, Y.; Takai, Y.; Kato, Y.; Kai, H.; Miyake, T.; Nishizawa, M., Stretchable biofuel cell with enzyme-modified conductive textiles. *Biosens. Bioelectron.* **2015,** *74*, 947-952.

[68] Kwon, C. H.; Park, Y. B.; Lee, J. A.; Choi, Y.-B.; Kim, H.-H.; Lima, M. D.; Baughman, R. H.; Kim, S. J., Mediator-free carbon nanotube yarn biofuel cell. *RSC Adv.* **2016,** *6* (54), 48346-48350.

[69] Kwon, C. H.; Ko, Y.; Shin, D.; Kwon, M.; Park, J.; Bae, W. K.; Lee, S. W.; Cho, J., High-power hybrid biofuel cells using layer-by-layer assembled glucose oxidase-coated metallic cotton fibers. *Nat. Commun.* **2018,** *9* (1), 4479.

[70] Sim, H. J.; Lee, D. Y.; Kim, H.; Choi, Y.-B.; Kim, H.-H.; Baughman, R. H.; Kim, S. J., Stretchable Fiber Biofuel Cell by Rewrapping Multiwalled Carbon Nanotube Sheets. *Nano Lett.* **2018,** *18* (8), 5272-5278.

[71] Zhao, M.; Gao, Y.; Sun, J.; Gao, F., Mediatorless Glucose Biosensor and Direct Electron Transfer Type Glucose/Air Biofuel Cell Enabled with Carbon Nanodots. *Anal. Chem.* **2015,** *87* (5), 2615-2622.

[72] Jeerapan, I.; Ciui, B.; Martin, I.; Cristea, C.; Sandulescu, R.; Wang, J., Fully edible biofuel cells. *Journal of Materials Chemistry B* **2018,** *6* (21), 3571-3578.

[73] Fischback, M. B.; Youn, J. K.; Zhao, X.; Wang, P.; Park, H. G.; Chang, H. N.; Kim, J.; Ha, S., Miniature Biofuel Cells with Improved Stability Under Continuous Operation. *Electroanalysis* **2006,** *18* (19-20), 2016-2022.

[74] Reuillard, B.; Abreu, C.; Lalaoui, N.; Le Goff, A.; Holzinger, M.; Ondel, O.; Buret, F.; Cosnier, S., One-year stability for a glucose/oxygen biofuel cell combined with pH reactivation of the laccase/carbon nanotube biocathode. *Bioelectrochemistry* **2015,** *106*, 73-76.

[75] Jeerapan, I.; Sempionatto, J. R.; You, J.-M.; Wang, J., Enzymatic glucose/oxygen biofuel cells: Use of oxygen-rich cathodes for operation under severe oxygen-deficit conditions. *Biosens. Bioelectron.* **2018,** *122*, 284-289.

[76] Shi, J.; Liu, S.; Zhang, L.; Yang, B.; Shu, L.; Yang, Y.; Ren, M.; Wang, Y.; Chen, J.; Chen, W.; Chai, Y.; Tao, X., Smart Textile-Integrated Microelectronic Systems for Wearable Applications. *Adv. Mater.* **2019,** *0* (0), 1901958.

[77] Andrew, T. L.; Zhang, L.; Cheng, N.; Baima, M.; Kim, J. J.; Allison, L.; Hoxie, S., Melding Vapor-Phase Organic Chemistry and Textile Manufacturing To Produce Wearable Electronics. *Acc. Chem. Res.* **2018,** *51* (4), 850-859.

[78] Zeng, W.; Shu, L.; Li, Q.; Chen, S.; Wang, F.; Tao, X.-M., Fiber-Based Wearable Electronics: A Review of Materials, Fabrication, Devices, and Applications. *Adv. Mater.* **2014,** *26* (31), 5310-5336.

[79] Van Lam, D.; Jo, K.; Kim, C.-H.; Won, S.; Hwangbo, Y.; Kim, J.-H.; Lee, H.-J.; Lee, S.-M., Calligraphic ink enabling washable conductive textile electrodes for supercapacitors. *J. Mater. Chem. A* **2016,** *4* (11), 4082-4088.

[80] Lee, S.-S.; Choi, K.-H.; Kim, S.-H.; Lee, S.-Y., Wearable Supercapacitors Printed on Garments. *Adv. Funct. Mater.* **2018,** *28* (11), 1705571.

[81] Shleev, S.; Andoralov, V.; Pankratov, D.; Falk, M.; Aleksejeva, O.; Blum, Z., Oxygen Electroreduction versus Bioelectroreduction: Direct Electron Transfer Approach. *Electroanalysis* **2016,** *28* (10), 2270-2287.

[82] Liu, Y.; Zhang, J.; Cheng, Y.; Jiang, S. P., Effect of Carbon Nanotubes on Direct Electron Transfer and Electrocatalytic Activity of Immobilized Glucose Oxidase. *ACS Omega* **2018,** *3* (1), 667-676.

[83] Prasad, K. P.; Chen, Y.; Chen, P., Three-Dimensional Graphene-Carbon Nanotube Hybrid for High-Performance Enzymatic Biofuel Cells. *ACS Appl. Mater. Interfaces* **2014,** *6* (5), 3387-3393.

[84] Kim, J.; Jeerapan, I.; Ciui, B.; Hartel, M. C.; Martin, A.; Wang, J., Edible Electrochemistry: Food Materials Based Electrochemical Sensors. *Adv. Healthcare Mater.* **2017,** *6* (22), 1700770-n/a.

[85] Zebda, A.; Alcaraz, J.-P.; Vadgama, P.; Shleev, S.; Minteer, S. D.; Boucher, F.; Cinquin, P.; Martin, D. K., Challenges for successful implantation of biofuel cells. *Bioelectrochemistry* **2018,** *124*, 57-72.

[86] Christwardana, M.; Kwon, Y., Effects of multiple polyaniline layers immobilized on carbon nanotube and glutaraldehyde on performance and stability of biofuel cell. *J. Power Sources* **2015,** *299*, 604-610.

[87] Rubenwolf, S.; Kerzenmacher, S.; Zengerle, R.; von Stetten, F., Strategies to extend the lifetime of bioelectrochemical enzyme electrodes for biosensing and biofuel cell applications. *Appl. Microbiol. Biotechnol.* **2011,** *89* (5), 1315-1322.

[88] Bioelectronics – An Introduction. In *Bioelectronics*, 10.1002/352760376X.ch1.

[89] Minteer, S. D., *Enzyme stabilization and immobilization*. Springer: 2017.

[90] Tu, T.; Wang, Y.; Huang, H.; Wang, Y.; Jiang, X.; Wang, Z.; Yao, B.; Luo, H., Improving the thermostability and catalytic efficiency of glucose oxidase from Aspergillus niger by molecular evolution. *Food Chem.* **2019,** *281*, 163-170.

[91] Reyes-De-Corcuera, J. I.; Olstad, H. E.; García-Torres, R., Stability and Stabilization of Enzyme Biosensors: The Key to Successful Application and Commercialization. *Annual Review of Food Science and Technology* **2018,** *9* (1), 293-322.

[92] Calabrese Barton, S., Oxygen transport in composite mediated biocathodes. *Electrochim. Acta* **2005,** *50* (10), 2145-2153.

[93] Yu, Y.; Xu, M.; Bai, L.; Han, L.; Dong, S., Recoverable hybrid enzymatic biofuel cell with molecular oxygen-independence. *Biosens. Bioelectron.* **2016,** *75*, 23-27.

[94] Bedekar, A. S.; Feng, J. J.; Krishnamoorthy, S.; Lim, K. G.; Palmore, G. T. R.; Sundaram, S., Oxygen Limitation In Microfluidic Biofuel Cells. *Chem. Eng. Commun.* **2007,** *195* (3), 256-266.

[95] Harvey, C. J.; LeBouf, R. F.; Stefaniak, A. B., Formulation and stability of a novel artificial human sweat under conditions of storage and use. *Toxicology in Vitro* **2010,** *24* (6), 1790-1796.

[96] Reid, R. C.; Minteer, S. D.; Gale, B. K., Contact lens biofuel cell tested in a synthetic tear solution. *Biosens. Bioelectron.* **2015,** *68*, 142-148.

[97] Bollella, P.; Fusco, G.; Stevar, D.; Gorton, L.; Ludwig, R.; Ma, S.; Boer, H.; Koivula, A.; Tortolini, C.; Favero, G.; Antiochia, R.; Mazzei, F., A Glucose/Oxygen

Enzymatic Fuel Cell based on Gold Nanoparticles modified Graphene Screen-Printed Electrode. Proof-of-Concept in Human Saliva. *Sens. Actuators, B* **2018,** *256*, 921-930.

[98] Jia, W.; Wang, X.; Imani, S.; Bandodkar, A. J.; Ramírez, J.; Mercier, P. P.; Wang, J., Wearable textile biofuel cells for powering electronics. *J. Mater. Chem. A* **2014,** *2* (43), 18184-18189.

[99] Falk, M.; Pankratov, D.; Lindh, L.; Arnebrant, T.; Shleev, S., Miniature Direct Electron Transfer Based Enzymatic Fuel Cell Operating in Human Sweat and Saliva. *Fuel Cells* **2014,** *14* (6), 1050-1056.

[100] Choleau, C.; Klein, J. C.; Reach, G.; Aussedat, B.; Demaria-Pesce, V.; Wilson, G. S.; Gifford, R.; Ward, W. K., Calibration of a subcutaneous amperometric glucose sensor implanted for 7 days in diabetic patients: Part 2. Superiority of the one-point calibration method. *Biosens. Bioelectron.* **2002,** *17* (8), 647-654.

[101] du Toit, H.; Rashidi, R.; Ferdani, D. W.; Delgado-Charro, M. B.; Sangan, C. M.; Di Lorenzo, M., Generating power from transdermal extracts using a multi-electrode miniature enzymatic fuel cell. *Biosens. Bioelectron.* **2016,** *78*, 411-417.

[102] Ó Conghaile, P.; Falk, M.; MacAodha, D.; Yakovleva, M. E.; Gonaus, C.; Peterbauer, C. K.; Gorton, L.; Shleev, S.; Leech, D., Fully Enzymatic Membraneless Glucose|Oxygen Fuel Cell That Provides 0.275 mA cm–2 in 5 mM Glucose, Operates in Human Physiological Solutions, and Powers Transmission of Sensing Data. *Anal. Chem.* **2016,** *88* (4), 2156-2163.

[103] Wang, T.; Milton, R. D.; Abdellaoui, S.; Hickey, D. P.; Minteer, S. D., Laccase Inhibition by Arsenite/Arsenate: Determination of Inhibition Mechanism and Preliminary Application to a Self-Powered Biosensor. *Anal. Chem.* **2016,** *88* (6), 3243-3248.

[104] Gu, C.; Kong, X.; Liu, X.; Gai, P.; Li, F., Enzymatic Biofuel-Cell-Based Self-Powered Biosensor Integrated with DNA Amplification Strategy for Ultrasensitive Detection of Single-Nucleotide Polymorphism. *Anal. Chem.* **2019,** *91* (13), 8697-8704.

[105] Gai, P.-P.; Ji, Y.-S.; Wang, W.-J.; Song, R.-B.; Zhu, C.; Chen, Y.; Zhang, J.-R.; Zhu, J.-J., Ultrasensitive self-powered cytosensor. *Nano Energy* **2016,** *19*, 541-549.

[106] Katz, E.; Bückmann, A. F.; Willner, I., Self-Powered Enzyme-Based Biosensors. *J. Am. Chem. Soc.* **2001,** *123* (43), 10752-10753.

[107] Stoppa, M.; Chiolerio, A., Wearable Electronics and Smart Textiles: A Critical Review. *Sensors* **2014,** *14* (7), 11957-11992.

[108] Yeknami, A. F.; Wang, X.; Jeerapan, I.; Imani, S.; Nikoofard, A.; Wang, J.; Mercier, P. P., A 0.3-V CMOS Biofuel-Cell-Powered Wireless Glucose/Lactate Biosensing System. *IEEE J. Solid-State Circuits* **2018,** *53* (11), 3126-3139.

[109] Falk, M.; Andoralov, V.; Silow, M.; Toscano, M. D.; Shleev, S., Miniature Biofuel Cell as a Potential Power Source for Glucose-Sensing Contact Lenses. *Anal. Chem.* **2013,** *85* (13), 6342-6348.

[110] Sekretaryova, A. N.; Beni, V.; Eriksson, M.; Karyakin, A. A.; Turner, A. P. F.; Vagin, M. Y., Cholesterol Self-Powered Biosensor. *Anal. Chem.* **2014,** *86* (19), 9540-9547.

[111] Pan, C.; Fang, Y.; Wu, H.; Ahmad, M.; Luo, Z.; Li, Q.; Xie, J.; Yan, X.; Wu, L.; Wang, Z. L.; Zhu, J., Generating Electricity from Biofluid with a Nanowire-Based Biofuel Cell for Self-Powered Nanodevices. *Adv. Mater.* **2010,** *22* (47), 5388-5392.

[112] Chu, M. X.; Miyajima, K.; Takahashi, D.; Arakawa, T.; Sano, K.; Sawada, S.-i.; Kudo, H.; Iwasaki, Y.; Akiyoshi, K.; Mochizuki, M.; Mitsubayashi, K., Soft contact lens biosensor for in situ monitoring of tear glucose as non-invasive blood sugar assessment. *Talanta* **2011,** *83* (3), 960-965.

[113] Koushanpour, A.; Gamella, M.; Katz, E., A Biofuel Cell Based on Biocatalytic Reactions of Lactate on Both Anode and Cathode Electrodes – Extracting Electrical Power from Human Sweat. *Electroanalysis* **2017,** *29* (6), 1602-1611.

[114] Pu, X.; Hu, W.; Wang, Z. L., Toward Wearable Self-Charging Power Systems: The Integration of Energy-Harvesting and Storage Devices. *Small* **2018,** *14* (1), 1702817.

[115] Xiao, X.; Conghaile, P. Ó.; Leech, D.; Ludwig, R.; Magner, E., An oxygen-independent and membrane-less glucose biobattery/supercapacitor hybrid device. *Biosens. Bioelectron.* **2017,** *98*, 421-427.

[116] Chen, X.; Yin, L.; Lv, J.; Gross, A. J.; Le, M.; Gutierrez, N. G.; Li, Y.; Jeerapan, I.; Giroud, F.; Berezovska, A.; K. O'Reilly, R.; Xu, S.; Cosnier, S.; Wang, J., Stretchable and flexible buckypaper-based lactate biofuel cell for wearable electronics. *Adv. Funct. Mater.* **2019**, 10.1002/adfm.201905785.

[117] Yu, Y.; Zhai, J.; Xia, Y.; Dong, S., Single wearable sensing energy device based on photoelectric biofuel cells for simultaneous analysis of perspiration and illuminance. *Nanoscale* **2017,** *9* (33), 11846-11850.

[118] Wang, L.; Shao, H.; Lu, X.; Wang, W.; Zhang, J.-R.; Song, R.-B.; Zhu, J.-J., A glucose/O2 fuel cell-based self-powered biosensor for probing a drug delivery model with self-diagnosis and self-evaluation. *Chem. Sci.* **2018,** *9* (45), 8482-8491.

[119] Renaud, L.; Selloum, D.; Tingry, S., Xurography for 2D and multi-level glucose/O2 microfluidic biofuel cell. *Microfluidics and Nanofluidics* **2015,** *18* (5), 1407-1416.

[120] Escalona-Villalpando, R. A.; Ortiz-Ortega, E.; Bocanegra-Ugalde, J. P.; Minteer, S. D.; Ledesma-García, J.; Arriaga, L. G., Clean energy from human sweat using an enzymatic patch. *J. Power Sources* **2019,** *412*, 496-504.

[121] Shitanda, I.; Nohara, S.; Hoshi, Y.; Itagaki, M.; Tsujimura, S., A screen-printed circular-type paper-based glucose/O2 biofuel cell. *J. Power Sources* **2017,** *360*, 516-519.

[122] Kai, H.; Suda, W.; Yoshida, S.; Nishizawa, M., Organic electrochromic timer for enzymatic skin patches. *Biosens. Bioelectron.* **2019,** *123*, 108-113.

[123] Amir, L.; Tam, T. K.; Pita, M.; Meijler, M. M.; Alfonta, L.; Katz, E., Biofuel Cell Controlled by Enzyme Logic Systems. *J. Am. Chem. Soc.* **2009,** *131* (2), 826-832.

[124] Bandodkar, A. J.; Choi, J.; Lee, S. P.; Jeang, W. J.; Agyare, P.; Gutruf, P.; Wang, S.; Sponenburg, R. A.; Reeder, J. T.; Schon, S.; Ray, T. R.; Chen, S.; Mehta, S.; Ruiz, S.; Rogers, J. A., Soft, Skin-Interfaced Microfluidic Systems with Passive Galvanic Stopwatches for Precise Chronometric Sampling of Sweat. *Adv. Mater.* **2019,** *0* (0), 1902109.

[125] Tan, Y.; Adhikari, R. Y.; Malvankar, N. S.; Pi, S.; Ward, J. E.; Woodard, T. L.; Nevin, K. P.; Xia, Q.; Tuominen, M. T.; Lovley, D. R., Synthetic Biological Protein Nanowires with High Conductivity. *Small* **2016,** *12* (33), 4481-4485.

[126] Atanassov, P.; Apblett, C.; Banta, S.; Brozik, S.; Barton, S. C.; Cooney, M.; Liaw, B. Y.; Mukerjee, S.; Minteer, S. D., Enzymatic biofuel cells. *Interface-Electrochemical Society* **2007,** *16* (2), 28-31.

[127] Franco, J. H.; Neto, S. A.; Hickey, D. P.; Minteer, S. D.; de Andrade, A. R., Hybrid catalyst cascade architecture enhancement for complete ethanol electrochemical oxidation. *Biosens. Bioelectron.* **2018,** *121*, 281-286.

[128] Zhu, Z.; Zhang, Y. H. P., In vitro metabolic engineering of bioelectricity generation by the complete oxidation of glucose. *Metab. Eng.* **2017,** *39*, 110-116.

[129] Son, D.; Lee, J.; Qiao, S.; Ghaffari, R.; Kim, J.; Lee, J. E.; Song, C.; Kim, S. J.; Lee, D. J.; Jun, S. W.; Yang, S.; Park, M.; Shin, J.; Do, K.; Lee, M.; Kang, K.; Hwang, C. S.; Lu, N.; Hyeon, T.; Kim, D.-H., Multifunctional wearable devices for diagnosis and therapy of movement disorders. *Nat Nano* **2014,** *9* (5), 397-404.

[130] Lee, H.; Choi, T. K.; Lee, Y. B.; Cho, H. R.; Ghaffari, R.; Wang, L.; Choi, H. J.; Chung, T. D.; Lu, N.; Hyeon, T.; Choi, S. H.; Kim, D.-H., A graphene-based electrochemical device with thermoresponsive microneedles for diabetes monitoring and therapy. *Nat Nano* **2016,** *11* (6), 566-572.

[131] Kim, D.-H.; Lu, N.; Ma, R.; Kim, Y.-S.; Kim, R.-H.; Wang, S.; Wu, J.; Won, S. M.; Tao, H.; Islam, A.; Yu, K. J.; Kim, T.-i.; Chowdhury, R.; Ying, M.; Xu, L.; Li, M.; Chung, H.-J.; Keum, H.; McCormick, M.; Liu, P.; Zhang, Y.-W.; Omenetto, F. G.; Huang, Y.; Coleman, T.; Rogers, J. A., Epidermal Electronics. *Science* **2011,** *333* (6044), 838.

[132] Hwang, S.-W.; Lee, C. H.; Cheng, H.; Jeong, J.-W.; Kang, S.-K.; Kim, J.-H.; Shin, J.; Yang, J.; Liu, Z.; Ameer, G. A.; Huang, Y.; Rogers, J. A., Biodegradable Elastomers and Silicon Nanomembranes/Nanoribbons for Stretchable, Transient Electronics, and Biosensors. *Nano Lett.* **2015,** *15* (5), 2801-2808.

[133] Jia, W.; Valdes-Ramirez, G.; Bandodkar, A. J.; Windmiller, J. R.; Wang, J., Epidermal biofuel cells: energy harvesting from human perspiration. *Angew. Chem. Int. Ed.* **2013,** *52* (28), 7233-6.

[134] Miyake, T.; Haneda, K.; Yoshino, S.; Nishizawa, M., Flexible, layered biofuel cells. *Biosens. Bioelectron.* **2013,** *40* (1), 45-49.

[135] Zhou, M.; Wang, J., Biofuel Cells for Self-Powered Electrochemical Biosensing and Logic Biosensing: A Review. *Electroanalysis* **2012,** *24* (2), 197-209.

[136] Li, M.; Li, Y.-T.; Li, D.-W.; Long, Y.-T., Recent developments and applications of screen-printed electrodes in environmental assays—A review. *Anal. Chim. Acta* **2012,** *734*, 31-44.

[137] Gaikwad, A. M.; Arias, A. C.; Steingart, D. A., Recent Progress on Printed Flexible Batteries: Mechanical Challenges, Printing Technologies, and Future Prospects. *Energy Technology* **2015,** *3* (4), 305-328.

[138] Matsuhisa, N.; Kaltenbrunner, M.; Yokota, T.; Jinno, H.; Kuribara, K.; Sekitani, T.; Someya, T., Printable elastic conductors with a high conductivity for electronic textile applications. *Nat. Commun.* **2015,** *6*.

[139] Vagin, M. Y.; Jeerapan, I.; Wannapob, R.; Thavarungkul, P.; Kanatharana, P.; Anwar, N.; McCormac, T.; Eriksson, M.; Turner, A. P. F.; Jager, E. W. H.; Mak, W. C., Water-processable polypyrrole microparticle modules for direct fabrication of hierarchical structured electrochemical interfaces. *Electrochim. Acta* **2016,** *190*, 495-503.

[140] Reuillard, B.; Le Goff, A.; Agnes, C.; Holzinger, M.; Zebda, A.; Gondran, C.; Elouarzaki, K.; Cosnier, S., High power enzymatic biofuel cell based on naphthoquinone-mediated oxidation of glucose by glucose oxidase in a carbon nanotube 3D matrix. *Phys Chem Chem Phys* **2013,** *15* (14), 4892-4896.

[141] Gray, D. S.; Tien, J.; Chen, C. S., High-Conductivity Elastomeric Electronics. *Adv. Mater.* **2004,** *16* (5), 393-397.

[142] Kim, J.; Jeerapan, I.; Imani, S.; Cho, T. N.; Bandodkar, A.; Cinti, S.; Mercier, P. P.; Wang, J., Noninvasive Alcohol Monitoring Using a Wearable Tattoo-Based Iontophoretic-Biosensing System. *ACS Sens.* **2016,** *1* (8), 1011-1019.

[143] Hocheng, H.; Chen, C.-M., Design, Fabrication and Failure Analysis of Stretchable Electrical Routings. *Sensors* **2014,** *14* (7), 11855-11877.

[144] Gonzalez, M.; Axisa, F.; Bulcke, M. V.; Brosteaux, D.; Vandevelde, B.; Vanfleteren, J., Design of metal interconnects for stretchable electronic circuits. *Microelectronics Reliability* **2008,** *48* (6), 825-832.

[145] Casalongue, H. S.; Kaya, S.; Viswanathan, V.; Miller, D. J.; Friebel, D.; Hansen, H. A.; Nørskov, J. K.; Nilsson, A.; Ogasawara, H., Direct observation of the oxygenated species during oxygen reduction on a platinum fuel cell cathode. *Nat Commun* **2013,** *4*.

[146] Scodeller, P.; Carballo, R.; Szamocki, R.; Levin, L.; Forchiassin, F.; Calvo, E. J., Layer-by-Layer Self-Assembled Osmium Polymer-Mediated Laccase Oxygen Cathodes for Biofuel Cells: The Role of Hydrogen Peroxide. *J. Am. Chem. Soc.* **2010,** *132* (32), 11132-11140.

[147] Cignini, P.; Pistoia, G., Discharge behaviour of AgO and Ag2O cathodes in lithium cells. *Electrochim. Acta* **1978,** *23* (10), 1099-1101.

[148] Pistoia, G., *Batteries for Portable Devices*. Elsevier Science B.V.: Amsterdam, 2005, p 33-76.

[149] Lee, P.; Lee, J.; Lee, H.; Yeo, J.; Hong, S.; Nam, K. H.; Lee, D.; Lee, S. S.; Ko, S. H., Highly Stretchable and Highly Conductive Metal Electrode by Very Long Metal Nanowire Percolation Network. *Adv. Mater.* **2012,** *24* (25), 3326-3332.

[150] Bauhofer, W.; Kovacs, J. Z., A review and analysis of electrical percolation in carbon nanotube polymer composites. *Compos. Sci. Technol.* **2009,** *69* (10), 1486-1498.

[151] Amjadi, M.; Kyung, K.-U.; Park, I.; Sitti, M., Stretchable, Skin-Mountable, and Wearable Strain Sensors and Their Potential Applications: A Review. *Adv. Funct. Mater.* **2016,** *26* (11), 1678-1698.

[152] Murray, B. J.; Li, Q.; Newberg, J. T.; Menke, E. J.; Hemminger, J. C.; Penner, R. M., Shape- and Size-Selective Electrochemical Synthesis of Dispersed Silver(I) Oxide Colloids. *Nano Lett.* **2005,** *5* (11), 2319-2324.

[153] Pham, Q.-T.; Huy, B. T.; Lee, Y.-I., New highly efficient electrochemical synthesis of dispersed Ag2O particles in the vicinity of the cathode with controllable size and shape. *J. Mater. Chem. C* **2015,** *3* (29), 7720-7726.

[154] Harn, Y.-W.; Yang, T.-H.; Tang, T.-Y.; Chen, M.-C.; Wu, J.-M., Facet-Dependent Photocatalytic Activity and Facet-Selective Etching of Silver(I) Oxide Crystals with Controlled Morphology. *ChemCatChem* **2015,** *7* (1), 80-86.

[155] Wang, W.; Zhao, Q.; Dong, J.; Li, J., A novel silver oxides oxygen evolving catalyst for water splitting. *Int. J. Hydrogen Energy* **2011,** *36* (13), 7374-7380.

[156] Sanli, E.; Uysal, B. Z.; Aksu, M. L., The oxidation of NaBH4 on electrochemicaly treated silver electrodes. *Int. J. Hydrogen Energy* **2008,** *33* (8), 2097-2104.

[157] Ozgit, D.; Hiralal, P.; Amaratunga, G. A. J., Improving Performance and Cyclability of Zinc–Silver Oxide Batteries by Using Graphene as a Two Dimensional Conductive Additive. *ACS Appl. Mater. Interfaces* **2014,** *6* (23), 20752-20757.

[158] Lund, E.; Galeckas, A.; Azarov, A.; Monakhov, E. V.; Svensson, B. G., Photoluminescence of reactively sputtered Ag2O films. *Thin Solid Films* **2013,** *536*, 156-159.

[159] Wang, J., Carbon-Nanotube Based Electrochemical Biosensors: A Review. *Electroanalysis* **2005,** *17* (1), 7-14.

[160] Rassaei, L.; Olthuis, W.; Tsujimura, S.; Sudhölter, E. J.; van den Berg, A., Lactate biosensors: current status and outlook. *Analytical and bioanalytical chemistry* **2014,** *406* (1), 123-137.

[161] Valenza, F.; Aletti, G.; Fossali, T.; Chevallard, G.; Sacconi, F.; Irace, M.; Gattinoni, L., Lactate as a marker of energy failure in critically ill patients: hypothesis. *CRITICAL CARE-LONDON*- **2005,** *9* (6), 588.

[162] Kemp, G., Lactate accumulation, proton buffering, and pH change in ischemically exercising muscle. *American Journal of Physiology - Regulatory, Integrative and Comparative Physiology* **2005,** *289* (3), R895-R901.

[163] Jia, W.; Wang, X.; Imani, S.; Bandodkar, A. J.; Ramírez, J.; Mercier, P. P.; Wang, J., Wearable textile biofuel cells for powering electronics. *J. Mater. Chem. A* **2014,** *2* (43), 18184-18189.

[164] Meredith, M. T.; Minteer, S. D., Biofuel Cells: Enhanced Enzymatic Bioelectrocatalysis. *Annual Review of Analytical Chemistry* **2012,** *5* (1), 157-179.

[165] Nelson, D. L.; Lehninger, A. L.; Cox, M. M., *Lehninger Principles of Biochemistry*. Macmillan: 2008.

[166] Cui, X.; Li, C. M.; Zang, J.; Yu, S., Highly sensitive lactate biosensor by engineering chitosan/PVI-Os/CNT/LOD network nanocomposite. *Biosens. Bioelectron.* **2007,** *22* (12), 3288-3292.

[167] Teymourian, H.; Salimi, A.; Khezrian, S., Fe3O4 magnetic nanoparticles/reduced graphene oxide nanosheets as a novel electrochemical and bioeletrochemical sensing platform. *Biosens. Bioelectron.* **2013,** *49*, 1-8.

[168] MacVittie, K.; Katz, E., Self-powered electrochemical memristor based on a biofuel cell - towards memristors integrated with biocomputing systems. *Chem. Commun.* **2014,** *50* (37), 4816-4819.

[169] Zhou, M.; Zhou, N.; Kuralay, F.; Windmiller, J. R.; Parkhomovsky, S.; Valdés-Ramírez, G.; Katz, E.; Wang, J., A Self-Powered "Sense-Act-Treat" System that is Based on a Biofuel Cell and Controlled by Boolean Logic. *Angew. Chem. Int. Ed.* **2012,** *51* (11), 2686-2689.

[170] Kalantar-zadeh, K.; Ha, N.; Ou, J. Z.; Berean, K. J., Ingestible Sensors. *ACS Sens.* **2017,** *2* (4), 468-483.

[171] Tao, H.; Brenckle, M. A.; Yang, M.; Zhang, J.; Liu, M.; Siebert, S. M.; Averitt, R. D.; Mannoor, M. S.; McAlpine, M. C.; Rogers, J. A.; Kaplan, D. L.; Omenetto, F. G., Silk-Based Conformal, Adhesive, Edible Food Sensors. *Adv. Mater.* **2012,** *24* (8), 1067-1072.

[172] Keller, A.; Pham, J.; Warren, H.; in het Panhuis, M., Conducting hydrogels for edible electrodes. *Journal of Materials Chemistry B* **2017,** *5* (27), 5318-5328.

[173] Kim, Y. J.; Wu, W.; Chun, S.-E.; Whitacre, J. F.; Bettinger, C. J., Biologically derived melanin electrodes in aqueous sodium-ion energy storage devices. *Proceedings of the National Academy of Sciences* **2013,** *110* (52), 20912-20917.

[174] Kim, Y. J.; Chun, S.-E.; Whitacre, J.; Bettinger, C. J., Self-deployable current sources fabricated from edible materials. *Journal of Materials Chemistry B* **2013,** *1* (31), 3781-3788.

[175] Wang, X.; Xu, W.; Chatterjee, P.; Lv, C.; Popovich, J.; Song, Z.; Dai, L.; Kalani, M. Y. S.; Haydel, S. E.; Jiang, H., Food-Materials-Based Edible Supercapacitors. *Adv. Mater. Technol.* **2016,** *1* (3), 1600059-n/a.

[176] Southcott, M.; MacVittie, K.; Halámek, J.; Halámková, L.; Jemison, W. D.; Lobel, R.; Katz, E., A pacemaker powered by an implantable biofuel cell operating under conditions mimicking the human blood circulatory system – battery not included. *Phys. Chem. Chem. Phys.* **2013,** *15* (17), 6278-6283.

[177] Koushanpour, A.; Gamella, M.; Guz, N.; Katz, E., A Biofuel Cell Based on Biocatalytic Reactions of Glucose on Both Anode and Cathode Electrodes. *Electroanalysis* **2017,** *29* (4), 950-954.

[178] Rabaey, K.; Verstraete, W., Microbial fuel cells: novel biotechnology for energy generation. *Trends Biotechnol.* **2005,** *23* (6), 291-298.

[179] Akyilmaz, E.; Dinckaya, E., A mushroom (Agaricus bisporus) tissue homogenate based alcohol oxidase electrode for alcohol determination in serum. *Talanta* **2000,** *53* (3), 505-509.

[180] Wang, J.; Lin, M. S., Mixed plant tissue carbon paste bioelectrode. *Anal. Chem.* **1988,** *60* (15), 1545-1548.

[181] Gu, Y.; Sattayasamitsathit, S.; Jia, W.; Kaufmann, K.; Wang, C.; Wang, J., High-Power Low-Cost Tissue-Based Biofuel Cell. *Electroanalysis* **2013,** *25* (4), 838-844.

[182] Yuhashi, N.; Tomiyama, M.; Okuda, J.; Igarashi, S.; Ikebukuro, K.; Sode, K., Development of a novel glucose enzyme fuel cell system employing protein engineered PQQ glucose dehydrogenase. *Biosens. Bioelectron.* **2005,** *20* (10), 2145-2150.

[183] Rubbens, J.; Brouwers, J.; Wolfs, K.; Adams, E.; Tack, J.; Augustijns, P., Ethanol concentrations in the human gastrointestinal tract after intake of alcoholic beverages. *European Journal of Pharmaceutical Sciences* **2016,** *86*, 91-95.

[184] Topcagic, S.; Minteer, S. D., Development of a membraneless ethanol/oxygen biofuel cell. *Electrochim. Acta* **2006,** *51* (11), 2168-2172.

[185] Beck, I. T.; Dinda, P. K., Acute exposure of small intestine to ethanol. *Digestive Diseases and Sciences* **1981,** *26* (9), 817-838.

[186] Fallingborg, J., Intraluminal pH of the human gastrointestinal tract. *Danish medical bulletin* **1999,** *46* (3), 183-196.

[187] Mason, H. S., Structures and Functions of the Phenolase Complex. *Nature* **1956,** *177* (4498), 79-81.

[188] Février, H.; Le Quéré, J.-M.; Le Bail, G.; Guyot, S., Polyphenol profile, PPO activity and pH variation in relation to colour changes in a series of red-fleshed apple juices. *LWT - Food Science and Technology* **2017,** *85*, 353-362.

[189] Ioniţă, E.; Gurgu, L.; Aprodu, I.; Stănciuc, N.; Dalmadi, I.; Bahrim, G.; Râpeanu, G., Characterization, purification, and temperature/pressure stability of polyphenol oxidase extracted from plums (Prunus domestica). *Process Biochem.* **2017,** *56*, 177-185.

[190] Montgomery, M. W.; Sgarbieri, V. C., Isoenzymes of banana polyphenol oxidase. *Phytochemistry* **1975,** *14* (5), 1245-1249.

[191] Gooding, P. S.; Bird, C.; Robinson, S. P., Molecular cloning and characterisation of banana fruit polyphenol oxidase. *Planta* **2001,** *213* (5), 748-757.

[192] Khan, M. W.; Murali, A., Modeling of alcohol oxidase enzyme of Candida boidinii and in silico analysis of competitive binding of proton ionophores and FAD with enzyme. *Molecular BioSystems* **2017,** *13* (9), 1754-1769.

[193] Zayats, M.; Willner, B.; Willner, I., Design of Amperometric Biosensors and Biofuel Cells by the Reconstitution of Electrically Contacted Enzyme Electrodes. *Electroanalysis* **2008,** *20* (6), 583-601.

[194] Fujita, S.; Yamanoi, S.; Murata, K.; Mita, H.; Samukawa, T.; Nakagawa, T.; Sakai, H.; Tokita, Y., A repeatedly refuelable mediated biofuel cell based on a hierarchical porous carbon electrode. *Sci. Rep.* **2014,** *4*, 4937.

[195] Min, K.; Ryu, J. H.; Yoo, Y. J., Mediator-free glucose/O2 biofuel cell based on a 3-dimensional glucose oxidase/SWNT/polypyrrole composite electrode. *Biotechnology and Bioprocess Engineering* **2010,** *15* (3), 371-375.

[196] Asav, E.; Akyilmaz, E., Preparation and optimization of a bienzymic biosensor based on self-assembled monolayer modified gold electrode for alcohol and glucose detection. *Biosens. Bioelectron.* **2010,** *25* (5), 1014-1018.

[197] Kulys, J.; Schmid, R. D., Bienzyme Sensors based on Chemically Modified Electrodes. *Biosens. Bioelectron.* **1991,** *6* (1), 43-48.

[198] Wijesuriya, D. C.; Rechnitz, G. A., Biosensors based on plant and animal tissues. *Biosens. Bioelectron.* **1993,** *8* (3), 155-160.

[199] Calabrese Barton, S.; Gallaway, J.; Atanassov, P., Enzymatic Biofuel Cells for Implantable and Microscale Devices. *Chem. Rev.* **2004,** *104* (10), 4867-4886.

[200] Zebda, A.; Cosnier, S.; Alcaraz, J. P.; Holzinger, M.; Le Goff, A.; Gondran, C.; Boucher, F.; Giroud, F.; Gorgy, K.; Lamraoui, H.; Cinquin, P., Single Glucose Biofuel Cells Implanted in Rats Power Electronic Devices. *Sci. Rep.* **2013,** *3*, 1516.

[201] MacVittie, K.; Katz, E., Self-powered electrochemical memristor based on a biofuel cell – towards memristors integrated with biocomputing systems. *Chem. Commun.* **2014,** *50* (37), 4816-4819.

[202] Reuillard, B.; Le Goff, A.; Agnès, C.; Holzinger, M.; Zebda, A.; Gondran, C.; Elouarzaki, K.; Cosnier, S., High power enzymatic biofuel cell based on naphthoquinone-mediated oxidation of glucose by glucose oxidase in a carbon nanotube 3D matrix. *Phys. Chem. Chem. Phys.* **2013,** *15* (14), 4892-4896.

[203] Ramanavicius, A.; Kausaite, A.; Ramanaviciene, A., Enzymatic biofuel cell based on anode and cathode powered by ethanol. *Biosens. Bioelectron.* **2008,** *24* (4), 761-766.

[204] Kavanagh, P.; Boland, S.; Jenkins, P.; Leech, D., Performance of a Glucose/O2 Enzymatic Biofuel Cell Containing a Mediated Melanocarpus albomyces Laccase Cathode in a Physiological Buffer. *Fuel Cells* **2009,** *9* (1), 79-84.

[205] Mano, N.; Mao, F.; Heller, A., Characteristics of a Miniature Compartment-less Glucose−O2 Biofuel Cell and Its Operation in a Living Plant. *J. Am. Chem. Soc.* **2003,** *125* (21), 6588-6594.

[206] Huckabee, W. E., RELATIONSHIPS OF PYRUVATE AND LACTATE DURING ANAEROBIC METABOLISM. II. EXERCISE AND FORMATION OF O2-DEBT. *The Journal of Clinical Investigation* **1958,** *37* (2), 255-263.

[207] Wang, J.-Y.; Nien, P.-C.; Chen, C.-H.; Chen, L.-C.; Ho, K.-C., A glucose bio-battery prototype based on a GDH/poly(methylene blue) bioanode and a graphite cathode with an iodide/tri-iodide redox couple. *Bioresour. Technol.* **2012,** *116*, 502-506.

[208] Lau, C.; Adkins, E. R.; Ramasamy, R. P.; Luckarift, H. R.; Johnson, G. R.; Atanassov, P., Design of Carbon Nanotube-Based Gas-Diffusion Cathode for O2 Reduction by Multicopper Oxidases. *Adv. Energy Mater.* **2012,** *2* (1), 162-168.

[209] Snyder, J.; Fujita, T.; Chen, M. W.; Erlebacher, J., Oxygen reduction in nanoporous metal–ionic liquid composite electrocatalysts. *Nat. Mater.* **2010,** *9* (11), 904-907.

[210] Snyder, J.; Livi, K.; Erlebacher, J., Oxygen Reduction Reaction Performance of [MTBD][beti]-Encapsulated Nanoporous NiPt Alloy Nanoparticles. *Adv. Funct. Mater.* **2013,** *23* (44), 5494-5501.

[211] Wang, J.; Lu, F., Oxygen-Rich Oxidase Enzyme Electrodes for Operation in Oxygen-Free Solutions. *J. Am. Chem. Soc.* **1998,** *120* (5), 1048-1050.

[212] Yan, Y.; Zheng, W.; Su, L.; Mao, L., Carbon-Nanotube-Based Glucose/O2 Biofuel Cells. *Adv. Mater.* **2006,** *18* (19), 2639-2643.

[213] Bankar, S. B.; Bule, M. V.; Singhal, R. S.; Ananthanarayan, L., Glucose oxidase — An overview. *Biotechnol. Adv.* **2009,** *27* (4), 489-501.

[214] Zhang, L.; Zhou, M.; Wen, D.; Bai, L.; Lou, B.; Dong, S., Small-size biofuel cell on paper. *Biosens. Bioelectron.* **2012,** *35* (1), 155-159.

[215] Agnès, C.; Holzinger, M.; Le Goff, A.; Reuillard, B.; Elouarzaki, K.; Tingry, S.; Cosnier, S., Supercapacitor/biofuel cell hybrids based on wired enzymes on carbon nanotube matrices: autonomous reloading after high power pulses in neutral buffered glucose solutions. *Energy Environ. Sci.* **2014,** *7* (6), 1884-1888.

[216] Kleppe, K., The Effect of Hydrogen Peroxide on Glucose Oxidase from Aspergillus niger*. *Biochemistry* **1966,** *5* (1), 139-143.

[217] Marković, N. M.; Schmidt, T. J.; Stamenković, V.; Ross, P. N., Oxygen Reduction Reaction on Pt and Pt Bimetallic Surfaces: A Selective Review. *Fuel Cells* **2001,** *1* (2), 105-116.

[218] Liu, H.; Liu, Y.; Li, J., Ionic liquids in surface electrochemistry. *Phys. Chem. Chem. Phys.* **2010,** *12* (8), 1685-1697.

[219] Brunel, L.; Denele, J.; Servat, K.; Kokoh, K. B.; Jolivalt, C.; Innocent, C.; Cretin, M.; Rolland, M.; Tingry, S., Oxygen transport through laccase biocathodes for a membrane-less glucose/O2 biofuel cell. *Electrochem. Commun.* **2007,** *9* (2), 331-336.

[220] Kwon, C. H.; Lee, J. A.; Choi, Y.-B.; Kim, H.-H.; Spinks, G. M.; Lima, M. D.; Baughman, R. H.; Kim, S. J., Stability of carbon nanotube yarn biofuel cell in human body fluid. *J. Power Sources* **2015,** *286*, 103-108.

[221] Brandon, N. P.; Brett, D. J., Engineering porous materials for fuel cell applications. *Philosophical Transactions of the Royal Society A: Mathematical, Physical and Engineering Sciences* **2006,** *364* (1838), 147-159.

[222] Lei, Y.; Sun, R.; Zhang, X.; Feng, X.; Jiang, L., Oxygen-Rich Enzyme Biosensor Based on Superhydrophobic Electrode. *Adv. Mater.* **2016,** *28* (7), 1477-1481.

[223] Carda–Broch, S.; Berthod, A.; Armstrong, D. W., Solvent properties of the 1-butyl-3-methylimidazolium hexafluorophosphate ionic liquid. *Analytical and Bioanalytical Chemistry* **2003,** *375* (2), 191-199.

[224] Gong, K.; Du, F.; Xia, Z.; Durstock, M.; Dai, L., Nitrogen-Doped Carbon Nanotube Arrays with High Electrocatalytic Activity for Oxygen Reduction. *Science* **2009,** *323* (5915), 760.

[225] Kongkanand, A.; Kuwabata, S.; Girishkumar, G.; Kamat, P., Single-Wall Carbon Nanotubes Supported Platinum Nanoparticles with Improved Electrocatalytic Activity for Oxygen Reduction Reaction. *Langmuir* **2006,** *22* (5), 2392-2396.

[226] Salazar, P. F.; Chan, K. J.; Stephens, S. T.; Cola, B. A., Enhanced Electrical Conductivity of Imidazolium-Based Ionic Liquids Mixed with Carbon Nanotubes: A Spectroscopic Study. *J. Electrochem. Soc.* **2014,** *161* (9), H481-H486.

[227] Lopez, F.; Zerria, S.; Ruff, A.; Schuhmann, W., An O2 Tolerant Polymer/Glucose Oxidase Based Bioanode as Basis for a Self-powered Glucose Sensor. *Electroanalysis* **2018,** *30* (7), 1311-1318.

[228] Cosnier, S.; Gross, A. J.; Giroud, F.; Holzinger, M., Beyond the hype surrounding biofuel cells: What's the future of enzymatic fuel cells? *Curr. Opin. Electrochem.* **2018,** *12*, 148-155.

[229] Choi, S.; Lee, H.; Ghaffari, R.; Hyeon, T.; Kim, D.-H., Recent Advances in Flexible and Stretchable Bio-Electronic Devices Integrated with Nanomaterials. *Adv. Mater.* **2016,** *28* (22), 4203-4218.

[230] Menciassi, A., Bioelectronic devices: Gut-powered ingestible biosensors. *Nature Biomedical Engineering* **2017,** *1* (3), 0050.

[231] Bettinger, C. J., Advances in Materials and Structures for Ingestible Electromechanical Medical Devices. *Angew. Chem. Int. Ed.* **2018,** *57* (52), 16946-16958.

[232] Steiger, C.; Abramson, A.; Nadeau, P.; Chandrakasan, A. P.; Langer, R.; Traverso, G., Ingestible electronics for diagnostics and therapy. *Nat. Rev. Mater.* **2019,** *4* (2), 83-98.

[233] Berglund, J., Technology You Can Swallow: Moving Beyond Wearable Sensors, Researchers Are Creating Ingestible Ones. *IEEE Pulse* **2018,** *9* (1), 15-18.

[234] Liu, X.; Steiger, C.; Lin, S.; Parada, G. A.; Liu, J.; Chan, H. F.; Yuk, H.; Phan, N. V.; Collins, J.; Tamang, S.; Traverso, G.; Zhao, X., Ingestible hydrogel device. *Nat. Commun.* **2019,** *10* (1), 493.

[235] Hwang, E. T.; Gu, M. B., Enzyme stabilization by nano/microsized hybrid materials. *Engineering in Life Sciences* **2013,** *13* (1), 49-61.

[236] Sarma, A. K.; Vatsyayan, P.; Goswami, P.; Minteer, S. D., Recent advances in material science for developing enzyme electrodes. *Biosens. Bioelectron.* **2009,** *24* (8), 2313-2322.

[237] Catalano, P. N.; Wolosiuk, A.; Soler-Illia, G. J. A. A.; Bellino, M. G., Wired enzymes in mesoporous materials: A benchmark for fabricating biofuel cells. *Bioelectrochemistry* **2015,** *106*, 14-21.

[238] Moehlenbrock, M. J.; Minteer, S. D., Introduction to the Field of Enzyme Immobilization and Stabilization. In *Enzyme Stabilization and Immobilization: Methods and Protocols*, Minteer, S. D., Ed. Springer New York: New York, NY, 2017, 10.1007/978-1-4939-6499-4_1pp 1-7.

[239] Conzuelo, F.; Ruff, A.; Schuhmann, W., Self-powered bioelectrochemical devices. *Curr. Opin. Electrochem.* **2018,** *12*, 156-163.

[240] El Youssef, J.; Castle, J.; Ward, W. K., A Review of Closed-Loop Algorithms for Glycemic Control in the Treatment of Type 1 Diabetes. *Algorithms* **2009,** *2* (1).